INTRACELLULAR ACTIVATION AND PROCESSING OF HUMAN DISINTEGRIN AND METALLOPROTEINASE 19 (hADAM 19)

Dissertation zur Erlangung des Doktorgrades der Naturwissenschaften (Dr. rer. nat.)

Fakultät für Chemie
Universität Bielefeld

vorgelegt von
TIEBANG KANG
aus Hunan, P. R. China

May, 2003

Contents

1. Summary

Adamalysin 19 (a disintegrin and metalloproteinase 19, ADAM19, or meltrin ß) is a plasma membrane metalloproteinase. In this dissertation, I revealed that hADAM19 zymogen contains two functional furin recognition sites (RXK/RR), $\underline{R}^{197}P\underline{RR}^{200}$ and $\underline{R}^{200}M\underline{KR}^{203}$, between its pro- and catalytic - domain by protein N-terminal sequencing, specific furin inhibitors, mutagenesis, and furin-deficient mammalian cell lines. $\underline{R}^{200}M\underline{KR}^{203}$ is the primary cleavage site, but $\underline{R}^{197}P\underline{RR}^{200}$ is an alternative site for activation when the primary site is abolished. Co-localization between furin and hADAM19 is also identified in the ER/Golgi complex and/or the trans-Golgi network. Furthermore, hADAM19 is processed at E^{586}-S^{587} within cysteine-rich domain by an autolytic mechanism and the sizes of the side chains of the residues at both E^{586} and S^{587} are critical for this processing. This proceesig is necessary for hADAM19 to exert its proteolytic activities *in vitro* as illustrated by mutagenesis, such as both E^{586} to D^{586} and S^{587} to T^{587}. Based on this processing, I also developed a flourescamine assay to determine the activity of soluble hADAM19 by using a peptide substrate of Ac-RPLESNV, which is identical to the sequence encompassing the processing site. Interestingly, the autolytic processing at E^{586}-S^{587} occurs intramolecularly, not intermolecularly, producing an N-terminal fragment associated with its C-terminal fragment through disulfide bonds. The cysteine residues at C^{605}, C^{633}, C^{639}, and C^{643} within the residual cysteine-rich domain of the C-terminal fragment are partially responsible for the covalent association of the C-fragment with the N-terminal fragment. A new processing site at at Lys^{543}-Val^{544} was identified in soluble mutants when these cysteine residues were individually mutated to serine residues. These soluble mutated proteins were properly folded and secreted, but were less stable and more easily degraded compared with the soluble wild type, as illustrated by trypsin digestion and inactive mutant studies, suggesting that the proteolytic activity and the stability of soluble hADAM19 may be regulated by the formation of disulfide bonds that include C^{605}, C^{633}, C^{639}, and C^{643}. Moreover, the new processing site resulted from autolytic cleavage and was shown

to be independent of the processing at E^{586}-S^{587} by utilizing the double mutations E^{586} to D or E^{346} to A in soluble representative mutants. Correspondingly, shed fragments are detectable in the media from MDCK cells stably expressing the full length mutant with C^{633} to S, but neither C^{643} to S nor the wild type. Finally, the processing or shedding of hADAM19 is unaffected by Ilomastat (GM6001), but is obviously enhanced by phorbol-12 myristate 13-acetate, a protein kinase C activator; however, A23187, a calcium ionphore, or calmodulin antagonists, such as calmidazolium (CLM), W7, and trifluoperazine (TFP) blocks or inhibits this processing or shedding, indicating the same complex signal pathways may be involved in both processing and shedding of hADAM19.

2. Introduction

2.1 *The family of ADAM proteins*

ADAM (A Disintegrin And Metalloprotease), also called MDC (Metalloprotease Disintegrin / Cysteine-rich) protein constitutes a large family with 33 members known so far. ADAM proteins play important roles in many biological processes involving cell-surface proteolysis and cell-cell or cell-matrix interactions (Wolfsberg and White 1996, Schlondorff and Blobel 1999, Kheradmand and Werb 2002, Seals and Courtneidge 2003). Therefore, ADAMs have been implicated in many vital functions during development (Rooke et al. 1996, Wolfsberg and White 1996, Peschon et al. 1998, Qi et al. 1999, Schlondorff and Blobel 1999, Kheradmand and Werb 2002) and in the pathogenesis of cancer (Kuno et al. 1997, Yavari et al. 1998, Iba et al. 1999, Matthews et al. 2000, Sandy et al. 2001, Kheradmand and Werb 2002, Seals and Courtneidge 2003), rheumatoid arthritis (Tortorella et al. 1999, Sandy and Verscharen. 2001), Alzheimer's disease (Buxbaum et al. 1998, Koike et al. 1999, Anders et al. 2001, Colciaghi et al. 2002, Hooper and Turner 2002), asthma and bronchial hyperresponsiveness (Van Eerdewegh et al. 2002, Seals and Courtneidge 2003), and inflammatory responses (Kuno et al. 1997, Sandy et al. 2000, 2001). Based on the location, this ADAMs family can be divided into two subgroups; The bigger group is the type I membrane-bound ADAMs, containing prodomain, metalloprotease and disintegrin domains, cysteine-rich domain, EGF-like domain, transmembrane domain, and cytoplasmic domain (Wolfsberg and White 1996, Blobel 1997, Black and White 1998, Stone et al. 1999, Primakoff and Myles 2000, Seals and Courtneidge 2003). The soluble ADAMs constitute the smaller subgroup, including soluble alternative splice variants of several membrane-bound ADAMs and ADAM-TS containing thrombospondin-like repeats, besides the prodomain, metalloprotease and disintegrin domain, cysteine-rich domain (Figure 1.) (Stone et al. 1999, Primakoff and Myles 2000, Tang 2001, Seals and Courtneidge 2003, Somerville et al., 2003).

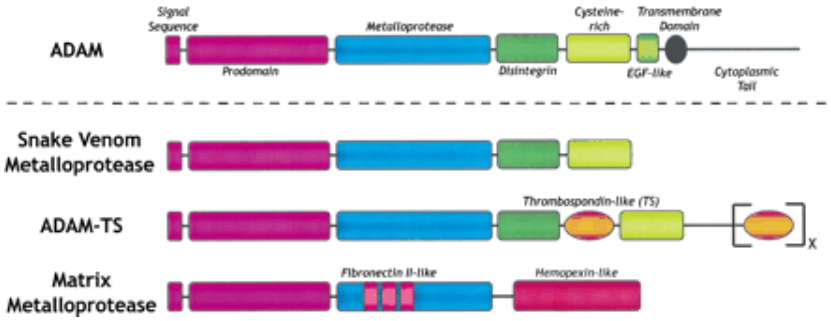

Figure 1. The topography of the ADAMs and related metalloproteases. Generalized domain structures of the ADAMs, SVMPs, ADAM-TS, and MMP families are shown. Note that ADAM-TS family members have a variable number of thrombospondin-like (TS) motifs. The MMP shown is of the gelatinase class. Other subclasses of MMPs lack hemopexin-like sequences and/or fibronectin type II-like sequences. The subclass of MT-MMPs have transmembrane domains and cytoplasmic tails in addition to the domains shown.

2.2 *Latency of ADAMs*

The classic cysteine switch mechanism for the latency and activation was originally proposed for MMPs (Van Wart and Birkedal-Hansen, 1990) and may be applied for many MMPs identified so far with the exception of MMP3, MMP23, and MMP26 (Chen et al. 1993, Galazka et al. 1996, Pei 1999, Velasco et al. 1999, Pei et al. 2000, Marchenko et al. 2002, Park et al. 2002). The conformation of proMMP3, which is different from its mature form, and a salt bridge in its precursor might contribute to the latency of the proenzyme (Chen et al. 1993, Galazka et al. 1996). The cysteine residue within the corresponding region of proMMP23/CA-MMP belongs to the type II membrane anchor, it is unable to coordinate with the zinc (II) in the catalytic domain to keep MMP23/CA-MMP latent (Pei 1999, Velasco et al. 1999, Pei et al. 2000). There is a unique cysteine-switch motif, PH81CGXXD, in the prodomain of proMMP-26, even if the conserved cysteine-switch sequence, PR81CGXXD, was restored by mutagenesis, the cysteine-switch activation mechanism was not induced (Marchenko et al. 2002), and the partial activation by autolysis produced the active forms containing this cysteine-switch sequence (Marchenko et al. 2002, Park et al. 2002).

Regarding the ADAM family members, the active ADAMs, such as ADAM1, 8, 9, 10, 12, 13, 15, 17, 19, 28, and ADAM-TS1, 4, 9, 12, contain a catalytic site consensus sequence (HEXXH) in their metalloprotease domains (Lum and Blobel 1997, Lum et al. 1998, Kuno et al. 1999, Loechel et al. 1998, 1999, Stone et al. 1999, Tortorella et al. 1999, Milla et al. 1999, Vu and Werb 2000, Primakoff and Myles 2000, Howard et al. 2000, 2001, Cal et al. 2001, Wei et al. 2001, Zhao et al. 2001, Shirakabe et al. 2001, Lopez-Perez et al. 2001, Guo et al. 2002, Cao et al. 2002, Gaultier et al. 2002, Schlomann et al. 2002, Kang et al. 2002b, 2002c, and submitted, Somerville et al. 2003). They may also have a putative cysteine-switch residue in their prodomains to keep them latent as proposed (Figure 2.) (Grams et al. 1993). For example, the latency and activation mechanism of ADAM12 is similar to the cysteine switch model as proposed for MMPs (Loechel et al. 1999); some ADAMs, such as ADAM9, 15, 17, and 19, showed enzyme activity against their substrates only after their prodomains were removed, suggesting that, at least, the removal of prodomains in these ADAMs is required for their proteolytic activities, resulting in a reasonable speculation that the latency of some ADAMs obey the cysteine switch model, although no direct evidence in many ADAMs, including ADAM9, 15, 17, and 19, has been provided to support the hypothesis that Cys-zinc coordination is required for latency (Lum et al. 1998, Milla et al. 1999, Roghani et al. 1999, Kang et al. 2002b).

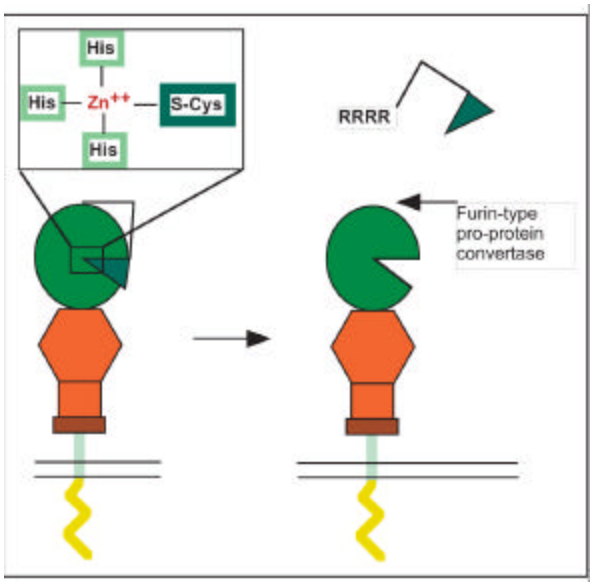

Figure 2. Cysteine-switch mechanism in a metalloproteinase-disintegrin. Metalloproteinases-disintegrins that have a catralytic-site consensus sequence contain an odd-numbered cysteine residues in their prodomains that has been proposed to function as a cysteine switch (Van Wart and Birkedal-Hansen, 1990). The Zn^{2+} is coordinated by three histidines in the catalytic site; the free sulfhydryl group of cysteine residue provides a fourth coordination site. This keeps the protease inactive (latent form) until the prodomain is removed. The predominant mechanism for the prodomain cleavage is mediated by furin or furin-like PCs in the secretory pathway.

2.3 *Activation of ADAMs*

By sequence alignment, two members in the ADAM family, ADAM8 (Yoshida et al. 1990) and ADAM28 (Howard et al. 2000) in mice, do not contain the conserved sequence, RXK/RR, which is generally cleaved by furin or furin-like proprotein convertases (PCs), in the boundary between pro- and metalloprotease- domains. Thus, for the removal of prodomains in ADAM zymogens, two mechanisms have been reported: One is the autolytic mechanism, which was shown in ADAM8 (Schlomann et al. 2002) and ADAM28 (Howard et al. 2000), because no processing of prodomains was observed in their inactive forms, in which the respective glutamate residue in their metalloproteinase domains was mutated to A or Q. The predominant mechanism for the removal of prodomains of ADAMs is mediated by furin or furin-like PCs in the secretory pathway. This mechanism has clearly been shown in many ADAMs, including ADAM1, 9, 12, 15, 17, 19, ADAM-TS1, 4, 9, 12, using N-terminal

sequencing, specific inhibitors of furin, blockers of protein trafficking from ER to Golgi, exogenous soluble furin *in vitro*, furin-deficient cell lines, and mutagenesis at the furin recognition site(s), RXK/RR, between the pro- and catalytic-domains (Lum and Blobel 1997, Lum et al. 1998, Loechel et al. 1998, Roghani et al. 1999, Kuno et al. 1999, Schlondorff et al. 2000, Cal et al. 2001, Guo et al. 2002, Cao et al. 2002, Kang et al. 2002b, Somerville et al., 2003). However, in some ADAMs, the removal of prodomain alone is not sufficient to activate the zymogens. For example, mature ADAM-TS4, which lacks its prodomain, has to be truncated at its C-terminus to display its aggrecanase activity (Guo et al. 2002); Soluble hADAM19 cleaved its prodomain by furin has to be processed within its cysteine-rich domain, producing an active enzyme shown by both alpha2-M and a peptide substrate assays *in vitro* (Kang et al. 2002c). In another case, the deletion of the prodomain destroys the proteolytic activity of ADAM10 (Fahrenholz et al. 2000, Anders et al. 2001). For ADAM12 and 17, the prodomains are not only an ihibitor of the catalytic domain, but also appear to act like a chaperone, facilitating secretion, folding, or both for the ADAM proteins (Milla et al. 1999, Roghani et al. 1999). In addition, many different mutants interfere with the folding or processing of ADAMs, resulting in a lack of proteolytic processing. For instance, the cysteine residue replaced with alanine in the prodomain of ADAM9 abolished its prodomain removal (Roghani et al. 1999). Both His^{346} and His^{350} substitutions with alanines in the metalloproteinase domain of mouse ADAM19 abrogated the processing of its prodomain (Shirakabe et al. 2001). The L73P mutant of ADAM12 resulted in complete retention of ADAM12 in the ER and inhibition of its processing (Cao et al. 2002). The soluble form of ADAM13 has never been converted into its mature form, indicating that the transmembrane domain, cytoplasmic domain, or both, are indispensable for the processing of the prodomain in ADAM13 (Gaultier et al. 2002). The removal of the disintegrin and cysteine-rich domains in TACE/ADAM17 resulted in the secretion of mature catalytic domain in association with

the precursor (pro) domain, demonstrating the cysteine-rich domain appears to play a role in the release of the prodomain (Milla et al. 1999).

2.4 *Functions of ADAMs*

ADAMs have been shown so far to possess four potential functions: proteolysis, cell adhesion, cell fusion, and cell signaling. One of the major functions for ADAMs is their proteolytic activities, acting as the sheddases responsible for the releasing of many membrane proteins, or as the proteinases for the digestion of components in the extracellular matrix or other proteins. Indeed, five ADAMs have been implicated in shedding processes so far. ADAM17/TACE, a major sheddase, has a role in the shedding of tumor necrosis factor-alpha (TNF-alpha), transforming growth factor-alpha (TGF-alpha), L-selectin, both TNF receptors, interleukin-1 receptor II, HER4, Notch, fractalkine, MUC1, TNF related activation-induced cytokine (TRANCE), and Collagen XVII. It also acts as a PMA-induced APP alpha-secretase (Black et al. 1997, Moss et al. 1997, Hooper et al. 1997, Peschon et al. 1998, Buxbaum et al. 1998, Lum et al. 1999, Schlondorff and Blobel 1999, Brou et al. 2000, Rio et al. 2000, Primakoff and Myles 2000, Blobel 2000, Garton et al. 2001, Kheradmand and Werb 2002, Sunnarborg et al. 2002, Franzke et al. 2002, Asai et al. 2003, Seals and Courtneidge 2003, Thathiah et al. 2003). ADAM10/KUZ, another major sheddase, is required for Notch signaling. It can cleave the Notch ligand Delta, heparin-binding epidermal growth factor (HB-EGF), TNF-alpha, L1 adhesion molecule, Collagen XVII and ephrin A2 and is an APP alpha-secretase (Hooper et al. 1997, Pan and Rubin 1997, Qi et al. 1999, Schlondorff and Blobel 1999, Fahrenholz et al. 2000, Primakoff and Myles 2000, Blobel 2000, Hattori et al. 2000, Mechtersheimer et al. 2001, Kheradmand and Werb 2002, Franzke et al. 2002, Asai et al. 2003, Seals and Courtneidge 2003). ADAM9/MDC9/meltrin gamma is believed to participate in the PMA-stimulated shedding of HB-EGF and is able to increase the shedding of Collagen XVII, and also can act as an APP alpha-secretase (Izumi et al. 1998, Koike et al. 1999,

Franzke et al. 2002, Asai et al. 2003, Seals and Courtneidge 2003). ADAM19/meltrin beta has been linked to shedding of the epidermal growth factor receptor ligand beta?type-neuregulins ?Shirakabe et al. 2001, Seals and Courtneidge 2003?. ADAM12/meltrin alpha ?has been shown to be responsible for endogenous shedding of HB-EGF in the heart (Asakura et al. 2002, Liao 2002, Seals and Courtneidge 2003).

Regarding the digestion of components of the extracellular matrix, ADAM10 cleaves type IV collagen *in vitro* (Millichip et al. 1998), ADAM15 cleaves type IV collagen and gelatin *in vitro* (Martin et al. 2002), and ADAM13-expressing cells degrade fibronectin (Alfandari et al. 2001). For the cleavage of other proteins, ADAM10 has first been shown to digest myelin basic protein (MBP) (Chantry et al. 1989), and MBP is also cleaved by ADAM8 (Schlomann et al. 2002). The soluble metalloprotease domain of MDC9 cleaves the insulin B-chain, a generic protease substrate (Roghani et al. 1999). A soluble ADAM12 exists as an alternatively spliced protein, which has been shown to cleave insulin-like growth factor-binding protein (IGFBP)-3 and -5 (Shi et al. 2000, Loechel et al. 2000). ADAM10 and ADAM17 contribute to the constitutive and PMA-regulated normal cleavage of the cellular prion protein (Vincent et al. 2001). For ADAM-TS proteins, ADAM-TS2 can degrade procollagen (Tortorella et al. 1999, Tang 2001), and ADAM-TS1, 4, 5, and 9 have been shown to cleave the lectican family of chondroitin sulfate proteoglycans *in vivo* and/or *in vitro*, such as versicans, aggrecans, and brevican (Abbaszade et al. 1999, Tortorella et al. 1999, 2000a, 2000b, Kuno et al. 2000, Sandy et al. 2000, Matthews et al. 2000, Sandy et al. 2001, Sandy and Verscharen. 2001, Guo et al. 2002, Rodriguez-Manzaneque et al. 2002, Westling et al. 2002, Somerville et al., 2003). In addition, there are some peptide substrates available to determine the activities of ADAM9, 10, 17, 19 (Roghani et al. 1999, Kang et al. 2002c), and ADAM9, 12, 15, 19 can form complex with alpha2-M and generate one or two products (Loechel et al. 1998, Lum et al. 1998, Roghani et al. 1999, Wei et al. 2001, Zhao et al. 2001, Kang et al. 2002b, 2002c).

Another major function for ADAMs is able to mediate cell-cell interaction or cell-cell fusions by their disintegrin/cysteine-rich (DC) domains. Six different ADAMs, ADAM2, 9, 12, 15, 23, 28 are able to interact with integrins such as alpha6beta1, alpha vbeta3, alpha9beta1, alpha vbeta5, alpha5beta1, and alpha4beta1, regulating cell-cell interactions in normal and pathological processes (Zhang et al. 1998, Nath et al. 1999, 2000, Eto et al. 2000, 2002, Zhou et al. 2001, Evans 2001, Bridges et al. 2002, Seals and Courtneidge 2003). For example, human ADAM15, the only one containing the RGD sequence in ADAMs, is able to bind to alphavbeta3, alpha5beta1 and alpha9beta1 (Zhang et al. 1998, Nath et al. 1999, Evans 2001). ADAM9 mediates cellular adhesion through alpha6beta1 or alpha vbeta5 integrins (Nath et al. 2000, Zhou et al. 2001, Evans 2001). The binding of integrin alpha9beta1 to the ADAM12 and 15 disintegrin domains mediates cell-cell interaction (Eto et al. 2000, 2002, Evans 2001). The lymphocyte metalloprotease MDC-L (ADAM 28) is a ligand for the integrin alpha 4beta1 (Bridges et al. 2002). The disintegrin and cysteine-rich domains of ADAM13 bind to both fibronectin and beta1-containing integrin receptors, and this binding can be inhibited by antibodies against the cysteine-rich domain (Gaultier et al, 2002). Furthermore, the recombinant disintegrin/cysteine-rich domain of ADAM8 mediates cell adhesion in cells expressing ADAM8 (Schlomann et al. 2002). The disintergrin and cysteine-rich domains of ADAM12 promotes the adhesion of fibroblasts and myoblasts (Zolkiewka, 1999). The disintegrin and cysteine-rich domains of full length ADAM12 supports cell adhesion through syndecans and triggers signaling events that lead to beta1 integrin-dependent cell spreading (Iba et al. 1999, 2000, Thodeti et al. 2003). Moreover, the disintegrin domains of ADAMs have been shown to mediate heterophilic and homophilic interactions, as in the cases of ADAM1, 2, 8. For instance, ADAM1 and ADAM2 can form heterodimers to mediate sperm-egg binding and fusion (Wolfsberg and White 1996). An alternatively spliced soluble ADAM12 interacts with IGFBP-3 through its cysteine-rich domain (Shi et al. 2000). The disintegrin and cysteine-rich domains of ADAM17 is required

for shedding of IL-1R-II while affecting the inhibitor sensitivity of TNF shedding (Reddy et al. 2000). Dr. DeSimone's group recently showed that the cysteine-rich domain of ADAM13 cooperates intramolecularly with the metalloproteinase domain of ADAM13 to regulate its function *in vivo* (Smith et al., 2002)

It is noteworthy that ADAMs have been shown to play roles in multiple signal transduction pathways. In the case of the transactivation of epidermal growth factor receptor (EGFR)-dependent signaling pathways upon stimulation of G-protein-coupled receptors (GPCRs), it is believed to be mediated by metalloproteinases, most likely by ADAMs, because the inhibition of proHB-EGF processing blocks GPCR-induced EGFR transactivation and downstream signals, and the treatment with the metalloproteinase inhibitor batimastat can inhibit the constitutive EGFR activity (Izumi et al. 1998, Prenzel et al, 1999, Nath et al. 2001, Yan et al. 2002). The cytoplasmic domains containing SH3 binding sites in ADAMs may also be related to some signal pathways. For example, ADAM15 associates with a number of different proteins including adaptors (endophilin I, SH3PX1, and Grb2), and three Src family tyrosine kinases (Src, Lck, and Hck) through its cytoplasmic domain (Howard et al. 1999, Poghosyan et al. 2002); ADAM9, like ADAM15, binds to endophilin I and SH3PX1 (Howard et al. 1999). ADAM12 cytoplasmic domain interacts with SH3 domains of Src and Grb2 and is phosphorylated by v-Src at Tyr-901 (Suzuki et al. 2000). Furthermore, endogenous ADAM12 associates with and activates endogenous Src in differentiating C2C12 cells by a direct and specific interaction between the SH3 binding sites in the cytoplasmic tail of ADAM12 and the SH3 domain of Src, and the direct interaction between the cytoplasmic tail of ADAM12 and the Src homology 3 domain of p85alpha activates phosphatidylinositol 3-kinase in C2C12 cells (Kang Q et al. 2000, 2001). The cytoplasmic tail of ADAM12 can also ineract with alpha-actinin-2, a muscle-specific actin-binding and cross-linking protein (Galliano et al. 2000, Cao et al. 2001). It was reported that PKC delta binds *in vivo* and *in vitro* to the cytoplasmic domain of MDC9/meltrin-gamma/ADAM9, regulating the TPA-induced,

ADAM9-mediated shedding of HB-EGF (Izumi et al. 1998), and that MDC9 is phosphorylated in cells upon PMA treatment (Roghani et al. 1999). In addition, mitotic arrest deficient 2 (MAD2), which is a component of the spindle assembly (or mitotic) checkpoint mechanism, as a binding partner of the ADAM17 cytoplasmic domain, and a MAD2-related protein, MAD2beta, as a binding partner of the MDC9 cytoplasmic domain were identified (Nelson et al. 1999). SH3 binding sites of ADAM19 cytoplasmic tail was shown to specifically interact with Arg, an oncoprotein, binding protein 1 (ArgBP1), beta-subunit of Coatomer protein (beta-cop), ubiquitin and another unknown protein by a yeast two-hybrid screening (Huang et al. 2002).

3. Results

3.1 The Journal of Biological Chemistry, Vol. 277, No 28, Issue of July 12, 2002, pp 25583-25591

Intracellular Activation of Human Adamalysin 19 (hADAM19) by Furin via two consecutive alternative recognition sites

Tiebang Kang‡, Yun-Ge Zhao‡, Duanqing Pei§, Joseph F. Sucic†, and Qing-Xiang Amy Sang‡

‡Department of Chemistry and Biochemistry and Institute of Molecular Biophysics, Florida State University, Tallahassee, Florida 32306-4390, USA;

§Department of Pharmacology, University of Minnesota, Minneapolis, Minnesota 55455, USA;

†Biology Department, University of Michigan-Flint, Flint, Michigan 48502-1950, USA

THE JOURNAL OF BIOLOGICAL CHEMISTRY
Vol. 277, No. 28, Issue of July 12, pp. 25583–25591, 2002

Printed in U.S.A.

Intracellular Activation of Human Adamalysin 19/Disintegrin and Metalloproteinase 19 by Furin Occurs via One of the Two Consecutive Recognition Sites*

Received for publication, April 12, 2002, and in revised form, April 29, 2002
Published, JBC Papers in Press, May 2, 2002, DOI 10.1074/jbc.M203532200

Tiebang Kang‡, Yun-Ge Zhao‡, Duanqing Pei§, Joseph F. Sucic¶, and Qing-Xiang Amy Sang‡‖

From the ‡Department of Chemistry and Biochemistry and Institute of Molecular Biophysics, Florida State University, Tallahassee, Florida 32306-4390, the §Department of Pharmacology, University of Minnesota, Minneapolis, Minnesota 55455, and the ¶Biology Department, University of Michigan, Flint, Michigan 48502-1950

Adamalysin 19 (a disintegrin and metalloproteinase 19, ADAM19, or meltrin β) is a plasma membrane metalloproteinase. Human ADAM19 zymogen contains two potential furin recognition sites (RX(K/R)R), ^{196}KRPR^{200}R and ^{199}RRMK^{203}R, between its pro- and catalytic domains. Protein N-terminal sequencing revealed that the cellular mature forms of hADAM19 started at ^{204}EDLNSMK, demonstrating that the preferred furin cleavage site was the ^{200}RMK^{203}R ↓ ^{204}EDLN. Those mature forms were catalytically active. Both Pittsburgh mutant of α_1-proteinase inhibitor and dec-Arg-Val-Lys-Arg-chloromethyl ketone, two specific furin inhibitors, blocked the activation of hADAM19. Activation of hADAM19 was also blocked by brefeldin A, which inhibits protein trafficking from the endoplasmic reticulum to the Golgi, or A23187, a calcium ionophore known to inhibit the autoactivation of furin. When ^{202}KR were mutated to AA, the proenzyme was also activated, suggesting that ^{197}RPRR is an alternative activation site. Furthermore, only pro-forms of hADAM19 were detected in the ^{199}RR to AA mutant, which abolished both furin recognition sites. Moreover, the zymogens were not converted into their active forms in two furin-deficient mammalian cell lines; co-expression of hADAM19 and furin in these two cell lines restored zymogen activation. Finally, co-localization between furin and hADAM19 was identified in the endoplasmic reticulum-Golgi complex and/or the trans-Golgi network. This report is the first thorough investigation of the intracellular activation of adamalysin 19, demonstrating that furin activated pro-hADAM19 in the secretory pathway via one of the two consecutive furin recognition sites.

The adamalysin, ADAM[1] (for a disintegrin and metalloprotease), or metalloprotease/disintegrin/cysteine-rich family includes proteins containing disintegrin- and metalloprotease-like domains. These proteinases are involved in diverse processes, such as development, cell-cell interaction, and protein ectodomain shedding (1–5). For example, ADAM10/kuzbanian (KUZ) and ADAM17/tumor necrosis factor-α convertase play key roles in the processing of both Notch1 receptor, which is critical in development, and amyloid precursor protein, which is related to the pathogenesis of Alzheimer's disease (3, 4, 6). Six different ADAMs, ADAM2, -9, -12, -15, -23, and -28, are able to interact with integrins such as $\alpha_6\beta_1$, $\alpha_v\beta_3$, $\alpha_9\beta_1$, $\alpha_v\beta_5$, $\alpha_5\beta_1$, and $\alpha_4\beta_1$, regulating cell-cell interactions in normal and pathological processes (7, 8). In the prodomain of ADAMs, there is a cysteine switch sequence similar to the motif found in matrix metalloproteases (MMPs) (9, 10), keeping ADAMs in latent forms (2, 3, 11, 12). There are one or more furin cleavage sites between the pro- and metalloprotease domains of almost all members of the ADAM family discovered (2, 13–15), but only several ADAM precursors, including ADAM1, -9, -12, -15, and -17 and ADAMTS1, -4, and -12, have been shown to be activated by furin or furin-like proprotein convertases (16–23).

Adamalysin 19/ADAM19, a type 1 membrane protein containing an intact zinc-binding site in its metalloprotease domain, was cloned from mice (24, 25) and humans (26, 27). Human adamalysin 19 was recently demonstrated to be an active metalloproteinase through its cleavage of α_2-macroglobulin (α_2-M) *in vitro* (27). The endopeptidase activity of adamalysin 19 was blocked by specific antibodies against its catalytic and disintegrin domain peptides (28). Mouse ADAM19 cleaved intracellular neuregulin, a member of the epidermal growth factor (EGF) family *in vivo* (29). Human ADAM19 and its mouse homolog are highly similar, sharing 80.6% identity in nucleotide sequences and 84.1% identity in amino acid sequences (24, 27). Among its many roles, hADAM19 may be important in osteoblast differentiation (24), as a marker for the differentiation and characterization of dendritic cells, in the distinction between macrophages and dendritic cells (26), and in the intracellular processing of neuregulin (29). ADAM19 is synthesized as a zymogen, and its mechanism of activation has not been thoroughly investigated.

* This work was supported in part by National Institutes of Health Grant CA78646; by Department of Defense United States Army Medical Research Acquisition Activity Grant DAMD17-02-1-0238; by American Cancer Society, Florida Division Grant F01FSU-1; and by a grant from the Florida State University Research Foundation (to Q.-X. A. S.), as well as by National Institutes of Health Grant CA76308 (to D. P.). The costs of publication of this article were defrayed in part by the payment of page charges. This article must therefore be hereby marked "*advertisement*" in accordance with 18 U.S.C. Section 1734 solely to indicate this fact.

‖ To whom correspondence should be addressed: Dept. of Chemistry and Biochemistry, 203 DLC, Chemistry Research Bldg., Rm. 203, Florida State University, Tallahassee, FL 32306-4390. Tel.: 850-644-8683; Fax: 850-644-8281; E-mail: sang@chem.fsu.edu.

[1] The abbreviations used are: ADAM, a disintegrin and metalloproteinase; ADAMTS, ADAM with thrombospondin-like motifs; α_2-M, α_2-macroglobulin; BACE, β-amyloid-converting enzyme; BFA, brefeldin A; decRVKR-CMK, dec-Arg-Val-Lys-Arg-chloromethyl ketone; DMEM, Dulbecco's modified Eagle's medium; EGF, epidermal growth factor; ER, endoplasmic reticulum; FBS, fetal bovine serum; MDCK, Madin-Darby canine kidney; MMP, matrix metalloproteinase; MT-MMP, membrane-type MMP; pAT, α_1-antitrypsin or α_1-proteinase inhibitor; α_1-PI, α_1-proteinase inhibitor; pATp, Pittsburgh mutant of α_1-antitrypsin/proteinase inhibitor; PACE4, paired basic amino acid-converting enzyme 4; PBS, phosphate-buffered saline; PC, proprotein convertase; 7.P15 cell, furin-deficient monkey kidney COS-7 strain cell; RIPA, radioimmune precipitation buffer; RPE.40 cell, furin-deficient Chinese hamster ovary-K1 strain cell; TGN, trans-Golgi network.

The proprotein convertases (PCs) are a large family of serine proteinases that recognize dibasic or R*X*(K/R)R motifs and cleave the peptide bond on the carboxyl side (30–32). As a major proprotein convertase, furin is concentrated in the trans-Golgi network (TGN) and cycles between this compartment and the cell surface through the endocytic pathway. The autoactivation and intracellular trafficking of furin are well characterized. Numerous studies have shown that furin activates a large number of proproteins in multiple compartments (30–32). For instance, furin has been demonstrated to mediate the activation of proenzymes, such as β-amyloid-converting enzyme (BACE), some matrix metalloproteinases (MMPs), including MMP-11, -14, -16, and -24, and some ADAMs, including ADAM1, -9, -12, -15, and -17 and ADAMTS1, -4, and -12 (16–23, 30, 31, 33–40). However, the molecular mechanism and pathway by which the cells regulate the potentially important interactions between these proenzymes and the proprotein convertase in cells are not fully understood. In this report, we present evidence that furin is responsible for the activation of hADAM19 and this activation can occur via one of the two consecutive recognition sites and that furin is co-localized with the substrate in the ER-Golgi complex and/or TGN.

EXPERIMENTAL PROCEDURES

Chemicals, Cell Lines, Cell Culture, and Immunological Reagents—All common laboratory chemicals, proteinase inhibitors, brefeldin A (BFA), anti-FLAG-M2 monoclonal antibody, and its agarose conjugates were purchased from Sigma. Anti-furin antibodies were from Affinity Bioreagents, Inc.(Golden, CO). Protein A/G PLUS agarose was from Santa Cruz Biotechnology, Inc. (Santa Cruz, CA). The CMK-based furin inhibitor dec-Arg-Val-Lys-Arg-chloromethyl ketone (decRVKR-CMK); a calcium ionophore, A23187; and a matrix metalloproteinase inhibitor, ilomastat (GM6001), were from BACHEM (Philadelphia, PA). Restriction enzymes were from Promega or Invitrogen. COS1, Madin-Darby canine kidney (MDCK), and derivative cells were maintained as described (40–43). The furin-deficient Chinese hamster ovary-K1 strain RPE.40 and furin-deficient COS-7 cell strain 7.P15 were cultured as described (44). Dulbecco's modified Eagle's medium (DMEM), fetal bovine serum (FBS), penicillin G, and streptomycin were from Invitrogen. α_2-M was from Roche Molecular Biochemicals. Goat anti-mouse conjugated with fluorescein isothiocyanate and goat anti-rabbit-conjugated rhodamine red were from Jackson Immunoresearch Laboratory, Inc. (West Grove, PA). Rabbit polyclonal hADAM19 antibodies pAb361 (anti-metalloproteinase domain) and pAb362 (anti-disintegrin domain) were generated by our laboratory as reported (28).

PCR Primers, Mutagenesis, and Expression Constructs—pCR3.1uni-ADAM19 wild type and mutants with or without the FLAG tag were generated by high fidelity polymerase chain reaction with *Pfu* polymerase (Stratagene) as described (40–43). The primer sequences for wild type ADAM19 were 5′-ACC ATG CCA GGG GGC GCA GGC GCC-3′ (forward primer) and 5′-GAT TTT CGA GCT AAT CAT CCC TCC-3′ (reverse primer). For deletion from the transmembrane domain to the cytoplasmic domain, sequences were 5′-ACC ATG CCA GGG GGC GCA GGC GCC-3′ (forward primer) and 5′-AGG ACC CAC ACT CTC AGG GGG-3′ (reverse primer). For ^{196}KR to AA mutant, sequences were 5′-CAG ACC AAG **GCG GCA** CCT CGC AGG-3′ (forward primer) and 5′-CCT GCG AGG **TGC CGC** CTT GGT CTG-3′ (reverse primer). For ^{199}RR to AA mutant, sequences were 5′-G AAG CGA CCT **GCC GCG** ATG AAA AGG-3′ (forward primer) and 5′-CCT TTT CAT **CGC GGC** AGG TCG CTT C-3′ (reverse primer). For ^{202}KR to AA mutant, sequences were 5′-CGC AGG ATG **GCA GCG** GAA GAT TTA AAC-3′ (forward primer) and 5′-GTT TAA ATC TTC **CGC TGC** CAT CCT GCG-3′ (reverse primer). Expression constructs for the wild type full-length form and the truncation form were named F46 and D52, respectively. The ^{196}KR to AA, ^{199}RR to AA, and ^{202}KR to AA mutants of full-length and truncation forms were called ^{196}RA-F, ^{196}RA-D, ^{199}RA-F, ^{199}RA-D, ^{202}RA-F, ^{202}RA-D, respectively. All constructs were confirmed by DNA sequencing. The expression vectors for furin and its soluble form, paired basic amino acid-converting enzyme 4 (PACE4), α_1-PI (pAT), and Pittsburgh mutant of α_1-PI (pATp) were constructed as previously described (37).

DNA Transfection and Generation of Stable hADAM19 Expression Cell Lines—LipofectAMINE 2000-mediated DNA transfections into MDCK cells were performed following the instructions provided by Invitrogen. Stable lines were selected in the presence of G418 (400 μg/ml) and screened by Western blotting as described (40–42).

Western Blotting—The experiments were carried out as described previously (40, 41). Briefly, cells were grown to 80% confluence and were treated as indicated. After centrifugation at 14,000 × *g* for 15 min at 4 °C to clear any debris, the serum-free media were prepared for SDS-PAGE. The cells were lysed with RIPA (50 mM Tris, pH 7.5, 150 mM NaCl, 0.25% sodium deoxycholate, 0.1% Nonidet P-40, 1 mM phenylmethylsulfonyl fluoride, 2.5 μM GM6001, 10 μg/ml aprotinin, 10 μg/ml E64, and 10 μg/ml pepstatin A) for 15 min in ice. The supernatant was collected after centrifugation at 14,000 × *g* for 20 min at 4 °C. After electrophoresis, the proteins were transferred onto nitrocellulose membranes and probed with anti-FLAG-M2 or anti-hADAM19 and developed as described (40, 41).

Purification of Soluble hADAM19 and Protein N-terminal Sequencing—All proteins were purified on anti-FLAG-M2 affinity columns as described (42, 43). Briefly, cells stably expressing wild type soluble hADAM19 (D52-5) or ^{199}RR to AA mutant (^{199}RA-D-6) were grown to 100% confluence, then washed with PBS twice and incubated for 48 h in serum-free medium containing GM6001 (to prevent the degradation of hADAM19). The conditioned media were collected, centrifuged to clear debris, and loaded onto an anti-M2 immuno-affinity column (1 ml of resuspended agarose) prewashed with Tris-buffered saline. The bound materials were extensively washed with Tris-buffered saline, eluted with FLAG peptides, and collected in 200-μl fractions. The fractions were analyzed by Western blot using anti-hADAM19 antibodies or anti-FLAG-M2. The fraction containing the highest hADAM19 protein concentration was prepared for protein N-terminal sequencing. After separation by SDS-PAGE, the samples were transferred to a polyvinylidene difluoride membrane and stained with Coomassie Blue R-250. After destaining, the hADAM19 bands were excised and sent to the Bioanalytical Core Facility at the Florida State University for N-terminal amino acid sequencing.

α_2-M Trapping Assay to Determine Endopeptidase Activity of hADAM19 Species—The detailed experimental procedure was previously reported (27, 28). Briefly, 10 μl of the fraction containing purified soluble hADAM19 was mixed with 24 μl of α_2-M (0.2 unit/ml), adjusted to a total volume of 100 μl by adding HEPES buffer (50 mM HEPES, pH 7.5, 200 mM NaCl, 10 mM $CaCl_2$, 25 μM $ZnCl_2$, 0.05% Brij-35), and incubated at 37 °C for 1–5 days. A 20-μl aliquot of the mixture was removed daily, put into 2× SDS-PAGE sample buffer, and boiled. Following SDS-PAGE, the protein bands in the gels were visualized by silver staining.

Transient Transfection into COS1, RPE.40, or 7.P15 Cells—COS1, RPE.40 or 7.P15 cells were seeded in 24- or 6-well plates for 16–24 h at 80% confluence prior to transfection. The cells were then transfected with the indicated plasmids using LipofectAMINE 2000. After 6–10 h, serum-free or 5% FBS DMEM containing 2.5 μM GM6001, with or without CMK, BFA, or A23187 at indicated concentrations, were added for another 24 h. The conditioned media and cell lysates were analyzed by Western blotting. For co-transfection experiments in these cells, the indicated plasmid was transfected alone as a control and then co-transfected with expression plasmids directing the production of furin, PACE4, pAT, pATp, furin and pAT, or furin and pATp. After 6–10 h, serum-free or 5% FBS DMEM containing GM6001 (2.5 μM) was added to the transfected cells for 16–24 h. Then, the conditioned media and cell lysates were analyzed by Western blotting as described above.

Glycosylation Analysis—N-Glycosylation *in vitro* was investigated by endoglycosidase F treatment as described previously (40, 41). Briefly, transfected cells were grown to 80% confluence and incubated in serum-free medium for 24 h. The conditioned media were then collected, and the cells were lysed with RIPA. After centrifugation, the conditioned media or the supernatant from RIPA were treated with glycosidase F (5 units, Roche Molecular Biochemicals) for 20 h at 37 °C and analyzed by Western blotting.

Confocal Microscopy—The procedures have been described in detail previously (38, 40). Briefly, MDCK cells expressing hADAM19 wild type or ^{199}RA mutant were grown on coverslips in six-well plates with or without treatment with CMK, BFA, or A23187. After fixing with Lina's fixation buffer for 30 min, the cells were permeabilized with buffer A (0.3% Triton X-100, 1% neutral detergent solution, 1% bovine serum albumin, and 0.01% NaN_3 in PBS) for 1 h and incubated for 3 h with anti-furin and anti-FLAG-M2 (1:100 dilution in buffer A) for double staining. After washing with PBS three times, secondary antibodies conjugated with either fluorescein isothiocyanate or rhodamine red were added to the cells for 1 h, followed by four washes with PBS. Confocal microscopy experiments were performed at the Biological Science Imaging Resource Facility at Florida State University.

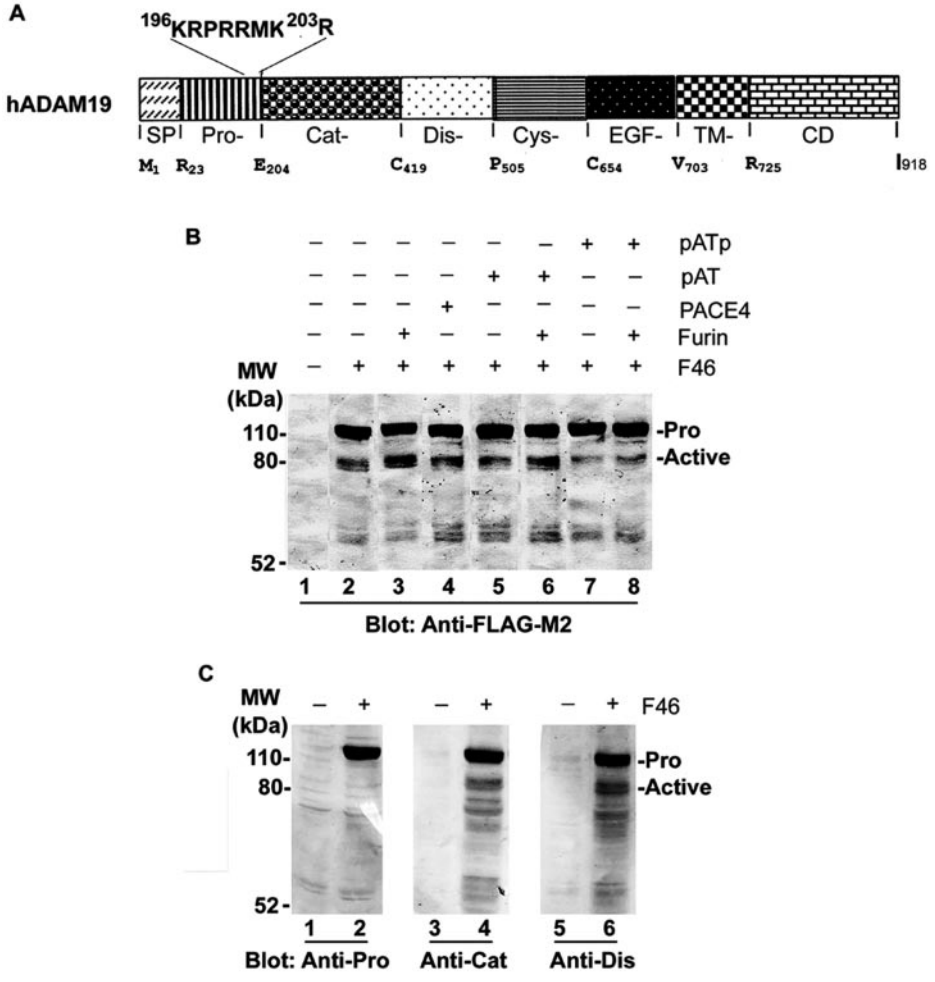

FIG. 1. **The prodomain removal of hADAM19 by furin.** *A*, a schematic diagram of the hADAM19 domain structure. The furin recognition sequence is shown *above* the border between the pro- and catalytic domains. *SP*, signal peptide; *Pro-*, prodomain; *Cat-*, catalytic domain; *Dis-*, disintegrin domain; *Cys-*, cysteine-rich domain; *EGF-*, EGF-like domain; *TM*, transmembrane domain; *CD*, cytoplasmic domain. *B*, detection of hADAM19 by Western blotting with anti-FLAG-M2 monoclonal antibody. Cell lysates from COS1 cells transfected with the blank vector (*lane 1*), pCR3.1-hADAM19 (F46) alone (*lane 2*), or co-transfected with plasmid encoding furin (*lane 3*), PACE4 (*lane 4*), pAT (*lane 5*), pAT and furin (*lane 6*), pATp (*lane 7*), or pATp and furin (*lane 8*). The pro- and active forms of hADAM19 are indicated. *C*, characterization of hADAM19 using polyclonal antibodies against different domains of hADAM19. Cell lysates from *lanes 1* and *2* in *B* were analyzed by Western blotting with the following hADAM19 polyclonal antibodies: anti-prodomain (*Pro*) (*lanes 1* and *2*), anti-catalytic domain (*Cat*) (*lanes 3* and *4*), or anti-disintegrin domain (*Dis*) (*lanes 5* and *6*).

RESULTS

Removal of the hADAM19 Prodomain Is Dependent on Furin Activity—The sequence of hADAM19 contains two potential furin recognition sites (R*X*(K/R)R), ^{196}KRPRRMK^{203}R, between its pro- and catalytic domains (Fig. 1*A*). To ascertain the role of furin in the cleaving of the hADAM19 prodomain, wild type hADAM19 (F46) with a C-terminal FLAG tag was transfected into COS1 cells alone or co-transfected with furin, PACE4, α_1-proteinase inhibitor (pAT), both furin and pAT, Pittsburgh mutant of α_1-proteinase inhibitor (pATp, a specific inhibitor of furin) (37, 45), or both furin and pATp. As shown in Fig. 1*B*, active hADAM19 forms were increased by the introduction of furin, but not PACE4. Furthermore, pATp blocked the processing of hADAM19; furin could not restore this processing when cells were co-transfected with furin and pATp (*lane 8*). pAT had little effect on endogenous or furin-induced processing of hADAM19 (*lanes 2*, *3*, *5*, and *6*). Because pATp did not completely block the hADAM19 processing, the low levels of endogenous processing may also be meditated by other proprotein convertases in addition to furin (*lanes 7* and *8*).

Interestingly, both the pro- and active forms of hADAM19 were doublets. These doublets may be differentially glycosylated forms. According to protein sequence analyses, hADAM19 has five potential glycosylation sites (27). Indeed, endoglycosidase F converted the doublets into a single pro- or active form, respectively (data not shown). To verify that the active hADAM19 lacks a prodomain, hADAM19 antibodies against the pro-, catalytic, or disintegrin domains (28) were used to probe the proteins in the cell lysates. The results in Fig. 1*C* clearly showed that the processed 80-kDa hADAM19 came from the removal of its prodomain because it was not recognized by the antibody against the prodomain peptide; however, it was detected with antibodies against its catalytic and disintegrin domains, respectively. These data showed that furin activity played a major role for the intracellular removal of hADAM19 prodomain.

To further demonstrate a direct role for furin in the activation of the hADAM19 zymogen, COS1 cells transfected with wild type hADAM19 (F46) were incubated with dec-Arg-Val-Lys-Arg-CMK (decRVKR-CMK), a widely used inhibitor of furin (17, 38, 40, 46, 47). As shown in Fig. 2*A*, decRVKR-CMK blocked the activation of hADAM19 in a dose-dependent manner. Because furin is mainly localized in TGN and the autoactivation of furin is calcium-dependent (48), we investigated whether hADAM19 activation occurred in the trans-Golgi network and required calcium. COS1 cells transfected with wild type hADAM19 were treated with BFA, which blocks protein trafficking from the ER to the Golgi apparatus (48, 49), or A23187, a calcium ionophore known to inhibit the maturation of furin (48). As shown in Fig. 2*B*, only the pro-forms of hADAM19 were detected upon treatment with either BFA or A23187. These results are consistent with furin-mediated activation of hADAM19.

Deletion of the Transmembrane Domain and the Cytoplasmic Tail of hADAM19 Does Not Alter the Processing of the Prodomain by Furin—To isolate soluble hADAM19 protein for enzyme activity assays, a construct encoding the extracellular domain (ectodomain) of hADAM19 containing a C-terminal FLAG tag was generated; this construct was called D52 and lacked the transmembrane domain and cytoplasmic domain

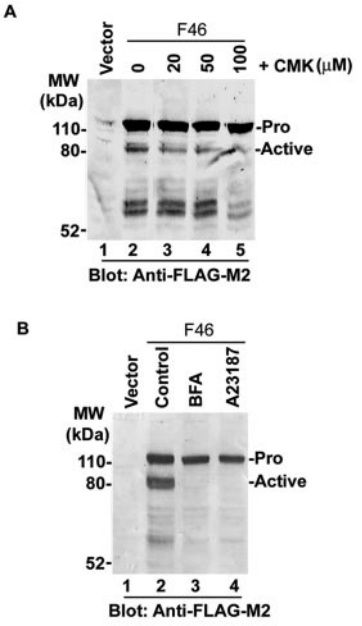

FIG. 2. **Blocking hADAM19 processing with CMK, BFA, or A23187.** *A*, dose-dependent inhibition of hADAM19 processing by decRVKR-CMK. COS1 cells transfected with the blank vector (*lane 1*) or pCR3.1hADAM19 (F46, *lanes 2–5*) were grown in 24-well plates with 0.1% methanol (v/v) (*lanes 1* and *2*) or CMK at 20 μM (*lane 3*), 50 μM (*lane 4*), or 100 μM (*lane 5*) for 24 h. The cell lysates were analyzed by Western blotting with anti-FLAG-M2. *B*, prevention of the hADAM19 prodomain removal by BFA and A23187. COS1 cells were transfected with the blank vector (*lane 1*) or F46 (*lanes 2–4*). Cells were grown in 24-well plates without (*lanes 1* and *2*) or with either 10 μg/ml BFA (*lane 3*) or 0.5 μM A23187 (*lane 4*) for 24 h. The cell lysates were analyzed as in *A*.

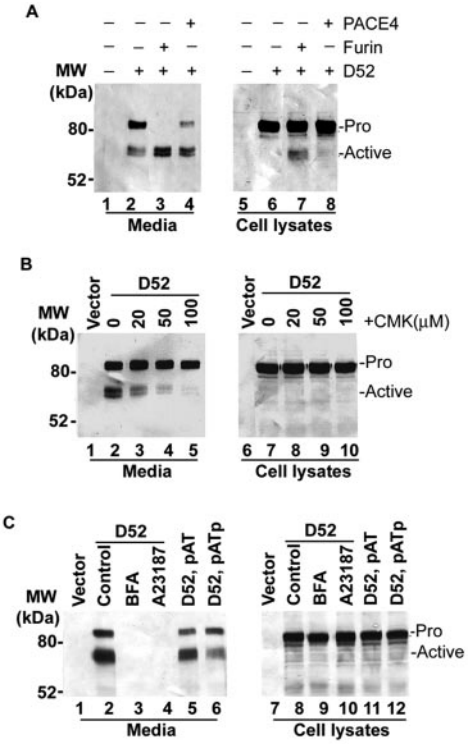

FIG. 3. **Activation of the ectodomain of hADAM19.** *A*, enhancement of the processing of soluble hADAM19 by furin. COS1 cells were transfected with the blank vector (*lanes 1* and *5*), or vector expressing soluble hADAM19 (D52) alone (*lanes 2* and *6*), or co-expressing with furin (*lanes 3* and *7*), or with PACE4 (*lanes 4* and *8*). Both conditioned media and cell lysates (*lanes 5–8*) were analyzed by Western blotting with anti-FLAG-M2. *B*, dose-dependent inhibition of the processing of soluble hADAM19 by CMK. The conditioned media (*lanes 1–5*) and cell lysates (*lanes 6–10*) were from COS1 cells transfected with the blank vector (*lanes 1* and *6*) or D52 (*lanes 2–5* and *7–10*). Cells were grown in 24-well plates with 0.1% methanol (v/v) (*lanes 1*, *2*, *6*, and *7*) or CMK at 20 μM (*lanes 3* and *8*), 50 μM (*lanes 4* and *9*), and 100 μM (*lanes 5* and *10*) for 12–16 h followed by incubation in serum-free media for 24 h. Samples were analyzed by Western blotting as in *A*. *C*, processing of soluble hADAM19 in the secretory pathway. COS1 cells were grown in 24-well plates overnight and then transfected with the blank vector (*lanes 1* and *7*) or D52 alone (*lanes 2–4* and *8–10*), or co-transfected with plasmids encoding either pAT (*lanes 5* and *11*) or pATp (*lanes 6* and *12*). The next day, cells were treated with either 10 μg/ml BFA (*lanes 3* and *9*) or 0.5 μM A23187 (*lanes 4* and *10*) in serum-free medium for 24 h. The conditioned media (*lanes 1–6*) or cell lysates (*lanes 7–12*) were analyzed as in *A*.

(Fig. 4*A*). This hADAM19 ectodomain construct was transfected into COS1 cells. As shown in Fig. 3*A*, only the active forms of soluble hADAM19 were detected in the media from COS1 cells co-expressing the hADAM19 ectodomain and furin. Both pro- and active forms were detected in the media from the cells co-transfected with PACE4 or transfected with the ectodomain construct alone. Additionally, the active forms were detected in the cell lysates only when cells were co-transfected with furin (Fig. 3*A*, *lanes 5–8*).

A dose-dependent inhibition of soluble hADAM19 activation by decRVKR-CMK was observed (Fig. 3*B*). However, there was no significant effect of decRVKR-CMK on the intracellular levels of hADAM19. Furthermore, there was no secretion of soluble hADAM19 in the transfected cells treated with either BFA or A23187 (Fig. 3*C*). Also, pATp dramatically decreased the amount of active forms in the medium when it was expressed in COS1 cells, but pAT failed to do so (Fig. 3*C*). Once again, no significant differences were seen in response to these treatments in the cell lysates (Fig. 3*C*). These results show that the soluble forms of hADAM19 were processed in the same manner as the full-length form and are consistent with furin-mediated activation of hADAM19.

There Are Two Alternative Furin Recognition Sites between the Pro- and Catalytic Domain of hADAM19—Upon the examination of the hADAM19 protein sequence, two consecutive furin recognition sites (R*X*(K/R)R), ^{196}KRPR^{200}R and ^{199}RRMK^{203}R, were found (Fig. 1*A*). We hypothesized that these two furin recognition sites are alternatively used for the intracellular activation of pro-ADAM19 by furin. To test this hypothesis, three mutants were generated in full-length and ectodomain hADAM19, which converted the ^{196}KR, ^{199}RR, and ^{202}KR into AA, respectively. These were named as ^{196}RA-F, ^{196}RA-D, ^{199}RA-F, ^{199}RA-D, ^{202}RA-F, and ^{202}RA-D, respectively, indicating that one (^{196}RA-F, ^{196}RA-D, ^{202}RA-F, or ^{202}RA-D) or no (^{199}RA) furin recognition site existed in the hADAM19 mutants (Fig. 4*A*).

All of the plasmids were transfected into COS1 cells to compare the levels of activated hADAM19 for the wild type and RA mutants in both the full-length (RA-F) and ectodomain forms (RA-D). As shown in Fig. 4 (*B* and *C*), no active forms of ^{199}RA mutants were detected as a result of the absence of a furin cleavage motif, whereas almost equivalent amounts of the active forms of the ^{196}RA and ^{202}RA mutants were detected. The wild type, full-length hADAM19 (Fig. 4*B*) and ectodomain form (Fig. 4*C*) were studied in parallel with the mutants. In addition, the protein levels of hADAM19 were almost equal among the cell lysates from these transfectants (Fig. 4, *B* and *C*). These results strongly supported the hypothesis that processing of the prodomain of hADAM19 was dependent on the presence of either one of the two consecutive furin recognition sites between the pro- and catalytic domains.

To further confirm that furin processed hADAM19 via one of the two alternative furin recognition sites, samples of the media from the four cell lines in Fig. 4*C* were incubated with the medium containing soluble furin, which was obtained from the

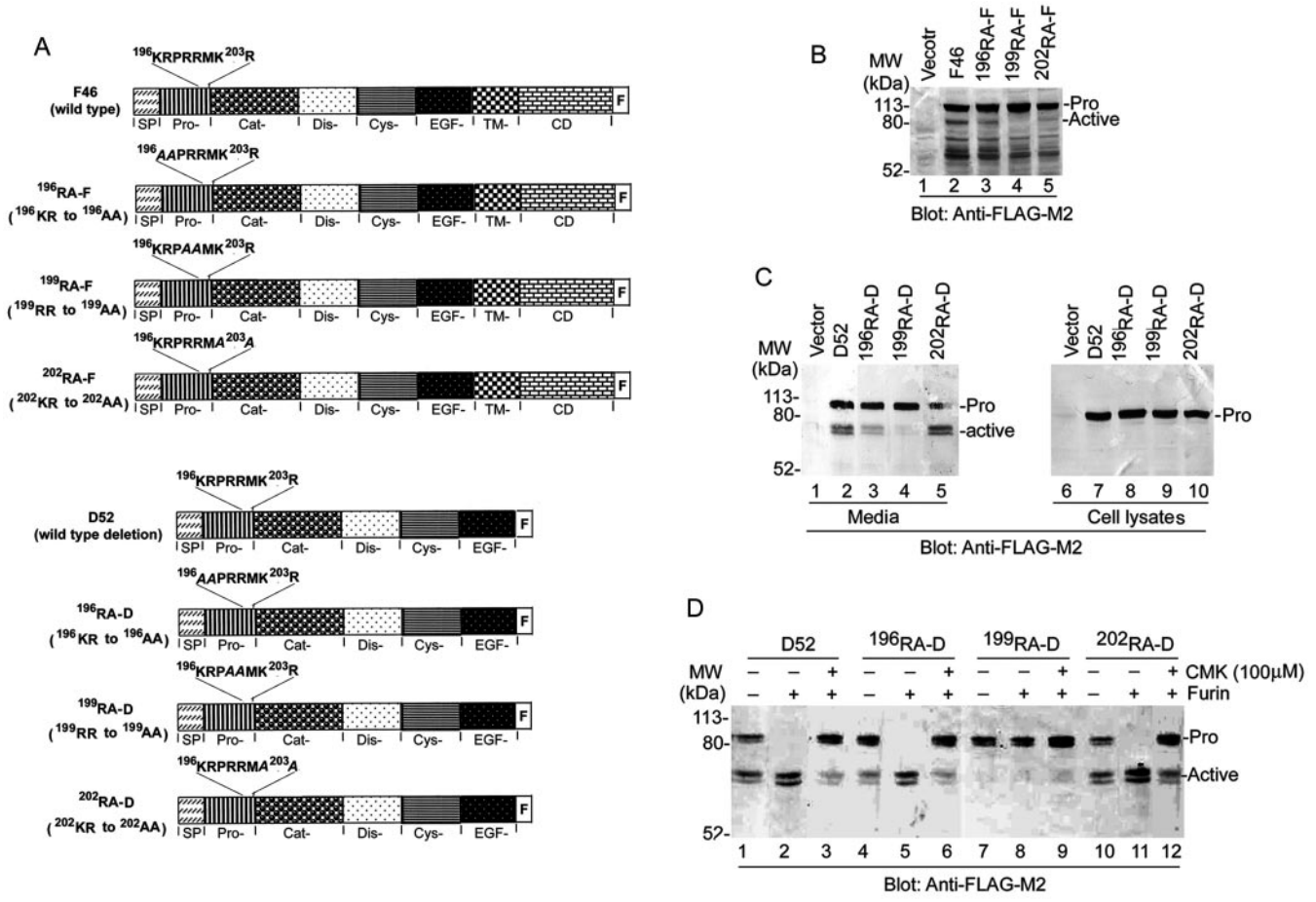

FIG. 4. **Requirement of furin motifs between the pro- and catalytic domains for the activation of hADAM19.** *A*, a schematic illustration for the wild type expression vector pCR3.1hADAM19 and its mutant constructs. All the constructs have a C-terminal FLAG tag. *SP*, signal peptide; *Pro-*, prodomain; *Cat-*, catalytic domain; *Dis-*, disintegrin domain; *Cys-*, cysteine-rich domain; *EGF-*, EGF-like domain; *TM*, transmembrane domain; *CD*, cytoplasmic domain; *F*, FLAG tag. *B*, processing of hADAM19 in the ^{199}RR to AA mutant is abolished. COS1 cells were transfected with the blank vector (*lane 1*), F46 (*lane 2*), ^{196}RA-F (*lane 3*), ^{199}RA-F (*lane 4*), or ^{202}RA-F (*lane 5*), and grown in 24-well plates for 24–36 h. The cells were lysed with RIPA followed by SDS-PAGE and Western blotting with anti-FLAG-M2. *C*, inhibition of the processing of the hADAM19 ectodomain in the ^{199}RR to AA mutant. The conditioned media (*lanes 1–5*) and cell lysates (*lanes 6–10*) were from COS1 cells transfected with the blank vector (*lanes 1* and *6*), D52 (*lanes 2* and *7*), ^{196}RA-D (*lanes 3* and *8*), ^{199}RA-D (*lanes 4* and *9*), or ^{202}RA-D (*lanes 5* and *10*) overnight, followed by incubation in serum-free medium for 24 h. The samples were analyzed by Western blotting with anti-FLAG-M2. *D*, activation of the soluble hADAM19 by exogenous soluble furin. The condition media from *lanes 2–4* in *C* were mixed with equal volumes of conditioned serum-free media from COS1 cells transfected with the blank vector (*lanes 1*, *4*, *7*, and *10*) or soluble furin (*lanes 2*, *3*, *5*, *6*, *8*, *9*, *11*, and *12*). After being incubated with (*lanes 3*, *6*, *9*, and *12*) or without 50 μM CMK (*lanes 1*, *2*, *4*, *5*, *7*, *8*, *10*, and *11*) at 37 °C for 24 h, the samples were analyzed by Western blotting as in *C*.

furin-transfected COS1 cell culture. The medium from COS1 cells transfected with a blank vector was used as a negative control. As shown in Fig. 4*D*, soluble furin did not process the ^{199}RA mutant of the soluble hADAM19. However, the wild type and the mutant soluble proteins containing a furin recognition motif were cleaved by furin. This furin-mediated processing was sensitive to decRVKR-CMK inhibition, consistent with the intracellular processing results obtained earlier (Figs. 3*A* and 4*C*). These results demonstrated that furin could activate hADAM19 at both furin cleavage sites between the prodomain and the catalytic domain of the zymogen.

Removal of the Prodomain Was Required for hADAM19 to Exert Its Proteolytic Activity—In our previous reports, an *in vitro* assay was established using α_2-M to test the activity of hADAM19 (27, 28). To assess the importance of zymogen activation to the proteolytic activity of hADAM19, stable lines of wild type hADAM19 and its ^{199}RA mutants were generated in MDCK cells, in which the endogenous furin activity is high (38, 40, 50). One stable line was chosen from each group as a representative to be treated with CMK, BFA, or A23187 and to examine whether hADAM19 would display the same processing as it did in COS1 cells. As predicted, CMK, BFA, or A23187 blocked the activation of wild type hADAM19 in the stably transfected MDCK cells called F46-4 (Fig. 5*A*). MDCK cells stably expressing the full-length ^{199}RA (^{199}RA-F-9) showed no conversion of the pro-hADAM19 to its active form (Fig. 5*A*). Furthermore, as shown in Fig. 5*B*, the active forms were only detected in the medium from MDCK cells stably expressing soluble hADAM19 (D52-5). When D52-5 cells were treated with decRVKR-CMK for 24 h, the pro-forms of soluble hADAM19 were predominantly detected from the cell culture medium. There were no active forms detected in the medium from the ^{199}RA-D6 mutant cells, which were MDCK cells stably expressing soluble hADAM19 with the ^{199}RA mutation (Fig. 5*B*).

Soluble hADAM19 proteins were purified from conditioned media of D52-5 and ^{199}RA-D6 cells. The endopeptidase activity of the purified metalloproteinases was tested using an α_2-M trapping and cleaving assay. As shown in Fig. 5*C*, only the wild type proteins could complex with α_2-M and generate two cleaved products. This activity was completely blocked by EDTA. The ^{199}RA mutant proteins were inactive, likely because the prodomain containing the cysteine switch residue

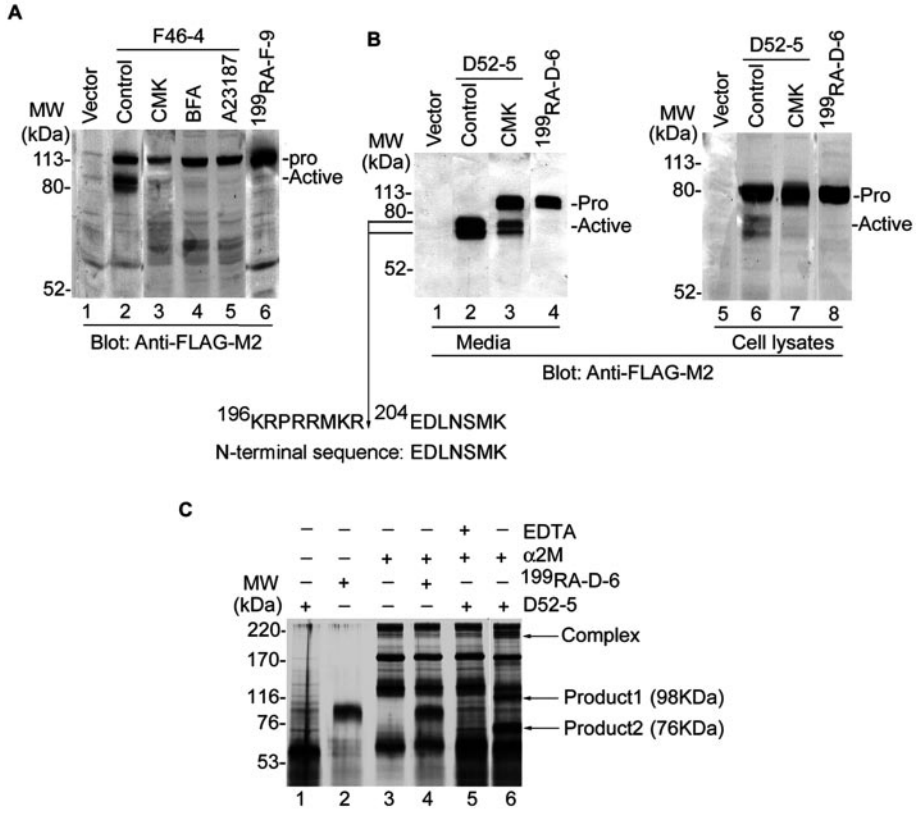

FIG. 5. **Requirement of the zymogen activation for the proteolytic activity of hADAM19.** *A*, processing of hADAM19 in stably transfected MDCK cells. MDCK cells stably expressing wild type hADAM19 (F46-4; *lanes 2–5*) or ^{199}RA mutant (^{199}RA-F-9; *lane 6*) were seeded in six-well plates at 50% confluence. The next day, cells were treated with CMK (100 μM, *lane 3*), BFA (10 μg/ml, *lane 4*), or A23187 (0.5 μM, *lane 5*). *Lanes 2* and *6* represent untreated controls. The cells were lysed with RIPA followed by analysis of Western blotting using anti-FLAG-M2. MDCK cells stably transfected with the blank vector were an additional control (*lane 1*). *B*, the requirement of furin in the processing of soluble hADAM19 in stably transfected MDCK cells. MDCK cells stably expressing soluble hADAM19 (D52-5) (*lanes 2*, *3*, *6*, and *7*) or soluble ^{199}RA mutant (^{199}RA-D-6) (*lanes 4* and *8*) were grown in 24-well plates to 100% confluence. Cells were incubated in serum-free media without (*lanes 1*, *2*, *4*, *5*, *6*, and *8*) or with CMK (100 μM, *lanes 3* and *7*) for 24 h. Both conditioned media (*lanes 1–4*) and lysates (*lanes 5–8*) were analyzed by Western blotting as in *A*. MDCK cells stably transfected with the blank vector is a control (*lane 1*). *C*, the proteolytic activity of soluble mature hADAM19. Purified soluble hADAM19 from D52-5 and ^{199}RA-D6 were incubated in reaction buffer alone (*lanes 1* and *2*) or with α_2-M in the absence (*lanes 4* and *5*) or presence of EDTA (*lane 5*) for 48 h. α_2-M in reaction buffer alone (48 h) was a control (*lane 3*). The α_2-M·hADAM19 complex and the cleavage products of α_2-M by hADAM19 are labeled on the *right*. Note that pro-soluble hADAM19 (^{199}RA-D-6) did not form the complex with α_2-M.

was not removed by furin (Fig. 5*B*). These results suggest that hADAM19 activation also obeys the cysteine-switch mechanism for zymogen latency and activation. Furthermore, N-terminal sequences of the purified hADAM19 proteins from the media revealed that the processed doublets (Fig. 5*B*, *lane 2*) had the identical N-terminal sequences of ^{204}EDLNSMK, suggesting that furin prefers to cleave hADAM19 using the recognition site of ^{200}RMK^{203}R rather than ^{197}RPR^{200}R. The doublets have different glycosylation patterns as verified by endoglycosidase F treatment experiments (data not shown). These results confirmed the prediction that hADAM19 was activated by furin through cleavage of the ^{203}R-^{204}E peptide bond at the sequence ^{199}RRMKR ↓ ^{204}EDLNSMK.

Two Furin-deficient Cell Strains (RPE.40 and 7.P15) Do Not Activate Pro-hADAM19, and the Introduction of Furin into These Cells Restores Zymogen Activation—To further confirm that furin activity was required for the intracellular activation of pro-hADAM19, the wild type of full-length and soluble forms of hADAM19 (F46 and D52) were transfected into RPE.40 cells and 7.P15 cells, two furin-deficient cell strains (44, 51). Processing of hADAM19 to its mature forms was negligible in these cell lines. However, the active forms were clearly detectable when cells co-expressed furin (data not shown). As shown in Fig. 6, there were barely detectable levels of the active forms of soluble hADAM19 in the media of the two D52-transfected cell lines. High levels of active forms were only detected in the media when the cells co-expressed furin, although PACE4 also increased the amount of active forms when it was co-expressed with D52 (Fig. 6, *A* and *B*). Curiously, the active forms were only detected in the lysates of cells co-expressing D52 and furin. These data further confirm that furin was responsible for the intracellular activation of hADAM19.

Furin Was Co-localized with hADAM19 in the ER-Golgi Complex and/or TGN—To verify that hADAM19 was a physiologically relevant substrate of furin, the cellular localization of furin and hADAM19 was examined by confocal microscopy using MDCK cells stably expressing hADAM19 (Fig. 7). Untreated cells are marked as F46-4 (control) (Fig. 7, *top panels*). Co-localization of hADAM19 and furin was clearly observed, and was consistent with ER-Golgi complex and/or TGN localizations (*top*, *middle panel*). Furthermore, hADAM19 was also seen at the edges of the plasma membrane (*right lane*, *top panel*) where furin was rare (*left lane*, *top panel*). Interestingly, a similar pattern of co-localization between the ^{199}RA mutant and furin was also observed (Fig. 7, *bottom panels*), suggesting that the co-localization was independent of the recognition sites for furin in hADAM19. To test whether the agents that block the activation of hADAM19 could prevent co-localization between furin and hADAM19 (Fig. 5*A*), the cells were treated with CMK, BFA, or A23187. None of these treatments interfered with the co-localization pattern of furin and hADAM19 (Fig. 7), suggesting that furin may be co-localized with

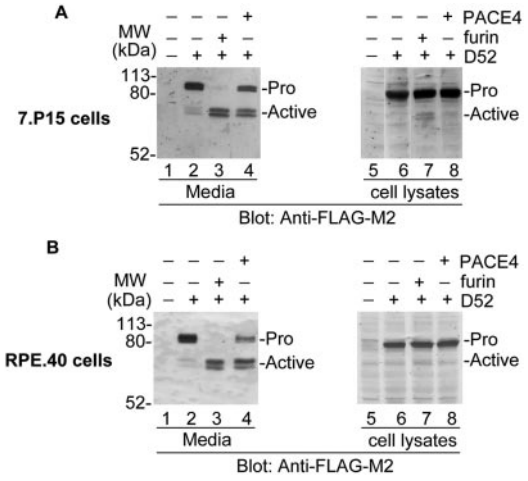

FIG. 6. **Processing the hADAM19 prodomain in furin-deficient mammalian cell lines.** *A*, hADAM19 in 7.P15 cells. 7.P15 cells were transfected with the blank vector (*lanes 1* and *5*) or D52 alone (*lanes 2* and *6*) or co-transfected with D52 and plasmids encoding furin (*lanes 3* and *7*) or PACE4 (*lanes 4* and *8*). Cells were grown in 24-well plates for 12–16 h followed by incubation in serum-free medium for 24 h. Conditioned media (*lanes 1–4*) and cell lysates (*lanes 5–8*) were analyzed by Western blotting with anti-FLAG-M2. *B*, hADAM19 in RPE.40 cells. RPE.40 cells were transfected with the blank vector (*lanes 1* and *5*) or D52 alone (*lanes 2* and *6*) or were co-transfected either D52 and plasmids encoding furin (*lanes 3* and *7*) or PACE4 (*lanes 4* and *8*). Cells were grown in 24-well plates overnight followed by incubation in serum-free media for 24 h. Conditioned media (*lanes 1–4*) and cell lysates (*lanes 5–8*) were analyzed by Western blotting as in *A*.

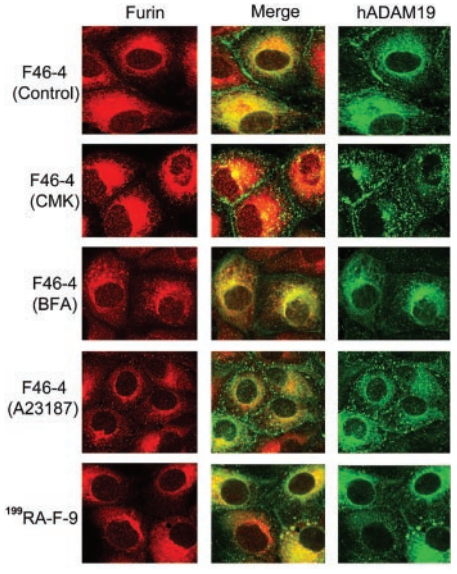

FIG. 7. **Co-localization of hADAM19 and furin.** MDCK cells stably expressing wild type hADAM19 (F46-4) or ^{199}RA mutant (^{199}RA-F-9) grown on coverslips in six-well plates were treated with nothing (control), 100 μM CMK, 10 μg/ml BFA, or 0.5 μM A23187 for 24 h. The fixed slides were stained for both hADAM19 with anti-FLAG-M2 (*right panels*) and furin with anti-furin (*left panels*). The merged pictures for both hADAM19 and furin are presented in the *middle column*. Note that hADAM19 is co-localized with furin, independent on furin motif, with neither CMK, BFA, nor A23187 altering the staining pattern.

hADAM19 in perinuclear ER-Golgi complex and/or TGN independent of the furin catalytic activity.

DISCUSSION

Proteolysis of the extracellular matrix and cell surface proteins mediated by metalloproteases, including MMPs and ADAMs, is of vital importance for tissue-remodeling processes during normal and pathological conditions, such as tissue morphogenesis, wound healing, inflammation, and tumor cell invasion and metastasis (3–7, 52, 53). Metalloproteases are synthesized as inactive proenzymes or zymogens, and their latency is maintained by a cysteine-switch residue in the propeptide domain in which the thiol group is coordinated to the active site zinc (II) (2, 9–12). To display any proteolytic activities, the prodomain located N-terminal to the catalytic domain must be removed from the zymogen in most cases. Recently, PCs, such as furin and or furin-like serine peptidases, have been recognized as very important enzymes for the zymogen activation, although various mechanisms have been proposed for the activation of pro-MMPs and pro-ADAMs. Furin or furin-like PCs mediate zymogen activation by recognizing a conserved R*X*(K/R)R motif in the boundary between pro- and catalytic domains. This motif is present in almost all ADAMs and nine MMPs (2, 13, 53). By analyzing the intracellular activation of hADAM19, we have demonstrated that both furin activity and one of the two consecutive sites in ^{197}RPRRMK^{203}R in ADAM19 are required for activation, which is dependent on calcium and proper secretory pathway trafficking. Furthermore, we have provided direct evidence that furin is co-localized with hADAM19 in ER-Golgi complex and/or TGN. This colocalization between furin and hADAM19 is independent of the furin recognition site and is resistant to a variety of treatments, such as CMK, BFA, and A23187, that inhibit furin activity, vesicular trafficking, and calcium signal, respectively. These findings are consistent with the report published recently showing that furin was co-localized with MMP16 independent of their apparent enzyme-substrate relationship (40).

Latency and Activation of ADAMs—The classic cysteine switch mechanism for pro-MMP latency and activation was originally proposed for MMPs (10) and may be applied for many MMPs discovered with the exception of MMP-3, MMP-23, and MMP-26 (41, 54–58). The activation of pro-MMP-3 by a mercurial compound was triggered by a perturbation of the conformation of the precursor rather than a direct disruption of the Cys-zinc interaction (54). A salt bridge in pro-MMP-3 might also contribute to the latency of the proenzyme (55). Organomercurial treatment failed to activate pro-MMP-26 with a unique cysteine-switch motif, P**H**^{81}CG*XX*D, and when the conserved cysteine-switch sequence, P**R**^{81}CG*XX*D, in the prodomain of pro-MMP-26 was restored by mutagenesis, the cysteine-switch activation mechanism was not induced (58).

Regarding the ADAM family members, the active ADAMs, such as ADAM1, -9, -10, -12, -15, -17, -19, -28, and ADAMTS1, -4, and -12, contain a catalytic site consensus sequence (HE*XX*H) in their metalloprotease domains (2, 11–14, 16–21, 27–29, 53, 59–61). They may also have a putative cysteine-switch residue in their prodomain to keep them inactive (9). For example, the investigation by Leochel *et al.* (11) demonstrated that the latency and activation mechanism of ADAM12 was similar to the cysteine switch model proposed for MMPs. ADAM9, -15, and -17 showed catalytic activity against their substrates only after their prodomains were removed (12, 21, 22). However, for many ADAMs, including ADAM19, no direct evidence has been provided to support the hypothesis that the Cys-zinc coordination is required for latency. For ADAM17/tumor necrosis factor-α convertase, the prodomain was not only an inhibitor of the catalytic domain, but also appeared to act like a chaperone, facilitating secretion, folding, or both of the ADAM protein (12). In this report, we have demonstrated that, after the removal of the prodomain of hADAM19 by furin, the enzyme has endopeptidase activity against α_2-M. However, furin is unable to cleave the prodomain of the ^{199}RR to AA hADAM19 mutant lacking a furin recognition site in the boundary of the pro- and catalytic domains. This mutant has no

proteolytic activity using an α_2-M trapping assay. These results demonstrate that at least one of the furin recognition sites is required for the removal of the propeptide domain by furin to activate pro-hADAM19. The detailed mechanism of pro-ADAM19 latency and activation and the role of the cysteine-switch sequence remain to be further investigated.

For the activation of ADAM zymogens, two mechanisms have been reported. One is the removal of the prodomain by autolysis, but it was shown only in ADAM28 (60). The predominant mechanism for the activation of ADAMs is mediated by furin or furin-like PCs in the secretory pathway. This mechanism has been shown in many ADAMs, including ADAM1, -9, -12, -15, -17, and -19, and ADAMTS1, -4, and -12, using N-terminal sequencing, specific inhibitors of furin, blockers of protein trafficking from ER to Golgi, exogenous soluble furin *in vitro*, furin-deficient cell lines, and mutagenesis at the furin recognition site(s) (R*X*(K/R)R) between the pro- and catalytic domain (Refs. 16–23; this report). In the present report, we provide a thorough investigation of ADAM zymogen activation mediated by furin (Figs. 1–6) and evidence that furin is co-localized with ADAMs in the ER-Golgi complex and/or TGN (Fig. 7), showing that ADAMs are similar to MMPs in these respects (38, 40).

There Are Two Consecutive Furin Recognition Sites in the Boundary of the Pro- and Catalytic Domains of hADAM19—The minimal furin recognition sequence requires basic residues at P_1 and P_4 (R*XX*R) and in some cases, at the P_1 position, an amino acid with a hydrophobic aliphatic side chain is not suitable (31). Typically, there is only one furin recognition site between the pro- and catalytic domain of the substrates of furin as found in most members of the ADAM family, seven MMPs, pro-BACE, and Notch1 receptor (2, 13–15, 30, 31, 33–40, 53, 62). In this report, we present evidence for the first time that there are two consecutive furin recognition sites, ^{197}RPR^{200}R and ^{200}RMK^{203}R, between the pro- and catalytic domain in hADAM19, which adhere to the rules for efficient cleavage by furin (31). Only pro-forms were detectable in the ^{199}RA mutant, which lacked a furin recognition site between its pro- and catalytic domain, whereas the mutants of both ^{196}RA and ^{202}RA, which possessed recognition sites, were converted into the active forms. Thus, the Arg residue at the P_4 site is required for the intracellular hADAM19 maturation mediated by furin (Figs. 4 and 5*B*). Interestingly, N-terminal sequencing of wild type mature forms (Fig. 5) confirmed that the preferred intracellular cleavage site for hADAM19 activation is the one nearer to the catalytic domain, ^{200}RMK^{203}R, as predicted before (26, 27). This motif is conserved in mice as ^{201}RMK^{204}R (24). The distal motif, ^{197}RPR^{200}R in humans, however, is replaced with ^{198}QPR^{201}R in mice, which is not efficiently cleaved by furin.

A notion that pro-hADAM19 activation by furin may be sequential, *i.e.* ^{200}R^{201}M is cleaved first followed by ^{203}R^{204}E, seems to be consistent with the partially activated soluble species seen for ^{196}RA-D compared with ^{202}RA-D data in Fig. 4*C*; however, it does not agree with the data shown in Fig. 4*B*, where it is seen that the presence of furin with the full-length ^{196}RA-F leads to more activated species than ^{202}RA-F. The delicate changes in the interactions between furin and the different mutants that have subtle structural and conformational differences might be partially responsible for the different activation levels observed. Moreover, among all the protein N-terminal sequence data of wild type hADAM19 activated species, only ^{204}EDLNSMK was found; the alternative cleavage site product of ^{201}MKRED was not detected. Most importantly, the minimal furin recognition sequence requires basic residues at P_1 and P_4 (R*XX*R) and the Arg residue at the P_4 site is required for the intracellular hADAM19 maturation mediated by furin (Figs. 4 and 5*B*). It may not be possible for furin, an endopeptidase, to effectively cleave the product of the ^{200}R-^{201}M cleavage because the ^{201}MK^{203}R-^{204}ED sequence lacks the required Arg at the P_4 site. Thus, our data suggest that the ^{203}R-^{204}E site is the predominant cleavage site and ^{200}R-^{201}M is an alternative cleavage site by furin when the predominant site is missing. This is consistent with the model proposed for wild type MT1-MMP, in which the pro-MT1-MMP is processed primarily at the ^{108}RRKR site to generate the active proteinase and the secondary site within ^{86}K*XX*RR*X*R is cleaved only when the primary ^{108}RRKR motif was mutated (39).

Notably, there are two potential consecutive furin recognition sites in other metalloproteinase zymogens, including ADAM11 (AB009675, ^{292}RLRRK^{297}R), ADAM22 (AF155382, ^{219}RPKRSK^{225}R), ADAMTS4 (AF148213, ^{206}RPRRAK^{212}R), MT2-MMP (NM_002428, ^{126}RRRRK^{131}R), and MT5-MMP (AJ010262, ^{118}RRRRNK^{224}R). The ones nearer to the catalytic domains are conserved in different species, whereas the distal ones might be acquired later during evolution. Although the significance of the two alternative recognition sites in these precursors remains poorly understood, we may speculate that the processing of these zymogens are crucial for some biological events; the zymogens may be activated by furin at a different cleavage site even if the primary site is abolished by mutation.

Significance of Furin and Its Related PC Pathways in the Processing of Precursors—Furin and its related PCs have been demonstrated as the major enzymes responsible for the maturation of many precursors, such as some ADAMs and MMPs (Refs. 16–23 and 37–40; this report). Furthermore, zymogens of BACE, a major enzyme related to Alzheimer's disease, and some growth factors and cell surface receptors, such as transforming growth factor β, insulin-like growth factor, hepatocyte growth factor receptor, and Notch1 receptor, are converted into their active forms by these PC pathways (30, 31, 33–36, 62). Thus, this activation mechanism by a PC may play key roles in many physiological and pathological events. In fact, furin knockout mice are embryonic lethal (63), and inhibition of furin results in absent or decreased invasion and tumorigenicity of human cancer cells (64, 65). The inability to activate many types of proproteins, including some pro-ADAMs and pro-MMPs, in furin null mice may contribute to the abnormal phenotypes during early development and morphogenesis in those mice. On the other hand, the design and synthesis of furin specific inhibitors may lead to a new strategy in the treatment of cancer and other diseases, such as Alzheimer's disease, in the human adult.

Acknowledgments—We thank Kim Riddle and Joe Ekman for excellent assistance in confocal microscopy at Biological Science Imaging Facility, Margaret Seavy at the Bioanalytical Facility for protein N-terminal sequencing, and Sara C. Monroe for editorial assistance with the manuscript preparation at the Florida State University. We appreciate Dr. Ping Wei at Human Genome Sciences Inc. for previous collaboration on the human ADAM19 project.

REFERENCES

1. Wolfsberg, T. G., and White, J. M. (1996) *Dev. Biol.* **180,** 389–401
2. Stone, A. L., Kroeger, M., and Sang, Q. X. (1999) *J. Protein Chem.* **18,** 447–465
3. Schlondorff, J., and Blobel, C. P. (1999) *J. Cell Sci.* **112,** 3603–3617
4. Blobel, C. P. (2000) *Curr. Opin. Cell Biol.* **12,** 606–612
5. Kheradmand, F., and Werb, Z. (2002) *Bioessays* **24,** 8–12
6. Esler, W. P., and Wolfe, M. S. (2001) *Science* **293,** 1449–1454
7. Evans, J. P. (2001) *Bioessays* **23,** 628–639
8. Bridges, L. C., Tani, P. H., Hanson, K. R. Roberts, C. M., Judkins, M. B., and Bowditch, R. D. (2002) *J. Biol. Chem.* **277,** 3784–3792
9. Grams, F., Huber, R., Kress, L. F., Moroder, L., and Bode W. (1993) *FEBS Lett.* **335,** 76–80
10. Van Wart, H. E., and Birkedal-Hansen, H. (1990) *Proc. Natl. Acad. Sci. U. S. A.* **87,** 5578–5582
11. Loechel, F., Overgaad, M. T., Oxvig, C., Albrechtsen, R., and Wewer, U. M. (1999) *J. Biol. Chem.* **274,** 13427–13433
12. Milla, M. E., Leesnitzer M. A., Moss. M. L., Clay, W. C. Carter, H. L., Miller, A. B., Su, J., Lambert, M. H., Willard, D. H., Sheeley, D. M., Kost, T. A., Burkhart, W., Moyer, M., Blackburn, R. K., Pahel, G. L., Mitchell, J. L., Hoffman, C. R., and Becherer, J. D. (1999) *J. Biol. Chem.* **274,** 30563–30570

13. Primakoff, P., and Myles, D. G. (2000) *Trends Genet.* **16,** 83–87
14. Tortorella, M. D., Burn, T. C., Pratta, M. A., Abbaszade, I., Hollis, J. M., Liu, R., Rosenfeld, S. A., Copeland, R. A., Decicco, C. P., Wynn, R., Rockwell, A., Yang, F., Duke, J. L., Solomon, K., George, H., Bruckner, R., Nagase, H., Itoh, Y., Ellis, D. M., Ross, H., Wiswall, B. H., Murphy, G., Hillman, M. C., Jr., Hollis, G. F., Newton, R. C., Magolda, R. L., Trzaskos, J. M., and Arner, E. C. (1999) *Science* **284,** 1664–1666
15. Yoshinaka, T., Nishii, K., Yamada, K., Sawada, H., Nishiwaki, E., Smith, K., Yoshino, K., Ishiguro, H., and Higashiyama, H. (2002) *Gene* (*Amst.*) **282,** 227–236
16. Cal, S., Arguees, J. M., Fernandez, P. L., and Lopez-Otin, C. (2001) *J. Biol. Chem.* **276,** 17932–17940
17. Gao, G., Westling, J., Thompson, V. P., Howell, T. D., Gottschall, P. E., and Sandy, J. D. (2002) *J. Biol. Chem.* **277,** 11034–11041
18. Kuno, K., Terashima, Y., and Matsushima, K. (1999) *J. Biol. Chem.* **274,** 18821–18826
19. Loechel, F., Gilpin, B. J., Engvall, E., Albrechtsen, R., and Wewer, U. M. (1998) *J. Biol. Chem.* **273,** 16993–16997
20. Lum, L., and Blobel, C. P. (1997) *Dev. Biol.* **191,** 131–145
21. Lum, L., Reid, M. S., and Blobel, C. P. (1998) *J. Biol. Chem.* **273,** 26236–26247
22. Roghani, M., Becherer, J. D., Moss, M. L., Atherton, R. E., Erdjument-Bromage, H., Arribas, J., Blackburn, R. K., Weskamp, G., Tempst, P., and Blobel, C. P. (1999) *J. Biol. Chem.* **274,** 3531–3540
23. Schlondorff, J., Becherer, J. D., and Blobel, C. P. (2000) *Biochem. J.* **347,** 131–138
24. Inoue, D., Reid, M., Lum, L., Kratzschmar, J., Weskamp, G., Myung, Y. M., Baron, R., and Blobel, C. P. (1998) *J. Biol. Chem.* **273,** 4180–4187
25. Kurohara, K., Masuda, Y., Nagabukuro, N., Tsuji, A., Amagasa, T., and Fujisawa-Sehara, (2000) *Biochem. Biophys. Res. Commun.* **270,** 522–527
26. Fritsche, J., Moser, M., Faust, S., Peuker, A., Buttner, R., Andreesen, R., and Kreutz, M. (2000) *Blood* **96,** 732–739
27. Wei, P., Zhao, Y.-G., Zhuang, L., Ruben, S., and Sang, Q.-X. (2001) *Biochem. Biophys. Res. Commun.* **280,** 744–755
28. Zhao, Y., Wei, P., and Sang, Q.-X. (2001) *Biochem. Biophys. Res. Commun.* **289,** 288–294
29. Shirakabe, K., Wasuda, S., Kurisaki, T., and Fujisawa-Sehara, A. (2001) *J. Biol. Chem.* **276,** 9352–9358
30. Molloy, S. S., Anderson, E. D., Jean, F., and Thomas, G. (1999) *Trends Cell Biol.* **9,** 28–35
31. Nakayama, K. (1997) *Biochem. J.* **327,** 625–635
32. Steiner, D. F. (1998) *Curr. Opin. Chem. Biol.* **848,** 45–62
33. Benjannet, S., Elagoz, A., Wickham, L., Mamarbachi, M., Munzer, J. S., Basak, A., Lazure, C., Cromlish, J. A., Sisodia, S., Chretien, M., and Seidah, N. G. (2001) *J. Biol. Chem.* **276,** 10879–10887
34. Bennett, B. D., Denis, P., Haniu, M., Teplow, D. B., Kahn, S., Louis, J. C., Citron, M., and Vassar, R. (2000) *J. Biol. Chem.* **275,** 37712–37717
35. Capell, A., Steiner, H., Willem, M., Kaiser, H., Meyer, C., Walter, J., Lammich, S., Multhaup, G., and Haass, C. (2000) *J. Biol. Chem.* **275,** 130849–130854
36. Creemers, J. W., Dominguez, D. I., Plets, E., Serneels, L., Taylor, N. A., Multhaup, G., Craessaaerts, K., Annaert, W., and De Strooper, B. (2001) *J. Biol. Chem.* **276,** 4211–4217
37. Pei, D., and Weiss, S. J. (1995) *Nature* **375,** 244–247
38. Wang, X., and Pei, D. (2001) *J. Biol. Chem.* **276,** 35953–35960
39. Yana, I., and Weiss, S. J. (2000) *Mol. Biol. Cell* **11,** 2387–2401
40. Kang, T., Nagase, H., and Pei, D. (2002) *Cancer Res.* **62,** 675–681
41. Kang, T., Yi, J., Yang, W., Wang, X., Jiang, A., and Pei, D. (2000) *FASEB J.* **14,** 2559–2568
42. Pei, D., Kang, T., and Qi, H. (2000) *J. Biol. Chem.* **275,** 33988–33997
43. Kang T, Yi, J., Guo, A., Wang, X., Overall, C. M., Jiang, W., Elde, R., Borregaard, N., and Pei, D. (2001) *J. Biol. Chem.* **276,** 21960–21968
44. Inocencio, N. M., Sucic, J. F., Moehring, J. M., Sepence, M. J., and Moehring, T. J. (1997) *J. Biol. Chem.* **272,** 1344–1348
45. Wasley, C. L., Rehemtulla, A., and Kaufman, R. J. (1993) *Curr. Opin. Biotechnol.* **3,** 560–565
46. Angliker, H., Wikstrom, P., Shaw, E., Brenner, C., and Fuller, R. S. (1993) *Biochem. J.* **293,** 75–81
47. Vey, M., Schafer, W., Berghofer, S., Klenk, H. D., and Garten, W. (1994) *J. Cell Biol.* **127,** 1829–1842
48. Fujiwara, T., Oda, T. K., Yokota, S., Takatsuki, A., and Ikehara, Y. (1988) *J. Biol. Chem.* **263,** 18545–18552
49. Hallenberger, S., Bosch, V., Angliker, H., Shaw, E., Klenk, H. D., and Garten, W. (1992) *Nature* **360,** 358–361
50. Shapiro, J., Sciaky, N., Lee, J., Bosshart, H., Angeletti, R. H., and Bonifacino, J. S. (1997) *J. Histochem. Cytochem.* **45,** 3–12
51. Bass, J., Turck, C., Rouard, M., and Steiner, D. F. (2000) *Proc. Natl. Acad. Sci. U. S. A.* **97,** 11905–11909
52. Chang, C., and Werb, Z. (2001) *Trends Cell Biol.* **11,** S37–S45
53. Vu, T. H., and Werb, Z. (2000) *Genes Dev.* **14,** 2123–2133
54. Chen, L. C., Noelken, M. E., and Nagase, H. (1993) *Biochemistry* **32,** 10289–10295
55. Galazka, G., Windsor, L. J., Birkedal-Hansen, H., and Engler, J. A. (1996) *Biochemistry* **35,** 11221–11227
56. Pei, D. (1999) *FEBS Lett.* **457,** 262–270
57. Velasco, G., Pendas, A. M., Fueyo, A., Knauper, V., Murphy, G., and Lopez-Otin, C. (1999) *J. Biol. Chem.* **274,** 4570–4576
58. Marchenko, N. D., Marchenko, G. N., and Strongin, A. Y. (2002) *J. Biol. Chem.* **277,** 18967–18972
59. Howard, L., Zhang, Y., Horrocks, M., Maciewicz, R. A., and Blobel, C. P. (2001) *FEBS Lett.* **498,** 82–86
60. Howard, L., Maciewicz, R. A., and Blobel, C. P. (2000) *Biochem. J.* **348,** 21–27
61. Lopez-Perez, E., Zhang, Y., Frank, S. J., Creemers, J., Seidah, N., and Checler, F. (2001) *J. Neurochem.* **76,** 1532–1539
62. Logeat, F., Bessia, C., Brou, C., LeBail, O., Jarrianlt, S., Seidah, N. G., and Israel, A. (1998) *Proc. Natl. Acad. Sci. U. S. A.* **95,** 8108–8112
63. Roebroek, A. J., Umans, L., Pauli, I. G., Robertson, E. J., van Leuven, F., Van de Ven, W. J., and Constam, D. B. (1998) *Development* **125,** 4863–4876
64. Bassi, D. E., De Cicco, R. L., Mahloogi, H., Zucker, S., Thomas, G., and Klei-Szanto, A. J. P. (2001) *Proc. Natl. Acad. Sci. U. S. A.* **98,** 10326–10331
65. Khatib, A.-M., Siegfried, G., Prat, A., Lius, J., Chretien, M., Metrakos, P., and Seidah, N. G. (2001) *J. Biol. Chem.* **276,** 30686–30693

3.2 The Journal of Biological Chemistry, Vol. 277, No 50, Issue of December 13, 2002, pp 48514-48522

Autolytic Processing at Glu(586)-Ser(587) within the Cysteine-rich Domain of Human Adamalysin 19/Disintegrin-metalloproteinase 19 is Necessary for its Proteolytic Activity.

Tiebang Kang†‡, Hyun I, Park†, Yewseok Suh†, Yun-Ge Zhao†, Harald Tschesche‡, and Qing-Xiang Amy Sang†

†Department of Chemistry and Biochemistry and Institute of Molecular Biophysics, Florida State University, Tallahassee, Florida 32306-4390, USA; ‡Department of Biochemistry I, Faculty of Chemistry, University Bielefeld, Bielefeld 33615, Germany.

THE JOURNAL OF BIOLOGICAL CHEMISTRY
Vol. 277, No. 50, Issue of December 13, pp. 48514–48522, 2002
Printed in U.S.A.

Autolytic Processing at Glu^{586}-Ser^{587} within the Cysteine-rich Domain of Human Adamalysin 19/Disintegrin-Metalloproteinase 19 Is Necessary for Its Proteolytic Activity*

Received for publication, September 3, 2002, and in revised form, October 15, 2002
Published, JBC Papers in Press, October 18, 2002, DOI 10.1074/jbc.M208961200

Tiebang Kang‡§, Hyun I. Park‡, Yewseok Suh‡, Yun-Ge Zhao‡, Harald Tschesche§, and Qing-Xiang Amy Sang‡¶

From the ‡Department of Chemistry and Biochemistry and Institute of Molecular Biophysics, Florida State University, Tallahassee, Florida 32306-4390 and the §Department of Biochemistry, Faculty of Chemistry, University of Bielefeld, Bielefeld 33615, Germany

We investigated the regulation of the proteolytic activity of human adamalysin 19 (a disintegrin and metalloproteinase 19, hADAM19). It was processed at Glu^{586}(P1)-Ser^{587}(P1′) site in the cysteine-rich domain as shown by protein N-terminal sequencing. This truncation was autolytic as illustrated by its R199A/R200A or E346A mutation that prevented the zymogen activation by furin or abolished the catalytic activity. Reagents that block furin-mediated activation of pro-hADAM19, decRVKR-CMK, A23187, and brefeldin A abrogated this processing. The sizes of the side chains of the P1 and P1′ residues are critical for the processing of hADAM19. The amount of processing product in the E586Q or S587A mutant with a side chain almost the same size as that in the wild type was almost equal. Conversely, very little processing was observed when the size of the side chain was changed significantly, such as in the E586A, E586G, or S587F mutants. Two mutants with presumably subtle structural distinctions from wild type hADAM19, E586D and S587T, displayed rare or little processing and had very low capacities to cleave α2-macroglobulin and a peptide substrate. Therefore, this processing is necessary for hADAM19 to exert its proteolytic activities. Moreover, a new peptide substrate, Ac-RPLE-SNAV, which is identical to the processing site sequence, was cleaved at the E-S bond by soluble hADAM19 containing the catalytic and disintegrin domains. This enzyme cleaved the substrate with K_m, k_{cat}, and k_{cat}/K_m of 2.0 mM, 2.4/min, and 1200 M^{-1} min^{-1}, respectively, using a fluorescamine assay. Preliminary studies showed that a protein kinase C activator, phorbol 12-myristate 13-acetate, promoted the cellular processing of hADAM19; however, three calmodulin antagonists, trifluoperazine, W7, and calmidazolium, impaired this cleavage, indicating complex signal pathways may be involved in the processing.

Ectodomain shedding is a process in which a wide variety of transmembrane proteins, such as growth factors and growth factor receptors, cytokines and their receptors, amyloid precursor protein (APP),[1] adhesion molecules, and enzymes, proteolytically release their extracellular domains. It is believed to play key roles in normal development, arthritis, inflammation, and tumorigenesis (1–5). Although the signal pathways regulating ectodomain shedding remain poorly understood, numerous studies have shown that structurally different proteins share common pathways (5–8). For example, phorbol 12 myristate 13-acetate (PMA), a protein kinase C (PKC) activator, is generally a potent inducer of ectodomain shedding. Other signals, such as calcium, calmodulin (CaM), tyrosine kinase, mitogen-activated protein kinase (MAPK), and phosphatase, also play roles in certain shedding processes (9–23). On the other hand, the shedding process, in most cases, is hindered by hydroxamate-based inhibitors of metalloproteinases, such as BB94, GM6001, and tumor necrosis factor-α proteinase inhibitor (TAPI) (5–8, 19, 24–26).

Inhibitor studies have shown that TIMP-3, not TIMP-1 or TIMP-2, impairs many shedding processes, indicating that the proteins comprising the a disintegrin and metalloprotease (ADAM)/adamalysin/metalloprotease, disintegrin, cysteine-rich (MDC) family, rather than the matrix metalloproteinase (MMP) family, are the predominant sheddases (27–30). Indeed, five ADAMs have been implicated in shedding processes so far. ADAM17/TACE, a major sheddase, has a role in the shedding of tumor necrosis factor-α (TNF-α), transforming growth factor-α (TGF-α), L-selectin, both TNF receptors, interleukin-1 receptor II, HER4, Notch, and TNF-related activation-induced cytokine (TRANCE). It also acts as a PMA-induced APP α-secretase (1–6, 31). ADAM10/Kuzbanian, another major sheddase, is required for Notch signaling. It can cleave the Notch ligand Delta, heparin-binding epidermal growth factor (HB-EGF), TNF-α, L1 adhesion molecule, and ephrin A2 and is

* This work was supported by National Institutes of Health Grant CA78646, by Department of Defense, U.S. Army Medical Research Acquisition Activity Grant DAMD17-02-1-0238, by American Cancer Society, Florida Division Grant F01FSU-1, by the Florida State University Research Foundation (to Q.-X. A. S.), and by the Deutsche Forschungsgemeinschaft (DFG), Bonn (SFB 549, project A05 and DFG Grant Ts 8-35/3) (to H. T.). The costs of publication of this article were defrayed in part by the payment of page charges. This article must therefore be hereby marked "*advertisement*" in accordance with 18 U.S.C. Section 1734 solely to indicate this fact.

¶ To whom correspondence should be addressed: Dept. of Chemistry and Biochemistry, Florida State University, 203 DLC, Chemistry Research Bldg., Rm. 203, Tallahassee, FL 32306-4390. Tel.: 850-644-8683; Fax: 850-644-8281; E-mail: sang@chem.fsu.edu.

[1] The abbreviations used are: APP, amyloid precursor protein; Ab, antibody; ADAM, a disintegrin and metalloproteinase; ADAMTS, a disintegrin and metalloproteinase with thrombospondin-like motifs; α2-M, α2-macroglobulin; CaM, calmodulin; decRVKR-CMK, decanoyl-Arg-Val-Lys-Arg-chloromethyl ketone; mAb, monoclonal antibody; MAPK, mitogen-activated protein kinase; MDC, metalloprotease/disintegrin/cysteine-rich; MDCK, Madin-Darby canine kidney; MMPs, matrix metalloproteinases; MT-MMPs, membrane-type MMPs; NRG, neuregulin; PKC, protein kinase C; PMA, phorbol 12-myristate 13-acetate; TACE, tumor necrosis factor α convertase; TAPI, tumor necrosis factor-α proteinase inhibitor; TIMPs, tissue inhibitors of metalloproteinases; TGF-α, transforming growth factor-α; TNF-α, tumor necrosis factor- α; TRANCE, TNF-related activation-induced cytokine; W7, *N*-(6-aminohexyl)-5-chloro-1-naphthalenesulfonamide.

an APP α-secretase (1–5, 32, 33). ADAM9 is believed to participate in the PMA-stimulated shedding of HB-EGF (34) and can function as an APP α-secretase (35). ADAM19/MDC β has been linked to shedding of the epidermal growth factor receptor-ligand neuregulin-β1 (36). ADAM12/MDC α has recently been shown to be responsible for endogenous shedding of HB-EGF in the heart (37). In addition, MMP7 has a functionally relevant role in shedding of TNF-α and FasL (38, 39), and MT1-MMP can be autolytically shed and is an enzyme capable of releasing both CD44 and TRANCE (21, 40, 41). However, not many proteinases responsible for ectodomain shedding of proteins have been identified.

Adamalysin 19/ADAM19/MDC β, cloned from mice (42, 43) and humans (44, 45), is a type I membrane-bound protein containing the basic domains of ADAMs, such as the prodomain, metalloprotease and disintegrin domain, cysteine-rich domain, transmembrane domain, and cytoplasmic domain (3). In addition to the processing of neuregulin (NRG) (36), human adamalysin 19 (hADAM19) is believed to play a role in osteoblast differentiation, in the distinction between macrophages and dendritic cells, and as a marker for the differentiation and characterization of dendritic cells (44). Recently, we demonstrated that hADAM19 is activated by furin in the secretory pathway and that the intracellular removal of the prodomain is required for its proteolytic activity, which was assessed with an α2-macroglobulin (α2-M) trapping assay *in vitro* (46). Emerging evidence indicates that metalloproteinase activity is regulated by the process of shedding or truncation, as in the cases of MT1-MMP, MT5-MMP, ADAM13, and ADAMTS4 (40, 47–49). Here we show that autolytic processing at $Glu^{586} \downarrow Ser^{587}$ of hADAM19 within its cysteine-rich domain is required for its endopeptidase activity and that efficient processing of hADAM19 is mainly dependent on the sizes of both Glu^{586} and Ser^{587}. We also show that PKC, CaM, and calcium signals may regulate the hADAM19 processing, which is not sensitive to GM6001 or TIMP-3. Moreover, we present a peptide substrate that mimics the processing site and may be used to determine the activity of soluble hADAM19 by a fluorescamine assay.

MATERIALS AND METHODS

Chemicals, Cell Lines, Cell Culture, and Immunological Reagents—All common laboratory chemicals, proteinase inhibitors, PMA, trifluoperazine, *N*-(6-aminohexyl)-5-chloro-1-naphthalenesulfonamide (W7), calmidazolium, PD98059, wortmannin, LY290042, pervanadate, and anti-FLAG-M2 monoclonal antibody (mAb) and its agarose conjugates were purchased from Sigma Chemical Co. (St. Louis, MO). The CMK-based furin inhibitor, dec-Arg-Val-Lys-Arg-chloromethyl ketone (decRVKR-CMK), and a matrix metalloproteinase inhibitor, ilomastat (GM6001), were purchased from Bachem (Philadelphia, PA). TIMP-3 was purchased from R & D Systems (Minneapolis, MN). Restriction enzymes were purchased from Promega (Madison, WI) or Invitrogen (Gaithersburg, MD). COS1 and Madin-Darby canine kidney (MDCK) cells and its derivatives were maintained as described (45). Dulbecco's modified Eagle's medium was purchased from Invitrogen (Gaithersburg, MD). Fetal bovine serum, penicillin G, and streptomycin were purchased from Invitrogen (Rockville, MD). α2-M was purchased from Roche Molecular Biochemicals (Indianapolis, IN). Rabbit polyclonal hADAM19 antibodies pAb361 (anti-metalloproteinase domain, anti-Cat) and pAb362 (anti-disintegrin domain, anti-Dis) were generated by our laboratory as reported previously (50).

PCR Primers, Mutagenesis, and Expression Constructs—All inserts tagged with FLAG at their C terminus were cloned into pCR3.1uni, including wild type hADAM19 (F46), soluble hADAM19 (D52), ^{199}RA-D (described in Ref. 46), and all mutants used in this study. The primer sequences for full-length (E346A-F) and soluble (E346A-D) $Glu^{346} \rightarrow$ Ala mutants were: forward primer, 5′-C ATG GCC CAC **GCG** ATG GGC CAC-3′; reverse primer, 5′-GTG GCC CAT **CGC** GTG GGC CAT G-3′. For deletion from the cysteine-rich domain to the end of the C terminus (D-CR): forward primer, 5′-ACC ATG CCA GGG GGC GCA GGC GCC-3′; reverse primer, 5′-GGT ACC ATC CAT CTG GTA GAA G-3′. For the soluble $Glu^{586} \rightarrow$ Ala mutant (E586A-D): forward primer, 5′-CGG CCC CTG **GCG** TCC AAC GCG-3′; reverse primer, 5′-CGC GTT GGA **CGC** CAG GGG CCG-3′. For the soluble $Glu^{586} \rightarrow$ Gly mutant (E586G-D): forward primer, 5′-CGG CCC CTG **GGG** TCC AAC GCG-3′; reverse primer, 5′-CGC GTT GGA **CCC** CAG GGG CCG-3′. For the soluble $Glu^{586} \rightarrow$ Asp mutant (E586D-D): forward primer, 5′-CGG CCC CTG **GAC** TCC AAC GCG-3′; reverse primer, 5′-CGC GTT GGA **GTC** CAG GGG CCG-3′. For the soluble $Glu^{586} \rightarrow$ Gln mutant (E586Q-D): forward primer, 5′-CGG CCC CTG **CAG** TCC AAC GCG-3′; reverse primer, 5′-CGC GTT GGA **CTG** CAG GGG CCG-3′. For the soluble $Ser^{587} \rightarrow$ Ala mutant (S587A-D): forward primer, 5′-CCC CTG GAG **GCC** AAC GCG GTG-3′; reverse primer, 5′-CAC CGC GTT **GGC** CTC CAG GGG-3′. For the soluble $Ser^{587} \rightarrow$ Thr mutant (S587T-D): forward primer, 5′-CCC CTG GAG **ACC** AAC GCG GTG-3′; reverse primer, 5′-CAC CGC GTT **GGT** CTC CAG GGG-3′. For the soluble $Ser^{587} \rightarrow$ Phe mutant (S587F-D): forward primer, 5′-CCC CTG GAG **TTC** AAC GCG GTG-3′; reverse primer, 5′-CAC CGC GTT **GAA** CTC CAG GGG-3′. All constructs were confirmed by DNA sequencing.

DNA Transfection and Generation of Stable Cell Lines—COS1 cells were seeded into 24-well plates for 16–24 h at 80% confluence and transfected with the indicated plasmids using LipofectAMINE2000 according to the instructions provided by Invitrogen (Gaithersburg, MD). After 6–10 h, serum-free Dulbecco's modified Eagle's medium and the indicated reagents were added, and the mixture was incubated for another 24 h. The conditioned media and cell lysates were then analyzed by Western blotting (46). The same transfection procedure was performed to generate stable MDCK cell lines, and the selection for hADAM19 was begun in the presence of G418 (400 μg/ml) after transfection for 24 h. The conditioned media and/or cell lysates of the clones were subjected to Western blotting to confirm the expression of hADAM19 (46).

Western Blotting—The experiments were carried out as described previously (46). Briefly, cells were grown to 80% confluence and were treated as indicated. After centrifugation for 15 min at 14,000 $\times$ *g* and 4 °C to clear any debris, the serum-free media were collected and prepared for SDS-PAGE. The cells were lysed with RIPA buffer (50 mM Tris, pH 7.5, 150 mM NaCl, 0.25% sodium deoxycholate, 0.1% Nonidet P-40, 1 mM phenylmethylsulfonyl fluoride, 2.5 μM GM6001, 10 μg/ml aprotinin, 10 μg/ml E64, and 10 μg/ml pepstatin A) for 15 min on ice. The supernatant was collected after centrifugation for 20 min at 14,000 $\times$ *g* and 4 °C. After electrophoresis, the proteins were transferred onto nitrocellulose membranes, probed with anti-FLAG-M2 or anti-hADAM19, and developed as before (46).

Purification of Soluble hADAM19 and N-terminal Sequencing—All proteins were purified on anti-FLAG-M2 affinity columns as described previously (46); however, HEPES buffer (50 mM HEPES, pH 7.5, 200 mM NaCl, 10 mM $CaCl_2$, 25 μM $ZnCl_2$, 0.05% Brij-35) was used instead of TBS buffer for the purpose of determining the activity of hADAM19 by a fluorescamine assay. Briefly, cells from stable lines expressing soluble hADAM19, D52-5, E586D-D, S587T-D, and D-CR, were grown to 100% confluence, washed twice with phosphate-buffered saline, and incubated for 48 h. in serum-free media. The conditioned media were collected, centrifuged to clear any debris, and loaded onto an anti-M2 immunoaffinity column (1 ml of resuspended agarose) that had been prewashed with HEPES buffer. The bound materials were extensively washed with HEPES buffer, eluted with FLAG peptides, and collected in 500-μl fractions. The fractions were analyzed by Western blot using anti-hADAM19 antibodies or anti-FLAG-M2, and the protein was quantified by its UV absorbance at 280 nm. The fractions containing the most wild type or mutant hADAM19 proteins were used for the α2-M trapping assay and fluorescamine assay. In the case of D52-5, the most concentrated fraction was also prepared for protein N-terminal sequencing to determine the shedding site. After separation by SDS-PAGE, the samples were transferred to a PVDF membrane and stained with Coomassie Blue R-250. After destaining, the hADAM19 bands were excised and sent to Margaret Seavy at the Bioanalytical Core Facility at the Florida State University for N-terminal amino acid sequencing.

α2-M Trapping Assay—The detailed experimental procedure was previously reported (46, 50). Briefly, equal amounts of purified wild type and mutated soluble hADAM19 were mixed with 24 μl of α2-M (0.2 unit/ml), respectively, adjusted to a total volume of 100 μl with HEPES buffer, and incubated at 37 °C for the indicated times. A 20-μl aliquot of the mixture was removed at the indicated times, put in 2$\times$ SDS-PAGE sample buffer, and boiled. Following SDS-PAGE, the protein bands in the gels were visualized by silver staining.

Determination of Kinetic Parameters of hADAM19 Using a New Peptide Assay—The N-terminal acetylated peptide (Ac-RPLESNAV) was synthesized by Dr. Umesh Goli at the Biochemical Analysis, Synthesis,

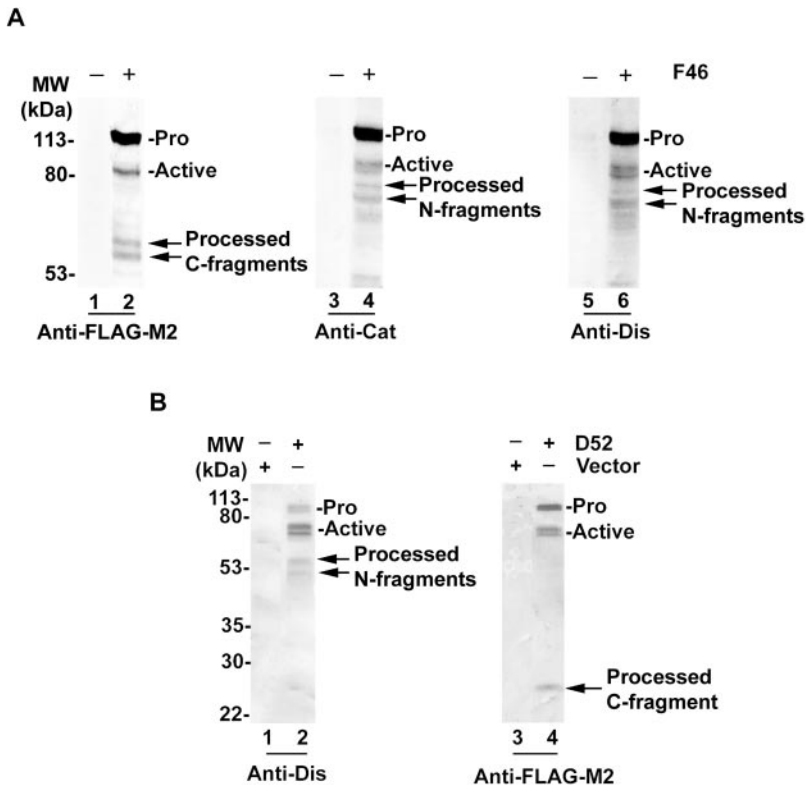

FIG. 1. **hADAM19 is processed within the cysteine-rich domain in COS1-transfected cells.** *A*, detection of hADAM19 by Western blotting with anti-FLAG-M2 mAb (*lanes 1* and *2*), anti-catalytic domain pAb (Anti-Cat) (*lanes 3* and *4*), or anti-disintegrin domain polyclonal antibody (Anti-Dis) (*lanes 5* and *6*). Cell lysates with radioimmune precipitation assay buffer from COS1 cells transfected with the blank vector (*lanes 1*, *3*, and *5*) or pCR3.1hADAM19 (F46) (*lanes 2*, *4*, and *6*). The pro, active, and processed forms of hADAM19 are indicated. *B*, characterization of soluble hADAM19. COS1 cells were transfected with the blank vector (*lanes 1* and *3*) or soluble hADAM19 (D52) (*lanes 2* and *4*). The conditioned media were analyzed by Western blotting using anti-disintegrin domain Ab (Anti-Dis) (*lanes 1* and *2*) and anti-FLAG-M2 mAb (*lanes 3* and *4*).

and Sequence Service Laboratory at Florida State University. The stock solutions of the peptide substrates were prepared in 0.05 M HEPES, pH 7.5, 0.2 M NaCl, 0.01 M $CaCl_2$, and 0.01% Brij-35. The peptide concentrations ranged from 0.2 to 4.0 mM, and the enzyme concentration was 160 nM. N-terminal sequencing for this released peptide was performed after overnight hydrolysis by the enzyme. Hydrolysis of the peptide by the enzyme was monitored by measuring fluorescence intensity (51). After incubation for the indicated times, the hydrolytic reaction was quenched by adding 20 μl of 100 mM 1,10-phenanthroline into 100 μl of reaction mixture. For the control sets, the 1,10-phenanthroline solution was added at the start of incubation. After the reaction was quenched, 100 μl of 0.1% fluorescamine in 10% Me_2SO/90% assay buffer was added into each reaction mixture. Relative fluorescence of the product coupled with fluorescamine was determined on a PerkinElmer Life Sciences LS-50B spectrofluorometer using an excitation wavelength of 386 nm and an emission wavelength of 477 nm. Excitation and emission slit widths were both 10 nm. Relative fluorescence was converted to nanomoles of product using a standard curve obtained with arginine. The final solution was diluted further with the assay buffer, if it was necessary. The values of k_{cat} and K_m were determined by fitting the data to the Michaelis-Menten equation. A molar extinction coefficient of 33,120 M^{-1} cm^{-1}, which was calculated by using Genetic Computer Group (GCG) software, was used to determine the concentration of soluble hADAM19.

RESULTS

hADAM19 Is Processed within the Cysteine-rich Domain—Shedding or truncation is increasingly being recognized as a key regulator of the activity of some metalloproteinases (40, 47–49). It was intriguing to investigate the possibility of shedding or truncation in hADAM19. As shown in Fig. 1*A*, in addition to the pro and active forms of hADAM19, we detected a doublet of protein of about 58 kDa by anti-FLAG-M2 in the lysate of the transfected COS1 cells expressing full-length hADAM19 with C-terminal FLAG tags (F46). We did not detect the doublet using antibodies against the catalytic and disintegrin domains of hADAM19, indicating that the 58-kDa protein is the processed C-terminal fragment lacking the metalloproteinase and disintegrin domains of hADAM19. On the other hand, another doublet of around 72 kDa was detected in the same lysate by these two hADAM19 antibodies but not anti-FLAG-M2 (Fig. 1*A*), suggesting that the 72-kDa protein is the processed N-terminal fragment containing the metalloproteinase and disintegrin domains of hADAM19. Taken together, a cellular processing occurs in hADAM19 after its disintegrin domain in the COS1-transfected cells. Notably, the doublets result from different forms of glycosylation as verified by glycosidase F treatment (Ref. 46 and data not shown). To probe the domain in which the processing occurs, we made two deletion forms of hADAM19 with C-terminal FLAG tags, soluble hADAM19 (D52), which lacked the transmembrane domain and cytoplasmic domain, and a form that lacked the cysteine-rich domain through the cytoplasmic domain (D-CR) (see Fig. 4). When D52 and D-CR were transfected into COS1 cells, we were able to detect several proteins in the conditioned media using both anti-FLAG-M2 and the antibody against the disintegrin domain, including the soluble pro and active forms of hADAM19. However, a 26-kDa protein in the conditioned medium from D52-transfected cells was clearly detectable using anti-FLAG-M2, but not the disintegrin domain antibody, suggesting that the 26-kDa protein is the processed C-terminal fragment of soluble hADAM19. In contrast, a doublet at 60–65 kDa was detected in the medium by the anti-disintegrin domain antibody, but not anti-FLAG-M2, indicating that the 60- to 65-kDa protein is the processed N-terminal fragment of soluble hADAM19 (Fig. 1*B*). There were no additional proteins detectable in the conditioned medium from the cells transfected with D-CR (data not shown); therefore, the processing of hADAM19 might be accounted for by shedding within its cysteine-rich domain.

PMA Up-regulates Processing of Full-length but Not Soluble hADAM19—PMA is a potent inducer of ectodomain shedding of many transmembrane proteins (5, 8–12, 14, 16, 19, 20, 34). To examine the effect of PMA on the processing of hADAM19, the COS1 cells transfected with F46 were treated with PMA overnight. As shown in Fig. 2*A*, PMA obviously enhanced hADAM19 processing in the COS1-transfected cells as detected under reducing conditions. Interestingly, we failed to detect the

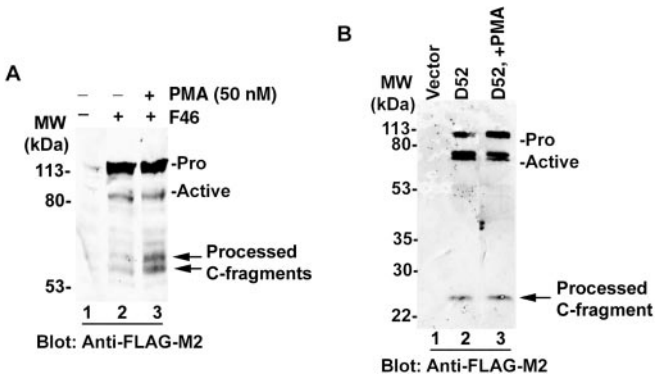

FIG. 2. **PMA enhances the processing at cysteine-rich domain of full-length, but not soluble, hADAM19.** *A*, enhancement of the processing at cysteine-rich domain of full-length hADAM19 by PMA. COS1 cells were transfected with the blank vector (*lane 1*) or F46 (*lanes 2* and *3*). After treated without (*lanes 1* and *2*) or with PMA (50 nM) (*lane 3*) overnight, the cells were lysed and probed with anti-FLAG-M2 mAb. *B*, PMA had no effect on the processing at cysteine-rich domain of soluble hADAM19. The conditioned media were collected from COS1 cells transfected with the blank vector (*lane 1*) or D52 (*lanes 2* and *3*) after overnight treatment with 50 nM PMA. The results were obtained from Western blots using anti-FLAG-M2 mAb.

processed N-terminal fragments in the conditioned media from the F46-transfected COS1 cells, even after PMA treatment (data not shown), suggesting that the processed N-terminal fragment may be still associated with the remaining C-terminal fragment or full-length of hADAM19 via one or more disulfide bonds. Therefore, according to the definition of ectodomain shedding, membrane-bound proteins release their soluble forms and the processing of hADAM19 within its cysteine-rich domain is not technically a form of shedding. To test if PMA-enhanced processing relies on the transmembrane and cytoplasmic domains, we treated the COS1 cells expressing D52 with PMA. As shown in Fig. 2*B*, PMA had a negligible effect on the processing of soluble hADAM19, suggesting that PMA might enhance the processing of hADAM19 via interaction with the cytoplasmic domain, transmembrane domain, or both. As a note, we used the processed C-terminal fragment at 26 kDa as a marker for the processing of soluble hADAM19 throughout this study.

The Processing at Glu^{586} ↓ Ser^{587} within the Cysteine-rich Domain Occurs by an Autolytic Mechanism—A recent report showed that ADAM13 shedding is dependent on its own metalloproteinase activity (48). We therefore hypothesized that the metalloproteinase activity of hADAM19 is also involved in its processing. To test this hypothesis, we used several independent approaches. As shown in Fig. 3*A*, rare processing was detected in the conditioned media from D52-transfected COS1 cells that were treated with decRVKR-CMK, which blocks the activation of hADAM19 (46). This indicates that prodomain removal is necessary for the processing at its cysteine-rich domain of hADAM19. Furthermore, ^{199}RA-D, an inactive mutant of soluble hADAM19 resistant to furin-mediated removal of its prodomain (46), displayed no processing, confirming that the soluble pro-form of hADAM19 lacks the capacity to process at its cysteine-rich domain (Fig. 3*A*). (The total protein level in the media was comparable to that in the media of the D52 cells.) We also generated another soluble inactive form of hADAM19 (E346A-D), in which the active residue Glu at 346 in the metalloproteinase domain was mutated to Ala, and transfected it into COS1 cells. Obviously, no processing at its cysteine-rich domain was observed in the media of these cells. Once again, the total protein level in the media was almost equal to that in the media of the D52 cells (Fig. 3*A*). These results strongly argue that the processing at its cysteine-rich domain of soluble hADAM19 depends on its own metalloproteinase activity. However, neither GM6001 nor TIMP-3, inhibitors that typically block sheddase activity (26–30), inhibited the autolytic processing of hADAM19 at its cysteine-rich domain (data not shown).

To further confirm that autolytic processing at its cysteine-rich domain occurs in soluble hADAM19, we generated stable MDCK cell lines called D52-5, ^{199}RA-D-6, and E346A-D-17, which expressed soluble D52, ^{199}RA, and E346A, respectively. As we expected, the 26-kDa-processed fragment was clearly detectable in the conditioned media from D52-5; the processing was dramatically inhibited by decRVKR-CMK (Fig. 3*B*). Furthermore, there was no processing at the cysteine-rich domain in ^{199}RA-D-6 and E346A-D-17 (Fig. 3*B*). (The total amount of soluble protein was comparable among the conditioned media of these cell lines). Once again, PMA, GM6001, and TIMP-3 failed to affect the processing of D52-5 (Figs. 2*B* and 3*B*, data not shown).

N-terminal sequencing revealed that the starting sequence of the purified 26-kDa protein was SNAVPIDT, which is identical to ^{596}SNAVPIDT^{594} within the cysteine-rich domain of hADAM19. This suggests that the processing of hADAM19 occurs at Glu^{586} ↓ Ser^{587} within its cysteine-rich domain (Fig. 3*B*).

The Sizes of Glu^{586} and Ser^{587} Are Critical for the Processing at Glu^{586} ↓ Ser^{587} of Soluble hADAM19—To examine the importance of the Glu^{586} (P1) and Ser^{587} (P1′) sites in the processing at Glu^{586} ↓ Ser^{587} of soluble hADAM19, we changed the size, charge, and polarity of these two residues by mutagenesis. The constructs are shown in Fig. 4. Shown in Fig. 5*A*, there was no or little detectable processing in the COS1 cells transfected with either E586D-D or S587T-D, suggesting that subtle changes in the sizes of residues at the P1 and P1′ positions can dramatically impair the processing. Furthermore, rare or little processing was observed when significant changes were made to the side chains of the residues at these sites, as in the cases of the Glu^{586} to Ala or Gly, and Ser^{587} to Phe mutants (Fig. 5*A*). On the other hand, the amount of processing product in the E586Q-D or S587A-D mutant, in which the side chain of the amino acid residue was almost the same size as that in wild type soluble hADAM19, was almost equal (Fig. 5*A*).

To further confirm the fate of processing at Glu^{586} ↓ Ser^{587} upon changes at the P1 and P1′ sites, we chose mutants with subtle changes and, presumably, structural similarities, Glu^{586} to Asp and Ser^{587} to Thr, to generate stable transfectants in MDCK cells. Shown in Fig. 5*B*, rare or little processing was detectable in the conditioned media from these stable MDCK transfectants, confirming that both soluble E586D-D and S587T-D have undetectable or little ability to process, even if they are cleaved by furin in the MDCK transfectants. (There were no significant differences in protein levels among the transfectants.)

The Signals of CaM and Calcium May Be Involved in the Processing at Glu^{586} ↓ Ser^{587} of hADAM19—In addition to the PKC pathway, there are several other signal pathways, involving tyrosine kinase, MAPKs, phosphatase, phosphatidylinositol 3-kinase, calcium, and CaM, which regulate the ectodomain-shedding process (10, 13–19, 21–23). Specific inhibitors were used to determine whether or not these signal pathways regulate the processing at Glu^{586} ↓ Ser^{587} of hADAM19. As shown in Fig. 6, only CaM inhibitors impaired the processing of soluble hADAM19. The other inhibitors, including genistein, PD98059, pervanadate, wortmannin, and LY290042, had no significant effects on the processing of soluble or full-length hADAM19 (data not shown). In addition, both A23187 and brefeldin A block the activation of both soluble and full-length

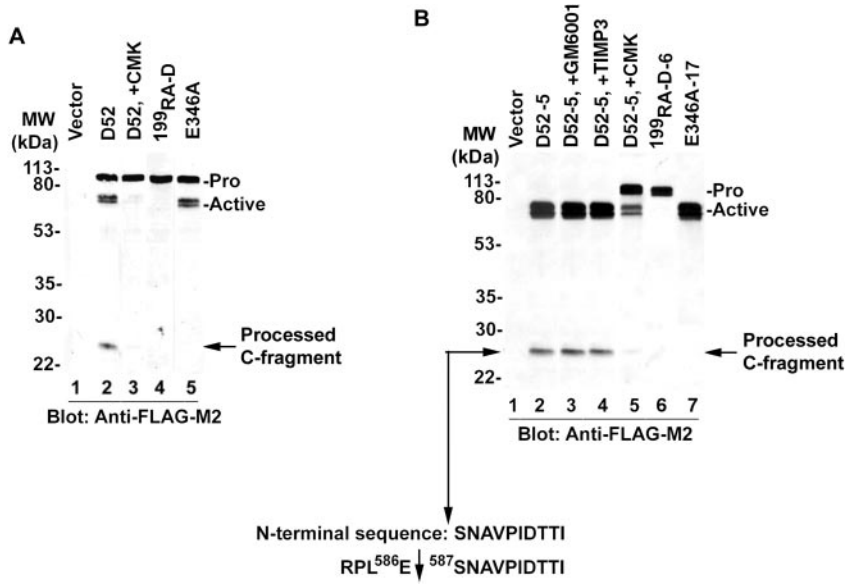

FIG. 3. **hADAM19 autolytically process at Glu^{586} ↓ Ser^{587} within the cysteine-rich domain.** *A*, autolytic processing at the cysteine-rich domain of soluble hADAM19 in COS1-transfected cells. COS1 cells were transfected with the blank vector (*lanes 1*), D52 (*lanes 2* and *3*), soluble mutant with ^{199}RR to ^{199}AA (^{199}RA-D) (*lane 4*), or soluble inactive mutant (E346A-D) (*lane 5*) and incubated without (*lanes 1*, *2*, *4*, and *5*) or with 100 μM CMK (*lane 3*) for 16 h. The conditioned media were analyzed by Western blotting with anti-FLAG-M2 mAb. *B*, processing at cysteine-rich domain of soluble hADAM19 in the stable MDCK transfectants. MDCK cells stably expressing soluble hADAM19 (D52-5) (*lanes 2–5*), soluble ^{199}RA mutant (^{199}RA-D-6) (*lane 6*), or the soluble inactive mutant (E346A-D-17) (*lane 7*) were treated without (*lanes 1*, *2*, *6*, and *7*) or with 5 μM GM6001 (*lane 3*), 100 nM TIMP-3 (*lane 4*), or 100 μM CMK (lane 5) overnight. The conditioned media were analyzed by Western blotting using anti-FLAG-M2 mAb. MDCK cells transfected with the blank vector were used as a control (*lane 1*). The sequence for the shed C-terminal protein is shown at the *bottom*.

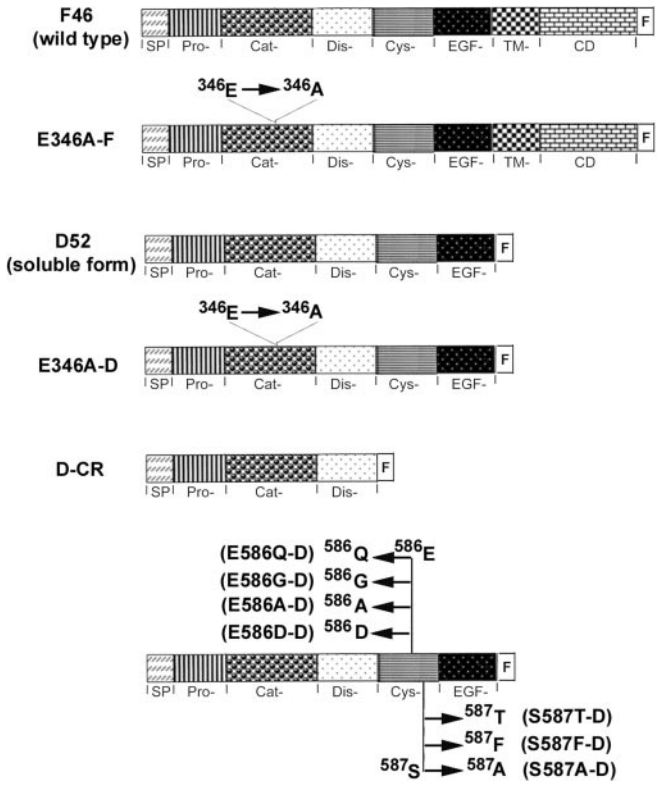

FIG. 4. **A schematic illustration of the wild type expression vector pCR3.1hADAM19 and its mutant constructs.** All of the constructs have a C-terminal FLAG tag. *SP*, signal peptide; *Pro-*, prodomain; *Cat-*, catalytic domain; *Dis-*, disintegrin domain; *Cys-*, cysteine-rich domain; *EGF-*, EGF-like domain; *TM*, transmembrane domain; *CD*, cytoplasmic domain; *F*, FLAG tag.

hADAM19 (46). There was no processing at Glu^{586} ↓ Ser^{587} detectable under the treatment of either A23187 or brefeldin A (data not shown), indicating that hADAM19 is activated and processed in the secretory pathway. Taken together, our results suggest that PKC, CaM, and calcium signal pathways may be related to the processing at Glu^{586} ↓ Ser^{587} of hADAM19.

The Processing at Glu^{586} ↓ Ser^{587} Is Necessary for hADAM19 to Exert Its Proteolytic Activity against α2-M—To assess the significance of the processing at Glu^{586} ↓ Ser^{587} of hADAM19, we purified the proteins from D52-5, E586D-D, and S587T-D, respectively. Intriguingly, the processed N-terminal fragments, containing the metalloproteinase, disintegrin, and parts of the cysteine-rich domain, were detected as mature forms using anti-disintegrin antibody (data not shown). This suggests that the processed N-terminal segments bind with unprocessed soluble forms or processed C-terminal-soluble fragments by one or more disulfide bonds, consistent with the results obtained early from the full-length hADAM19 (data not shown). When we probed the purified proteins with anti-FLAG-M2, as shown in Fig. 7*A*, S587T-D displayed relatively more processing than E586D-D, in which a very low level of processing was detected. D52-5 showed much more processing than E586D-D and S587T-D. As shown in Fig. 7*B*, D52-5 protein had a much greater ability to form a complex with α2-M and generate two products compared with both E586D-D and S587T-D proteins, which displayed much lower activities. Obviously, S587T-D had a relatively higher activity than E586D-D, which showed very low activity. These results perfectly coincide with the Western blot shown in Fig. 7*A*, indicating that the more that hADAM19 processed at Glu^{586} ↓ Ser^{587}, the more proteolytic activity it exerted against α2-M *in vitro*.

Ac-RPLE-SNAV Is Cleaved by Active hADAM19—To test hADAM19 activity, we synthesized a new peptide, Ac-RPLE-SNAV, which encompasses the processing site of hADAM19 and is conserved among humans and mice (42, 45). Because the processing at Glu^{586} ↓ Ser^{587} is mediated by its own metalloproteinase activity (Fig. 3), we were able to use this peptide to assay soluble hADAM19 activity and obtained the similar results as from the α2-M assay (Fig. 7*B*). Once again, the highest

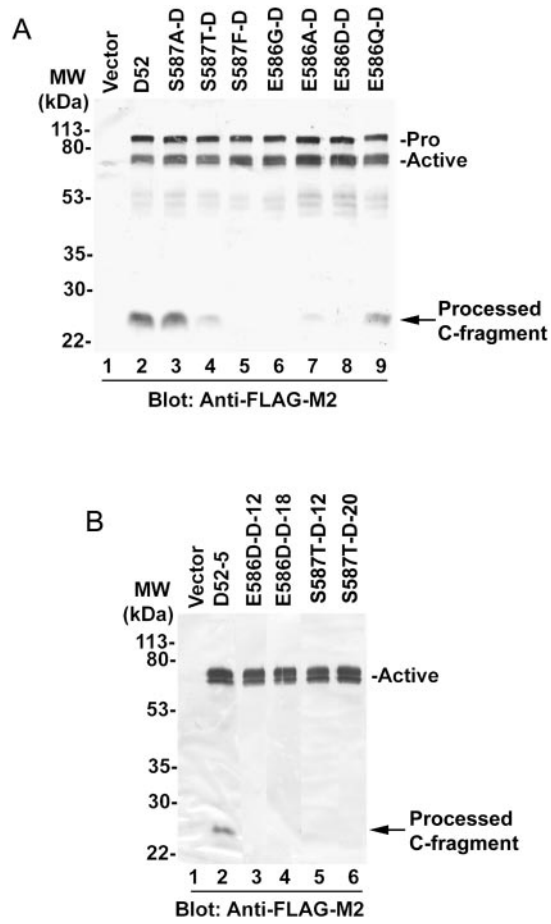

FIG. 5. **The residue sizes at both Glu^{586} and Ser^{587} are critical for the processing at Glu^{586} ↓ Ser^{587} of hADAM19.** *A*, processing profile at Glu^{586} ↓ Ser^{587} of soluble mutants in COS1-transfected cells. COS1 cells were transfected with the blank vector (*lane 1*), D52 (*lane 2*), soluble mutants with Ser^{587} to Ala (S587A-D) (*lane 3*), Thr (S587T-D) (*lane 4*), or Phe (S587F-D) (*lane 5*), or Glu^{586} → Gly (E586G-D) (*lane 6*), Ala (E586A-D) (*lane 7*), Asp (E586D-D) (*lane 8*), or Gln (E586Q-D) (*lane 9*). The conditioned media were subjected to SDS-PAGE and Western blotting with anti-FLAG-M2 mAb. *B*, detection of the processing at Glu^{586} ↓ Ser^{587} of hADAM19 in MDCK cells stably expressing soluble hADAM19 mutants. Four MDCK cells stably expressing soluble hADAM19 with Glu^{586} → Asp (E586D-D-12 and E586D-D-18) (*lanes 3* and *4*) or Ser^{587} to Ala (S587A-D-12 and S587A-D-20) (*lanes 5* and *6*) were prepared in serum-free media overnight. The conditioned media were analyzed by Western blotting using anti-FLAG-M2 mAb. MDCK cells transfected with the blank vector (*lane 1*) and D52-5 cells (*lane 2*) were used as controls.

activity was seen in D52-5 with 1% cleavage after incubation overnight. E586D-D and S587T-D only showed 30 and 10% the activity exerted by D52-5, respectively (data not shown). As we knew, the activity at 1% was not enough for a fluorescence assay. However, given that D52-5 was not fully processed (maybe 25% of the mature hADAM19 got processed according to the Western blotting result as shown in Fig. 7*A*), we decided to generate another stable line in MDCK cells expressing D-CR (Fig. 4). The reason we deleted the whole cysteine-rich domain is that we surmised that this domain has a potential interaction with the metalloproteinase domain, disintegrin domain, or both that might decrease the activity. Fortunately, purified D-CR from the MDCK transfectants had a higher activity for cleaving our new peptide substrate, and the cleavage product detected by N-terminal sequencing was peptide SNAV, confirming that the peptide substrate was cleaved at the E-S bond, which is identical to the processing site in the hADAM19 protein. Furthermore, as shown in Fig. 8, the k_{cat}, K_m, and k_{cat}/K_m values for 150-min incubation were 2.4 min^{-1}, 2.0 mM, and

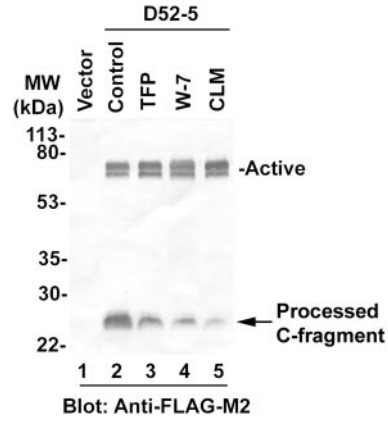

FIG. 6. **Processing at Glu^{586} ↓ Ser^{587} of hADAM19 is inhibited by calmodulin inhibitors.** MDCK cells stably expressing soluble hADAM19 (D52-5) (*lanes 2–5*) were treated without (*lanes 1* and *2*) or with 100 μM trifluoperazine (*lane 3*), 25 μM W7 (*lane 4*), or 50 μM calmidazolium (*lane 5*) for 16 h. The conditioned media were then analyzed by Western blotting using anti-FLAG-M2 mAb. MDCK cells transfected with the blank vector were used as a control (*lane 1*).

1200 M^{-1} min^{-1}, respectively. Thus, we developed a peptide substrate for determining soluble hADAM19 activity by a fluorescamine assay.

DISCUSSION

In the current report, we have demonstrated that processing of hADAM19 occurs at Glu^{586} ↓ Ser^{587} within the cysteine-rich domain by its own metalloproteinase activity and is a necessary step to display its proteolytic activity against both a peptide substrate and α2-M *in vitro*. We have also revealed that the processing at Glu^{586} ↓ Ser^{587} of hADAM19 is regulated by a unique pathway, distinguishable from those shown for other ADAMs, MT-MMPs, and other membrane-bound proteins.

Shedding or Processing of Metalloproteinases—Growing evidence suggests that shedding is of vital importance for the regulation of metalloproteinase activity. For MT-MMPs, Pei's group reported that MT5-MMP is shed by furin, down-regulating its activity, and that interleukin-8 triggers the signal for both release and activation of MT6-MMP by an unknown mechanism (47, 52). The activity of MT1-MMP can be autolytically terminated directly on the cell surface or via production of a soluble functional fragment, consequently down-regulating enzyme activity on the cell surface (40). Among ADAMs, ADAM13 is the only one that has been shown to shed its ectodomain intracellularly by an autolytic mechanism, producing an active enzyme able to bind with α2-M and integrins (48). In addition, truncation of mature ADAMTS4 at its C terminus is required for its aggrecanase activity (49). In this report, we demonstrate that hADAM19 carries out processes within its cysteine-rich domain, resulting in an active enzyme shown by both α2-M and peptide substrate assays *in vitro* (Figs. 3, 7, and 8). It might, therefore, be a general regulatory mechanism that MT-MMPs, such as MT1-MMP and MT5-MMP, are down-regulated by shedding to release active forms from the cell surface, whereas ADAMs must shed, carry out process, or become truncated at the C terminus to exert their functions, such as acting as a sheddase, binding with integrins on the cell surface, or digesting components of the extracellular matrix.

Regulation of the Processing at Glu^{586} ↓ Ser^{587} of hADAM19—The signal pathways involved in shedding or truncation processes, especially of ADAMs, are poorly understood. In the present report, we provide unique characteristics of the regulation of the processing at Glu^{586} ↓ Ser^{587} of hADAM19. We found that PMA, a common inducer of shedding, also enhances the processing at Glu^{586} ↓ Ser^{587} of hADAM19 (Fig.

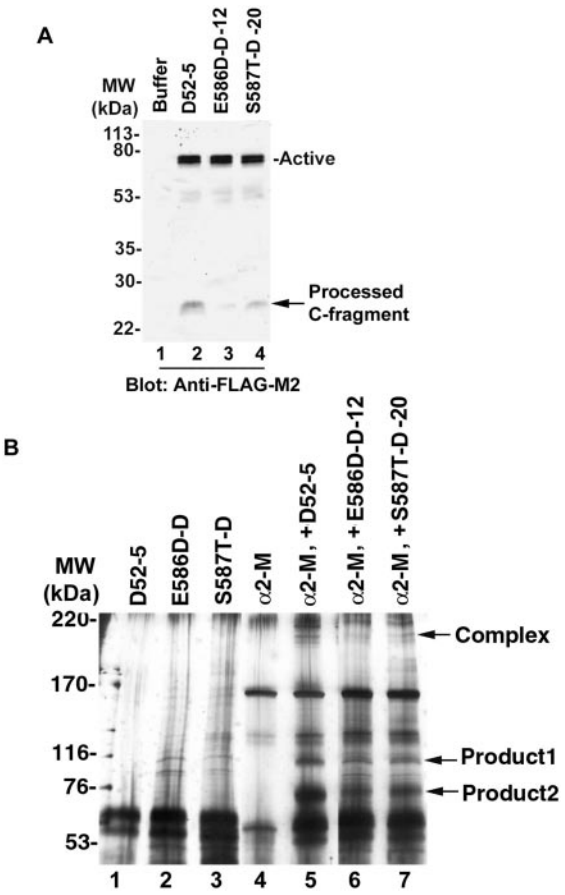

FIG. 7. **Requirement of the processing at Glu^{586} ↓ Ser^{587} for the proteolytic activity of hADAM19.** *A*, processing status at Glu^{586} ↓ Ser^{587} of purified proteins from the stable MDCK transfectants. MDCK cells stably expressing soluble hADAM19 (D52-5) (*lane 2*), soluble Glu^{586} → Asp (E586D-D-12) (*lane 3*), or soluble Ser^{587} to Ala (S587A-D-20) (*lane 4*) were prepared for purification as described under "Materials and Methods." Western blots using anti-FLAG-M2 mAb were performed on equal amounts of these purified proteins. *B*, the proteolytic activity of soluble hADAM19 using α2-M *in vitro*. The purified hADAM19 from D52-5 (*lanes 1* and *5*), E586D-D-12 (*lanes 2* and *6*), or S587A-D-20 (*lanes 3* and *7*) were normalized and incubated in reaction buffer alone (*lanes 1–3*) or with α2-M (*lanes 5–7*) for 24 h. α2-M in reaction buffer alone (24 h) was a control (*lane 3*). The α2-M·hADAM19 complex and the cleavage products of α2-M by hADAM19 are labeled on the *right*.

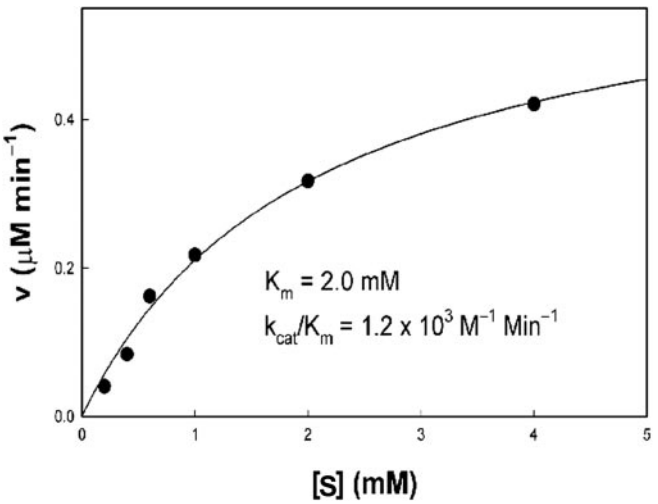

FIG. 8. **The hydrolysis of Ac-RPLE-SNAV by hADAM19.** The peptide (Ac-RPLE-SNAV) (0.2–4.0 mM), which mimics the processing site of hADAM19, was incubated with 0.26 μM soluble, active ADAM19 for 150 min. The formation of product was measured by monitoring the coupling of fluorescamine with the amino group newly formed from the cleavage. The nonlinear regression analysis of the data indicates k_{cat} = 2.4 min^{-1}, K_m = 2.0 mM, and k_{cat}/K_m = 1200 M^{-1} min^{-1}.

2*A*). The mechanism probably involves the cytoplasmic domain, transmembrane domain, or both, because PMA did not alter the processing of soluble hADAM19 (Fig. 2*B*). This is consistent with reports showing that the cytoplasmic domain of ADAM9 is required for PMA-induced shedding (34) and that the membrane anchor of TACE is necessary for its processing of TNF-α (53, 54). In addition, there are a few reports that have demonstrated the requirement of the cytoplasmic tail for shedding of pro-NRG, APP, pro-TGF, and L1 adhesion molecules (17, 55, 56). However, in most cases, endogenous and/or inducer-mediated shedding is independent of the cytoplasmic domain (Fig. 2*B*) (14, 17, 19, 22, 24). Calcium ionophore, A23187, is another potent inducer of most protein-shedding processes (13–16). Nevertheless, we found that A23187 and brefeldin A block the activation of both full-length and soluble hADAM19. Subsequently, no processing at Glu^{586} ↓ Ser^{587} was detectable, suggesting that hADAM19 is activated and processed in the secretory pathway (46, data not shown). Inhibitors of CaM have been shown to stimulate the shedding of several proteins, including MT1-MMP, pro-TGFα, pro-NRG, and APP, by a mechanism independent of both PKC and calcium (17–20). However, in our study, a reverse result was obtained; the processing at Glu^{586} ↓ Ser^{587} was inhibited by the CaM inhibitors (Fig. 6). Finally, we found that tyrosine kinase, MAPK, phosphatase, or phosphatidylinositol 3-kinase do not seem to play roles in the processing at Glu^{586} ↓ Ser^{587} of hADAM19 (data not shown), although they have been previously shown to participate in some shedding processes (9–12, 21–23, 29).

In addition, the proteinases responsible for the shedding of many cell surface molecules seem to have broad sequence specificity as revealed by mutational analysis of residues around the cleavage site of pro-TGFα, APP, IL-6 receptor, L-selectin, and pro-TNFα (57–61). In this report, we used mutagenesis to show that the residue sizes of the side chains at both the Glu^{586} and Ser^{587} sites are extremely important for normal processing at Glu^{586} ↓ Ser^{587} of hADAM19. Even delicate changes, such as Glu^{586} → Asp and Ser^{587} → Thr, caused dramatic decreases in the processing. Notably, many studies have shown that some potent synthetic inhibitors of metalloproteinases, such as TAPI, BB94, and GM6001, can block most, if not all, shedding processes and that many shedding processes are sensitive to TIMP-3, a matrix-associated TIMP that preferably inhibits ADAMs (5–8, 19, 24–30). However, neither GM6001 nor TIMP-3 inhibits the autolytic processing at Glu^{586} ↓ Ser^{587} of hADAM19 (Fig. 3*B*), which is consistent with some reports showing that the shedding of MT5-MMP, MT6-MMP, and IL-6 receptor is not affected by metalloproteinase inhibitors (47, 52, 62). One possibility, we speculate, is that shedding, in most cases, occurs at membrane-proximal regions on the cell surface, which are easily accessible to hydroxamate-based inhibitors and TIMP-3 (5, 25, 60, 63). Human ADAM19 processing takes place at a region distal from the transmembrane domain in the secretory pathway, which is less accessible to GM6001 and TIMP-3 (Fig. 3*B*). How hADAM19 initiates the processing at Glu^{586} ↓ Ser^{587} and what the roles for the disintegrin- and cysteine-rich domains are during the processing at Glu^{586} ↓ Ser^{587} remain to be uncovered. Perhaps dimerization through the disintegrin- and/or cysteine-rich domains is the key step for the processing as proposed for other ADAMs (3). This might also be an explanation for the fact that the processed N-terminal fragments, containing the metalloproteinase, disintegrin, and parts of the cysteine-rich domain, were not detected in the conditioned medium from the transfected COS1 cells with full-

length hADAM19 and were present among the purified soluble hADAM19 proteins (data not shown).

A New Peptide Substrate Based on the Processing Site Sequence for hADAM19—The peptide substrates currently used to measure MMP activity are synthesized based on the cleavage sites of protein substrates. Because hADAM19 processes at $Glu^{586} \downarrow Ser^{587}$ by its own metalloproteinase activity, we surmised that a peptide encompassing the processing site would be an ideal substrate. Indeed, this peptide, Ac-RPLE-SNAV, was suitable for a fluorescamine assay of enzyme activity and was cleaved at the *E*-S site as determined by peptide N-terminal sequencing. Although the wild type hADAM19 showed a minimally detectable activity by this method, D-CR, containing the metalloproteinase and disintegrin domains, displayed a higher activity to determine kinetic parameters after incubation for 150 min using our fluorescamine assay (Fig. 8). The kinetic parameters, k_{cat}, K_m, and k_{cat}/K_m, were 2.4 min^{-1}, 2.0 mM, and 1200 M^{-1} min^{-1}, respectively, demonstrating that this is a poor substrate and will have a limited usage. It is necessary that the peptide substrates will be optimized by creating analogs that are hydrolyzed more efficiently by hADAM19 in the near future. Our preliminary data show that TIMP-3 can inhibit hADAM19 activity in this peptide-based assay,[2] which is similar to the results for ADAM10, -12, and -17 and ADAMTS4 and -5 *in vitro* (64–67), and confirm that the TIMP-3 we used was active. However, TIMP-3 had no effect on the cellular processing at $Glu^{586} \downarrow Ser^{587}$ of soluble hADAM19 (Fig. 3*B*), indicating that this processing occurred intracellularly, to where TIMP-3 molecules might not be accessible. Interestingly, ADAMTS4 is truncated at $Glu^{373} \downarrow Ala^{374}$, the site for the cleavage of ADAMTS4 and ADAMTS5, not MMPs. In contrast, the truncation site at $Asn^{341} \downarrow Phe^{342}$ is mediated by MMPs, not aggrecanases (49, 68). Our mutational data showed that the $Glu^{586} \downarrow Ala^{587}$ processing site was also optimal for autolytic processing of hADAM19 (Fig. 5*B*), indicating that our peptide substrate might be useful to determine the activity of other ADAMs, such as aggrecanases. This peptide substrate may also be used for testing metalloproteinase inhibitors against hADAM19 and other ADAMs.

Acknowledgments—We thank Sara C. Monroe at Florida Statue University for her editorial assistance with the manuscript preparation and Dr. Jörg-Walter Bartsch at the University of Bielefeld for his critical review of the manuscript.

REFERENCES

1. Schlondorff, J., and Blobel, C. P. (1999) *J. Cell Sci.* **112,** 3603–3617
2. Kheradmand, F., and Werb, Z. (2002) *Bioessays* **24,** 8–12
3. Primakoff, P., and Myles, D. G. (2000) *Trends Genet.* **16,** 83–87
4. Blobel, C. P. (2000) *Curr. Opin. Cell Biol.* **12,** 606–612
5. Hooper, N. M., Karran, E. H., and Turner, A. J. (1997) *Biochem. J.* **321,** 265–279
6. Peschon, J. J., Slack, J. L., Reddy, P., Stocking, K. L., Sunnarborg, S. W., Lee, D. C., Russell, W. E., Castner, B. J., Johnson, R. S., Fitzner, J. N., Boyce, R. W., Nelson, N., Kozlosky, C. J., Wolfson, M. F., Rauch, C. T., Cerretti, D. P., Paxton, R. J., March, C. J., and Black, R. A. (1998) *Science* **282,** 1281–1284
7. Arribas, J., Coodly, L., Vollmer, P., Kishimoto, T. K., Rose-John, S., and Massague, J. (1996) *J. Biol. Chem.* **271,** 11376–11382
8. Mullberg, J., Rauch, C. T., Wolfson, M. F., Castner, B., Fitzner, J. N., Otten-Evans, C., Mohler, K. M., Cosman, D., and Black, R. A. (1997) *FEBS Lett.* **401,** 235–238
9. Desdouits-Magnen, J., Desdouits, F., Takeda, S., Syu, L. J., Saltiel, A. R., Buxbaum, J. D., Czernik, A. J., Nairn, A. C., and Greengard, P. (1998) *J. Neurochem.* **70,** 524–530
10. Gutwein, P., Oleszewski, M., Mechtersheimer, S., Agmon-Levin, N., Krauss, K., and Altevogt, P. (2000) *J. Biol. Chem.* **275,** 15490–15497
11. Fan, H., and Derynck, R. (1999) *EMBO J.* **18,** 6962–6972
12. Gechtman, Z., Alonso, J. L., Raab, G., Ingber, D. E., and Klagsbrun, M. (1999) *J. Biol. Chem.* **274,** 28828–28835
13. Vecchi, M., Baulida, J., and Carpenter, G. (1996) *J. Biol. Chem.* **271,** 18989–18995
14. Dethlefsen, S. M., Raab, G., Moses, M. A., Adam, R. M., Klagsbrun, M., and Freeman, M. R. (1998) *J. Cell. Biochem.* **69,** 143–153
15. Yee, N. S., Langen, H., and Besmer, P. (1993) *J. Biol. Chem.* **268,** 14189–14201
16. Pandiella, A., and Massague, J. (1991) *J. Biol. Chem.* **266,** 5769–5773
17. Kahn, J., Walcheck, B., Migaki, G. I., Jutila, M. A., and Kishimoto, T. K. (1998) *Cell* **92,** 809–812
18. Annabi, B., Pilorget, A., Bousquet-Gagnon, N., Gingras, D., and Beliveau, R. (2001) *Biochem. J.* **359,** 325–333
19. Diaz-Rodriguez, E., Esparis-Ogando, A., Montero, J. C., Yuste, L., and Pandiella, A. (2000) *Biochem. J.* **346,** 359–367
20. Fors, B. P., Goodarzi, K., and von Andrian, U. H. (2001) *J. Immunol.* **167,** 3642–3651
21. Schlondorff, J., Lum, L., and Blobel, C. P. (2001) *J. Biol. Chem.* **276,** 14655–14674
22. Vecchi, M., Rudolph-Owen, L. A., Brown, C. L., Dempsey P. J., and Carpenter, G. (1998) *J. Biol. Chem.* **273,** 20589–20595
23. Manna, S. K., and Aggarwal, B. B. (1998) *J. Biol. Chem.* **273,** 33333–33341
24. Crowe, P. D., Walter, B. N., Mohler, K. M., Otten-Evans, C., Black, R. A., and Ware, C. F. (1995) *J. Exp. Med.* **181,** 1205–1210
25. Arribas, J., Lopez-Casillas, F., and Massague, J. (1997) *J. Biol. Chem.* **272,** 17160–17165
26. Ilan, N., Mohsenin, A., Cheung, L., and Madri, J. A. (2001) *FASEB J.* **15,** 362–372
27. Borland, G., Murphy, G., and Ager, A. (1999) *J. Biol. Chem.* **274,** 2810–2815
28. Fitzgerald, M. L., Wang, Z., Park, P. W., Murphy, G., and Bernfield, M. (2000) *J. Cell Biol.* **148,** 811–824
29. Nath, D., Williamson, N. J., Jarvis, R., and Murphy, G. (2001) *J. Cell. Sci.* **114,** 1213–1220
30. Hargreaves, P. G., Wang, F., Antcliff, J., Murphy, G., Lawry, J., Russell, R. G., and Croucher, P. I. (1998) *Br. J. Haematol.* **101,** 694–702
31. Lum, L., Wong, B. R., Josien, R., Becherer, J. D., Erdjument-Bromage, H., Schlondorff, J., Tempst, P., Choi, Y., and Blobel, C. P. (1999) *J. Biol. Chem.* **274,** 13613–13618
32. Mechtersheimer, S., Gutwein, P., Agmon-Levin, N., Stoeck, A., Oleszewski, M., Riedle, S., Fogel, M., Lemmon, V., and Altevogt, P. (2001) *J. Cell Biol.* **155,** 661–673
33. Hattori, M., Osterfied, M., and Flanagan, J. (2000) *Science* **289,** 1360–1365
34. Izumi, Y., Hirata, M., Hasuwa, H., Iwamoto, R., Umata, T., Miyado, K., Tamai, Y., Kurisaki, T., Sehara-Fujisawa, A., Ohno, S., and Mekada, E. (1998) *EMBO J.* **17,** 7260–7272
35. Koike, H., Tomioka, S., Sorimachi, H., Saido, T. C., Maruyama, K., Okuyama, A., Fujisawa-Sehara, A., Ohno, S., Suzuki, K., and Ishiura, S. (1999) *Biochem. J.* **343,** 371–375
36. Shirakabe, K., Wakatsuki, S., Kurisaki, T., and Fujisawa-Sehara, A. (2001) *J. Biol. Chem.* **276,** 9352–9358
37. Asakura, M., Kitakaze, M., Takashima, S., Liao, Y., Ishikura, F., Yoshinaka, T., Ohmoto, H., Node, K., Yoshino, K., Ishiguro, H., Asanuma, H., Sanada, S., Matsumura, Y., Takeda, H., Beppu, S., Tada, M., Hori, M., and Higashiyama, S. (2002) *Nat. Med.* **8,** 35–40
38. Haro, H., Crawford, H. C., Fingleton, B., Shinomiya, K., Spengler, D. M., and Matrisian, L. M. (2000) *J. Clin. Invest.* **105,** 143–150
39. Powell, W. C., Fingleton, B., Wilson, C. L., Boothby, M., and Matrisian, L. M. (1999) *Curr. Biol.* **9,** 1441–1447
40. Toth, M., Hernandez-Barrantes, S., Osenkowski, P., Bernardo, M. M., Gervasi, D. C., Shimura, Y., Meroueh, O., Kotra, L. P., Galvez, B. G., Arroyo, A. G., Mobashery, S., and Fridman, R. J. (2002) *J. Biol. Chem.* **277,** 26340–26350
41. Kajita, M., Itoh, Y., Chiba, T., Mori, H., Okada, A., Kinoh, H., and Seiki, M. (2001) *J. Cell Biol.* **153,** 893–904
42. Inoue, D., Reid, M., Lum, L., Kratzschmar, J., Weskamp, G., Myung, Y. M., Baron, R., and Blobel, C. P. (1998) *J. Biol. Chem.* **273,** 4180–4187
43. Kurohara, K., Matsuda, Y., Nagabukuro, A., Tsuji, A., Amagasa, T., and Fujisawa-Sehara, A. (2000) *Biochem. Biophys. Res. Commun.* **270,** 522–527
44. Fritsche, J., Moser, M., Faust, S., Peuker, A., Buttner, R., Andreesen, R., and Kreutz, M. (2000) *Blood* **96,** 732–739
45. Wei, P., Zhao, Y.-G., Zhuang, L., Ruben, S., and Sang, Q.-X. (2001) *Biochem. Biophys. Res. Commun.* **280,** 744–755
46. Kang, T., Zhao, Y. G., Pei, D., Sucic, J. F., and Sang, Q. X. (2002) *J. Biol. Chem.* **277,** 25583–25591
47. Wang, X., and Pei, D. (2001) *J. Biol. Chem.* **276,** 35953–35960
48. Gaultier, A., Cousin, H., Darribere, T., and Alfandari, D. (2002) *J. Biol. Chem.* **277,** 23336–23344
49. Gao, G., Westling, J., Thompson, V. P., Howell, T. D., Gottschall, P. E., and Sandy, J. D. (2002) *J. Biol. Chem.* **277,** 11034–11043
50. Zhao, Y. G., Wei, P., and Sang Q. X. (2001) *Biochem. Biophys. Res. Commun.* **289,** 288–294
51. Netzel-Arnett, S., Sang, Q.-X., Moore, W. G. I., Narve, M., Birkedal-Hansen, H., and Van Wart, H. E. (1993) *Biochemistry* **32,** 6427–6432
52. Kang, T., Yi, J., Guo, A., Wang, X., Overall, C. M., Jiang, W., Elde, R., Borregaard, N., and Pei, D. (2001) *J. Biol. Chem.* **276,** 21960–21968
53. Reddy, P., Slack, J. L., Davis, R., Cerretti, D. P., Kozlosky, C. J., Blanton, R. A., Shows, D., Peschon, J. J., and Black, R. A. (2000) *J. Biol. Chem.* **275,** 14608–14614
54. Itai, T., Tanaka, M., and Nagata, S. (2001) *Eur. J. Biochem.* **268,** 2074–2082
55. Bosenberg, M. W., Pandiella, A., and Massague, J. (1992) *Cell* **71,** 1157–1165
56. Liu, X., Hwang, H., Cao, L., Wen, D., Liu, N., Graham, R. M., and Zhou, M. (1998) *J. Biol. Chem.* **273,** 34335–34340
57. Wong, S. T., Winchell, L. F., McCune, B. K., Earp, H. S., Teixidó, J., Massagué, J., Herman, B., and Lee, D. C. (1989) *Cell* **56,** 495–506
58. Sisodia, S. S. (1992) *Proc. Natl. Acad. Sci. U. S. A.* **89,** 6075–6079
59. Müllberg, J., Oberthür, W., Lottspeich, F., Mehl, E., Dittrich, E., Graeve, L., Heinrich, P. C., and Rose-John, S. (1994) *J. Immunol.* **152,** 4958–4968
60. Migaki, G. I., Kahn, J., and Kishimoto, T. K. (1995) *J. Exp. Med.* **182,** 549–557
61. Tang, P., Hung, M. C., and Klostergaard, J. (1996) *Biochemistry* **35,** 8226–8233

[2] T. Kang, H. Park, and Q. X. Sang, unpublished data.

62. Mullberg, J., Durie, F. H., Otten-Evans, C., Alderson, M. R., Rose-John, S., Cosman, D., Black, R. A., and Mohler, K. M. (1995) *J. Immunol.* **155,** 5198–5205
63. Alfalah, M., Parkin, E. T., Jacob, R., Sturrock, E. D., Mentele, R., Turner, A. J., Hooper, N. M., and Naim, H. Y. (2001) *J. Biol. Chem.* **276,** 21105–21109
64. Amour, A., Knight, C. G., Webster, A., Slocombe, P. M., Stephens, P. E., Knauper, V., Docherty, A. J., and Murphy, G. (2000) *FEBS Lett.* **473,** 275–279
65. Amour, A., Slocombe, P. M., Webster, A., Butler, M., Knight, C. G., Smith, B. J., Stephens, P. E., Shelley, C., Hutton, M., Knauper, V., Docherty, A. J., and Murphy, G. (1998) *FEBS Lett.* **435,** 39–44
66. Loechel, F., Fox, J. W., Murphy, G., Albrechtsen, R., and Wewer, U. M. (2000) *Biochem. Biophys. Res. Commun.* **278,** 511–515
67. Kashiwagi, M., Tortorella, M., Nagase, H., and Brew, K. (2001) *J. Biol. Chem.* **276,** 12501–12504
68. Westling, J., Fosang, A. J., Last, K., Thompson, V. P., Tomkinson, K. N., Hebert, T., McDonagh, T., Collins-Racie, L. A., LaVallie, E. R., Morris, E. A., and Sandy, J. D. (2002) *J. Biol. Chem.* **277,** 16059–16066

3.3 Submitted to the Journal of Biological Chemistry, 2003

Regulation of Enzyme Stability by the Cysteine Residues of the Residual Cysteine-rich Domain of the C-terminal Fragment Retained by the Autocatalytic Processing at Glu^{586}-Ser^{587} of Human Adamalysin 19/ADAM19

Tiebang Kang†#, Harald Tschesche#, and Qing-Xiang Amy Sang†

†Department of Chemistry and Biochemistry and Institute of Molecular Biophysics, Florida State University, Tallahassee, Florida 32306-4390, USA; #Department of Biochemistry I, Faculty of Chemistry, University Bielefeld, Bielefeld 33615, Germany.

Regulation of Enzyme Stability by the Cysteine Residues of the Residual Cysteine -rich Domain of the C -terminal Fragment Retained by the Autocatalytic Processing at Glu^{586}-Ser^{587} of Human Adamalysin 19/ADAM19*

Tiebang Kang†#, Harald Tschesche#, and Qing-Xiang Amy Sang†¶
†Department of Chemistry and Biochemistry and Institute of Molecular Biophysics, Florida State University, Tallahassee, Florida 32306-4390, USA; #Department of Biochemistry, Faculty of Chemistry, University Bielefeld, Bielefeld 33615, Germany.

*Supported in part by grants from the National Institutes of Health, CA78646, the DOD U.S. Army Medical Research Acquisition Activity, DAMD17-02-1-0238, the American Cancer Society, Florida Division F01FSU-1, and the Florida State University Research Foundation (to Q-X. A. S.), as well as the Deutsche Forschungsgemeinschaft, Bonn, by the SFB 549, project A05 and the DFG-grant, Ts 8-35/3 (to H.T.)

Running Title: Disulfide Bonds Affect the Processing of hADAM19

¶To whom correspondence should be addressed:
Prof. Q.-X. Amy Sang
Department of Chemistry and Biochemistry
Florida State University
203 DLC, Chemistry Research Building, Room 203
Tallahassee, Florida 32306-4390
Tel: 850-644-8683; Fax: 850-644-8281
E-mail: sang@chem.fsu.edu
http://www.chem.fsu.edu/editors/sang/sang.htm

ABBREVIATIONS

ADAM, a disintegrin and metalloproteinase; ADAMTS, a disintegrin and metalloproteinase with thrombospondin-like motifs; alpha 2-M, alpha-2-macroglobulin; APP, amyloid precursor protein; CaM, calmodulin; DMEM, Dulbecco's modified Eagle´s medium; ECM, extracellular matrix; FBS, fetal bovine serum; IL-1R-II , interleukin 1 receptor II; MDC, Metalloprotease/Disintegrin/Cysteine-rich; MDCK, Madin-Darby canine kidney; NRG, neuregulin; pAb, polyclonal antibody; PBS, phosphate buffered saline; PKC, protein kinase C; PMA, phorbol-12 myristate 13-acetate; SDS-PAGE, sodium dodecyl sulfate polyacrylamide gel electrophoresis; TACE, tumor necrosis factor alpha convertase; TIMPs, tissue inhibitor of matrix metalloproteinases; TGF-alpha, transforming growth factor-alpha; TGN, *trans*-Golgi networks; TNF-alpha , tumor necrosis factor-alpha; W7, N-(6-aminohexyl)-5-chloro-1-naphthalenesulfonamide.

SUMMARY

We reported that human adamalysin 19 (a disintegrin and metalloproteinase 19, hADAM19, meltrin beta) is activated by furin-mediated cleavage of the prodomain followed by an autolytic processing at Glu^{586}-Ser^{587} within the cysteine-rich domain (Kang *et al. J. Biol. Chem.*, 277: 25583-25591 and 48514-48522, 2002). Here we demonstrated that this autolytic processing at Glu^{586}-Ser^{587} occurred intramolecularly, producing an NH_2-terminal fragment (N-fragment) associated with its COOH-terminal fragment (C-fragment) through disulfide bonds. Cys^{605}, Cys^{633}, Cys^{639}, and Cys^{643} within the residual cysteine-rich domain of the C-fragment are partially responsible for the covalent association of the C-fragment with the N-fragment. A new processing site at Lys^{543}-Val^{544} was identified in soluble mutants when these cysteine residues were individually mutated to serine residues. These mutated proteins were folded, secreted, and had enzymatic activity, but were less stable and more easily degraded than the soluble wild type, as illustrated by trypsin digestion and inactive mutant studies. The proteolytic activity and the stability of soluble hADAM19 may be regulated by the formation of disulfide bonds between cysteine residues within the N-fragment and C^{605}, C^{633}, C^{639}, and C^{643} at the C-fragment. Moreover, the new processing site resulted from autolytic cleavage was independent of the processing at Glu^{586}-Ser^{587} by utilizing the double mutations of Cys633Ser/Glu586Asp or Cys639Ser/Glu586Asp. Shed fragments are also detectable in the media from Madin-Darby canine kidney cells stably expressing the full length Cys633Ser mutant. Ilomastat (GM6001), a potent matrix metalloproteinase inhibitor, only had little effect on the shedding process although it inhibited digestion of a peptide substrate by purified hADAM19, suggesting that this shedding process may be an intracellular event. Thus, the cysteine-rich domain may regulate the enzyme stability and activity of ADAMs via the formation of inter-fragment disulfide bond(s).

INTRODUCTION

Ectodomain shedding, a process by which transmembrane proteins proteolytically release their extracellular domains, plays a critical role in many physiological and pathological conditions (1-3). Numerous studies have shown that ADAMs (A Disintegrin And Metalloprotease), also called adamalysin/ MDC (Metalloprotease, Disintegrin, Cysteine-rich), such as ADAM17/TACE, ADAM10/Kuzbanian (KUZ), ADAM9, ADAM19/MDC beta??and ADAM12/MDC alpha, are the predominant sheddases responsible for the shedding of most molecules identified so far, such as tumor necrosis factor-alpha (TNF-alpha), transforming growth factor-alpha (TGF-alpha), interleukin 1 receptor II (IL-1R-II), Notch and its ligand Delta, amyloid precursor protein (APP), heparin-binding epidermal growth factor (HB-EGF), mucin MUC1, and neuregulin-beta?(NRG-beta1) (3-5). The activities of ADAMs are regulated at multiple levels including transcription, translation, zymogen activation, and inhibition by tissue inhibitors of matrix metalloproteinases (TIMPs) (2-6). The principle regulatory step is zymogen activation, which has been attractive to a number of investigators with the predominant focus on the regulation rela ted to prodomain removal (6-18). Synthesized as zymogens, ADAMs must undergo prodomain cleavage by either furin or furin-like proprotein convertases before they display any proteolytic activities, as in the cases of ADAM1, 9, 12, 15, 17, 19, a disintegrin and metalloproteinase with thrombospondin 1-like motifs (ADAM-TS) 1, 4, 12, (6-16), or by autolysis, as seen in ADAM8 (17) and ADAM28 (18). However, in some ADAMs, the prodomains have functions involved in their catalytic activities. For example, deletion of the prodomain destroys the proteolytic activity of ADAM10 (19, 20). In the cases of ADAM12 and 17, the prodomains are not only an inhibitor of the catalytic domain, but also appear to act like a chaperone, facilitating secretion, folding, or both for the ADAM proteins (12, 21). In addition, many mutations interfere with the folding or processing of ADAMs, resulting in a lack of proteolytic processing. For instance, the cysteine residue replaced with alanine in the prodomain of ADAM9 abolished its

prodomain removal (12); both His^{346} and His^{350} substitutions with alanines in the metalloproteinase domain of mouse ADAM19 abrogated the processing of its prodomain (22); the L73P mutant of ADAM12 resulted in complete retention of ADAM12 in the endoplasmic reticulum (ER) and inhibition of its processing (14); the soluble form of ADAM13 has never been converted into its mature form, indicating that the transmembrane domain, cytoplasmic domain, or both, are indispensable for the processing of the prodomain in ADAM13 (23); the removal of the disintegrin and cysteine-rich domains in the tumor necrosis factor-alpha converting enzyme (TACE)/ADAM17 resulted in secretion of the mature catalytic domain in association with the precursor (pro) domain, demonstrating that the disintegrin and cysteine-rich domains appear to play a role in the release of the prodomain (21).

Most recently, there is increasing evidence showing that C-terminal truncation plays a critical role in the regulation of the proteolytic activity of ADAMs, as illustrated by ADAM8, 13, and 19, and ADAM-TS4 (16, 17, 23-25). This truncation produces active enzymes or functional fragments to exert their functions, such as acting as sheddases, binding with integrins on the cell surface, or digesting components of the extracellular matrix (ECM) (16, 17, 23-25). However, the regulation of this processing remains to be uncovered. Intriguingly, Smith *et al.* showed that the cysteine-rich domain affects the proteolytic activity of ADAM13 *in vivo*, probably by an intramolecular interaction with its metalloproteinase domain, and that this model might be applied to other ADAMs (26). This prompted us to explore how this intramolecular interaction occurs in ADAMs, since we demonstrated that an autolytic processing of hADAM19 at E^{586}-S^{587} within the cysteine-rich domain takes place in the secretory pathway (24). Based on the fact that the E^{586}-S^{587} processed active N-fragment containing metalloproteinase and disintegrin domains and a segment of the cysteine-rich domain is not released from the C-fragment containing the C-terminal part of the cysteine-rich domain and epidermal growth factor (EGF)-like domain under non-reducing conditions (24),

we hypothesized that interfragment disulfide bond(s) may play a crucial role in the processing of hADAM19. This report provides evidence that a critical role in the stability of the processed hADAM19 is played by disulfide bonds formed between cysteine residues in the N-fragment and those in the segment of the cysteine-rich domain of the processed C-fragment.

MATERIALS AND METHODS

Chemicals, Cell Lines, Cell Culture, and Immunological Reagents---All common laboratory chemicals, proteinase inhibitors, phorbol-12 myristate 13-acetate (PMA), N-(6-aminohexyl)-5-chloro-1-naphthalenesulphonamide (W7), trypsin, soybean trypsin inhibitor, and anti-FLAG-M2 monoclonal antibody and its agarose conjugates were purchased from Sigma (St. Louis, MO). A matrix metalloproteinase inhibitor, Ilomastat (GM6001), was purchased from BACHEM (Philadephia, PA). Restriction enzymes were purchased from Promega (Madison, WI) or Invitrogen (Gaithersburg, MD). COS1, Madin Darby canine kidney (MDCK) cells and its derivatives were maintained as described (13, 24). Dulbecco's modified Eagle's medium (DMEM) was purchased from Invitrogen Gibco BRL (Gaithersburg, MD). Fetal bovine serum (FBS), penicillin G, and streptomycin were purchased from Life Technologies (Rockville, MD). alpha2-macroglobulin (alpha 2-M) was purchased from Roche Molecular Biochemicals (Indianapolis, IN). Rabbit polyclonal hADAM19 antibody pAb361 (anti-metalloproteinase domain, anti-Cat) was generated by our laboratory as reported (27).

Polymerase Chain Reaction (PCR) Primers, Mutagenesis, and Expression Constructs---All inserts tagged with FLAG at their C-terminus were cloned into pCR3.1uni, including wild type hADAM19 (F46), soluble hADAM19 (D52), D-E346A, D-E586D, D-CR (described in Ref. 24), and all mutants used in this study. For D586 deleted from S587 to the end of the C-terminal: forward primer, 5'- ACC ATG CCA GGG GGC GCA GGC GCC-3'; reverse primer, 5'- CTC CAG GGG CCG GGC CTC AGA G -3'. For the soluble C^{605} to S^{605} mutants (D-C605S): forward primer, 5'- CAG ATC CAG **TCC** CGG GGC ACC CAC-3';

reverse primer, 5'- GGT GCC CCG **GGA** CTG GAT CTG CC-3'. For the full length and soluble C^{633} to S^{633} mutants (F-C633S and D-C633S): forward primer, 5'- GGA ACC AAG **TCT** GGC TAC AAC C-3'; reverse primer, 5'- GTT GTA GCC **AGA** CTT GGT TCC AG-3'. For the soluble C^{639} to S^{639} mutant (D-C639S): forward primer, 5'- C AAC CAT ATT **TCC** TTT GAG GGG CAG-3'; reverse primer, 5'- CCC CTC AAA **GGA** AAT ATG GTT G-3'. For the full length and soluble C^{643} to S^{643} mutants (F-C643S and D-C643S): forward primer, 5'- GAG GGG CAG **TCC** AGG AAC ACC TC-3'; reverse primer, 5'- GGT GTT CCT **GGA** CTG CCC CTC AAA G-3'. For the double mutants, including E^{586} to D^{586} and C^{633} to S^{633} (D-C633S/E586D), E^{586} to D^{586} and C^{639} to S^{639} (D-C639S/E586D), E^{346} to A^{346} and C^{633} to S^{633} (F- C633S/E346A and D-C633S/E346A), and E^{346} to A^{346} and C^{643} to S^{643} (F-C643S/E346A and D-C643S/E346A), we used D-E586D or D-E346A as the template and the primers for C^{633} to S^{633} or C^{639} to S^{639}, respectively. All constructs were confirmed by DNA sequencing.

DNA Transfection and Generation of Stable Cell Lines---COS1 cells were seeded in 24-well plates for 16-24 hrs at 80% confluence and transfected or co-transfected with the indicated plasmids using LipofectAMINE2000 according to the instructions provided by Invitrogen (Gaithersburg, MD). After 6-10 hrs, serum-free DMEM media and the indicated reagents were added and incubated for another 24 hrs. The conditioned media and cell lysates were then analyzed by Western blotting (13, 24). The same transfection procedure was performed to generate stable MDCK cell lines, and the selection for hADAM19 was begun in the presence of G418 (400 ug/ml) after transfection for 24 hours. The conditioned media and/or cell lysates of the clones were subjected to Western blotting to confirm the expression of hADAM19 (13, 24). For co-culture cells, the indicated MDCK stable lines were equally mixed in the same wells overnight, followed by serum-free media for 24 hours, and the media were then analyzed by Western blotting.

Western Blotting----The experiments were carried out as described previously (13, 24). Briefly, cells were grown to 80% confluence and were treated as indicated. After centrifugation for 15 mins at 14,000 x *g* and 4ºC to clear any debris, the serum-free media were collected and prepared for SDS-PAGE. The cells were lysed with RIPA buffer (50 mM Tris, pH 7.5, 150 mM NaCl, 0.25% sodium deoxycholate, 0.1% NP-40, 1 mM phenyl-methyl-sulfonyl-fluoride, 1 mM of 1, 10-phenasrol, 10 ug/ml aprotinin, 10 ug/ml E64, and 10 ug/ml pepstatin A) for 15 min on ice. The supernatant was collected after centrifugation for 20 min at 14,000 x *g* and 4ºC. After electrophoresis, the proteins were transferred onto nitrocellulose membranes, probed with anti-FLAG-M2 or anti-Dis, and developed as before (13, 24).

Purification of Soluble hADAM19 and Co-incubation with Purified Proteins--- The proteins of D-CR and D-E346A were produced earlier in our laboratory, all proteins were purified on anti-FLAG-M2 affinity columns as described previously (24). Briefly, cells from stable lines expressing soluble hADAM19, D586, D-C633S, or D-C633S/E586D, were grown to 100% confluence, washed twice with phosphate buffered saline (PBS), and incubated for 48 hours in serum-free media. The conditioned media were collected, centrifuged to clear any debris, and loaded onto an anti-M2 immunoaffinity column (1 ml of resuspended agarose) that had been prewashed with HEPES buffer. The bound materials were extensively washed with HEPES buffer, eluted with FLAG peptides, and collected in 500 ul fractions. The fractions were analyzed by Western blot using anti-hADAM19 antibodies or anti-FLAG-M2, and the protein concentration was quantified by absorbance at 280 nm. The fraction containing the highest interested proteins was characterized by protein N-terminal sequencing as described previously (13, 24), and the fractions containing the most wild type or mutant hADAM19 proteins were used for the flourescamine assay or the co-incubation of purified proteins to test substrate cleavage. For the co-incubation of purified proteins, we mixed the purified protein of D-E346A with D-CR or D586 equally at 100 ng/ul overnight, then the processing of D-E346A by D-CR or D586 was detected by Western blotting with Anti-FLAG-M2 as above.

Trypsin Digestion Experiment---The protocol followed was from a report by Dr. Bond's group (28). Briefly, Trypsin was added to the conditioned media from D-52-5, D-C633S-4, or D586 at a final concentration of 5, 10, 20, or 40 ng/ul in 20 mM Tris-HCl, pH 7.5. After incubation at 37ºC for 30 min, soybean trypsin inhibitor was added at a 2-fold excess of trypsin. Samples were incubated at 25ºC for 15 min, followed immediately by Western blotting using anti-FLAG-M2.

Determination of the Activity of hADAM19 Using a Peptide Assay---Procedural details were described previously (24). Stock solutions of the peptide substrates at 20 mM were prepared in 0.05 M HEPES, pH 7.5, 0.2 M NaCl, 0.01 M $CaCl_2$, and 0.01% Brij-35, and the enzyme concentration was about 160 nM. Hydrolysis of the peptide by the enzyme following incubation for 2.5 hours was monitored by measuring fluorescence intensity using fluorescamine assay.

RESULTS

Autolytic Processing at E^{586}-S^{587} of hADAM19 is an Intramolecular Interaction. We recently developed a peptide substrate to determine the activity of hADAM19 by a fluorescamine assay, and reported that the autolytic processing at E^{586}-S^{587} within the cysteine-rich domain is necessary for its proteolytic activities against both this peptide substrate and ?2-M (24). To directly prove that the processed N-fragment, containing metalloproteinases and disintegrin domains and a part of the cysteine-rich domain, is active, we generated a truncated form of hADAM19, from the beginning to E^{586} and tagged with C-terminal FLAG tag (D586) (see Fig. 3), which was found to have the same activity as D-CR against this peptide substrate (24, data not shown). To determine if processing at E^{586}-S^{587} of hADAM19 is an inter- or intra-molecular interaction, we used several independent approaches. As shown in Fig. 1, the inactive soluble hADAM19 (D-E346A) (24) was not processed by either one of its active

soluble forms, D586 and D-CR, when co-cultured with their stably-expressing MDCK cells, suggesting that the processing at E^{586}-S^{587} of hADAM19 is an intramolecular interaction. Furthermore, either D586 or D-CR failed to process D-E346A when we performed a transient co-transfection using D-E346A with either D586 or D-CR in COS1 cells, or incubated their purified proteins *in vitro* using D-E346A with D586 or D-CR (data not shown). These results strongly argue that an intramolecular interaction results in the processing of hADAM19 at E^{586}-S^{587}.

Disulfide Bonds are Responsible for the Association of the N-fragment with the C-fragment Processed at E^{586}-S^{587} of hADAM19. We have previously suggested that the processed N-fragment at E^{586}-S^{587} of hADAM19 may be associated with its processed C-fragment via one or more disulfide bonds (24). To further explore this possibility, we ran the conditioned media from MDCK cells stably expressing D52 (D52-5) side by side under either reducing or non-reducing condition. As showed in Fig. 2A and 2B, the mature forms of hADAM19 were detected under both reducing and non-reducing conditions. However, the fragment at 26 kDa representing the processed C-fragment at E^{586}-S^{587} of hADAM19 was detectable only under reducing condition (Fig. 2A). Moreover, the processed N-fragments emerged together with the mature forms under non-reducing conditions (Fig. 2B). Therefore, we may draw the conclusion that the processed C-fragment containing a part of the cysteine-rich domain and EGF-like domain forms disulfide bonds with the processed N-fragment including metalloproteinase and disintegrin domains and a segment of the cysteine-rich domain, in soluble hADAM19.

Since the processing at E^{586}-S^{587} of hADAM19 is an intramolecular interaction (Fig. 1), and the proteolytic activity of ADAM13 has recently been shown to be regulated by its cysteine-rich domain through intramolecular functioning with its metalloproteinase domain (26), we hypothesized that the disulfide bonds formed by the cysteine residues of the N-fragment and those within the part of the cysteine-rich domain retained by the processed C-

fragment may play a critical role in the processing of hADAM19 at E^{586}-S^{587}. To evaluate this, we mutated the cysteine residues at C^{605}, C^{633}, C^{639}, and C^{643} to S^{605}, S^{633}, S^{639}, and S^{643} within this region of soluble hADAM19, respectively (Fig. 3), then transiently transfected these mutants into COS1 cells. The results shown in Fig. 2C revealed that all mutants produced a new C-fragment at around 32 kDa, while the normal processing of the 26 kDa fragment at E^{586}-S^{587} remained unchanged in the mutants with C^{605}, C^{633}, and C^{639} to S^{605}, S^{633}, and S^{639}, respectively. However, the levels of both 26 and 32 kDa fragments in the mutant of C^{643} to S^{643} were decreased dramatically. When running these samples under non-reducing conditions, we found that the processed C-fragments at 26 and 32 kDa were not associated with their processed N-fragments, suggesting that the association of the N-fragment with the C-fragment of hADAM19 processed at E^{586}-S^{587} was destroyed by the disruption of one or more disulfide bonds formed between any cysteine residue at C^{605}, C^{633}, C^{639}, or C^{643} and a cysteine residue(s) in the N-fragment.

Disulfide Bonds Linked by C^{605}, C^{633}, C^{639} or C^{643} and Cysteine Residues in the N-fragment are Involved in the Stability of Soluble hADAM19. To further investigate the functions of different disulfide bonds that include C^{605}, C^{633}, C^{639}, or C^{643}, we generated MDCK cells stably expressing the soluble mutants of C^{605}, C^{633}, C^{639}, and C^{643} to S^{605}, S^{633}, S^{639}, and S^{643}, called D-C605S, D-C633S, D-C639S, and D-C643S, respectively. As shown in Fig. 4A, a high expression of soluble hADAM19 was detected in the cell lysates from D-C643S, but the proteins in the media contained negligible mature or processed forms of soluble hADAM19, indicating that the proteins expressed by D-C643S are not folded or secreted properly, or are less stable and more easily degraded when the disulfide bond formed between C^{643} and a cysteine residue at N-fragment is destroyed. However, aside from the mature forms, we also detected the fragments at 26 and 32 kDa by anti-FLAG-M2 in the media from D-C605S, D-C633S, and D-C639S at different levels (Fig. 4A). Once again, the protein expression level of D-C633S is the highest among the mutants, consistent with the results obtained in the COS1

transient transfection as shown in Fig. 2C, suggesting that the proteins of D-C633S, D-C639S, and D-C605S are more stable and more difficult to degrade, or have fewer problems related to folding and secretion than the proteins of D-C643S. However, compared with proteins from the soluble wild type hADAM19, lower levels of hADAM19 were detectable in the media from D-C633S, D-C639S and D-C605S. The protein levels among these transfects were comparable as shown in Fig. 4A, indicating that the disulfide bonds formed between cysteine residues at N-fragment and one or more cysteine residues at C^{605}, C^{633}, C^{639}, and C^{643} play different roles in soluble hADAM19.

We chose D-C633S and D-C643S as representatives to generate inactive enzymes, in which a catalytic residue E^{346} was mutated to A^{346}. As shown in Fig. 4B, the protein levels in the media from MDCK cells stably expressing both double mutants, D-C633S/E346A and D-C643S/E346A, were comparable with those in the media from cells expressing the soluble inactive form (D-E346A), demonstrating that the disruption of one or more disulfide bonds formed between cysteine residues in N-fragment and one or more cysteine residues of C^{605}, C^{633}, C^{639}, and C^{643} within the cysteine-rich domain does not disturb the folding and secretion of soluble hADAM19. Taken together, we speculate that soluble hADAM19 is stabilized and prevented from its autolysis by one or more interfragment disulfide bonds formed between cysteine residues at N-fragment and one or more cysteine residues at C^{605}, C^{633}, C^{639}, and C^{643}.

To further confirm above speculation related to the function of these cysteine residues within the part of the cystein-rich domain retained by the C-fragment processed at E^{586}-S^{587} of soluble hADAM19, we tested the susceptibility of these soluble hADAM19 mutants to trypsin digestion, as used in the case of meprin A (28), which showed that cysteine mutants in the MAM domain of meprin A were more susceptible to activation by trypsin. The medium of D-C633S-4, containing the highest expression level of mature and processed forms of hADAM19 among the stable lines (Fig. 4A), was chosen for comparison with soluble

hADAM19, D52-5. As shown in Fig. 5, the products of the trypsin digestion in the medium from D52-5 were more stable than those from D-C633S-4, suggesting again that one or more mutated cysteines in this region may result in less stability or more vulnerability to the degradation of soluble hADAM19. This conclusion was further supported by another experiment using the protein of D586, which lacked the C-fragment processed at E^{586}-S^{587} of hADAM19 and was more susceptibility to trypsin digestion than D52-5 (Fig. 5). Considered together, our results suggest that one or more of the interfragment disulfide bonds formed between cysteine residues at the N-fragment and one or more cysteine residues at C^{605}, C^{633}, C^{639}, and C^{643} accounts for much of the stability of hADAM19. Less stability and more degradation, but not incorrect folding and secretion, of these mutated proteins, may be responsible for the decreased levels of mature or processed forms of soluble hADAM19 detected in the media from the MDCK cells stably transfected with these Cys to Ser mutants.

The New Processing at K^{543}-V^{544} is Independent of the Processing at E^{586}-S^{587}. Since the autolytic processing at E^{586}-S^{587} of soluble hADAM19 is necessary for its proteolytic activity (24), and the new processing is also an autolysis (Fig. 4B), it was very intriguing to determine if this new processing is dependent of the processing at E^{586}-S^{587}. To address this issue, we made two soluble double mutants, C^{633} to S^{633} and E^{586} to D^{586} (D-C633S/E586D), and C^{639} to S^{639} and E^{586} to D^{586} (D-C639S/E586D) (Fig. 3) because there was rare processing at E^{586}-S^{587} when E^{586} was mutated to D^{586} as described in our previous report (24). We then performed transient transfection with these mutants into COS1 cells. As shown in Fig. 6A, the protein at 32 kDa was detectable in these double mutants, although the protein at 26 kDa, representing the processing at E^{586}-S^{587}, disappeared in these media, suggesting that the new processing is independent of, but not followed by, the processing at E^{586}-S^{587}. This independence was further confirmed when we generated MDCK cells stably expressing the soluble double mutants of D-C633S/E586D, as shown in Fig. 6B. To determine the new peptide bond cleavage site, we chose one stable MDCK transfectant, D-C633S/E586D-9, as the

representative to purify the proteins from their media by anti-FLAG-M2 affinity column and electrophoresis. N-terminal sequencing revealed that the starting sequence of the purified 32 kDa protein was VNVAGDT, which is identical to ^{544}VNVAGDT within the cysteine-rich domain of hADAM19. This suggests that the processing of hADAM19 at K^{543}-V^{544} is an alternative site within its cysteine-rich domain when the primary site at E^{587}-S^{587} is impaired dramatically or its intramolecular disulfide bonds are destroyed

The Shedding is Detectable in the Full Length of hADAM19 with C^{633} to S^{633}, and This Shedding is Regulated by Protein Kinase C (PKC), calmodulin (CaM), and Calcium Signals. Based upon the results shown in Figs. 2C, 4A, and 6, the shedding ability of the full length mutants with Cys to Ser was further examined by choosing C^{633} to S^{633} (F-C633S) and C^{643} to S^{643} (F-C643S) as representatives with different stabilities. As shown in Fig. 7A, three shed proteins around 44~53 kDa were clearly detected in the media from the MDCK cells stably transfected with F-C633S, but neither with the wild type (F46) nor with F-C643S. Expression levels were comparable among these stable transfectants, consistent with the results obtained earlier with their soluble forms (Figs. 2C, 4A). The double mutants F-C633S/E346A also failed to shed (data not shown), demonstrating that F-C633S undergoes autolytic shedding. Moreover, we revealed that phorbol-12-myristate 13-acetate (PMA), a PKC activator, apparently enhanced the shedding of full length hADAM19 with C^{633} to S^{633}, and that W7, an inhibitor of CaM, and A23187, a calcium ionophore, inhibited this shedding, consistent with our recent report showing that PKC, CaM and calcium signal pathways may be involved in the processing of hADAM19 at E^{586}-S^{587} (24). A potent and broad-spectrum matrix metalloproteinase inhibitor, Ilomastate (GM6001), had only little effect on the shedding of MDCK cells stably expressing F-C633S of hADAM19 (Fig. 7B) although it was a blocker of many shedding processes (3, 29). Interestingly, GM6001 was able to dramatically inhibit the activity of soluble hADAM19 against our peptide substrate used previously (24, data not shown), indicating GM6001 was not easily accessible to the intracellular environment during

the shedding process. Our current results also support the concept that the processing of hADAM19 at E^{586}-S^{587} takes place intracellularly (24).

DISCUSSION

In this current report, we provide evidence that any one of the cysteine residues within the fraction of the cysteine-rich domain of the C-fragment of hADAM19 processed at E^{586}-S^{587} is indispensable for the association of the processed N-terminal with its C-terminal, and plays a critical role in the stability of hADAM19. This may lead the first report that the cysteine-rich domain likely forms disulfide bonds to regulate the proteolytic activity of ADAMs *in vitro*.

Significance of Autolytic Processing or Shedding in hADAM19. Among ADAMs, ADAM8, 13, 19 and ADAM-TS4 have been shown to be processed intracellularly by autolysis (16, 17, 23-25), producing an active enzyme or a functional fragment responsible for binding with alpha2-M or integrins, mediating cell adhesion, or digesting components in the ECM. Following our previous report (24), we have demonstrated in this report that hADAM19 processing or shedding occurs at a different site, K^{543}-V^{544}, within its cysteine-rich domain, which is prior to the normal processing site at E^{586}-S^{587}, under certain conditions, as in the case of the disruption of disulfide bonds by mutation or reduction. This also produces an active enzyme, as shown in Figs. 2C, 4A, 6, and 7, because the processing or shedding of hADAM19 depends on its own proteolytic activity (Fig. 4B, and Ref. 24), but is independent of the normal processing at E^{586}-S^{587} (Fig. 6). Notably, the processing site of E^{586}-S^{587} is the predominant one even in the case of the disruption of the intramolecular disulfide bonds (Fig. 2A, 4C, 6). However, the site of K^{543}-V^{544} become the major one when the intramolecular disulfide bonds are destroyed and its primary site is mutated (Fig. 6). Given that the processing at E^{586}-S^{587} within the cysteine-rich domain is necessary for its proteolytic activities (24), we speculate that there is an alternative site, such as K^{543}-V^{544}, for the processing or shedding of hADAM19 within the cysteine-rich domain to produce a fully

activated hA DAM19, indicative of its very important roles in both physiological and pathological conditions.

The Functions of the Cysteine-rich Domain in ADAMs. The "cysteine-rich domain" is sometimes referred to the cysteine-rich domain together with the disintegrin domain. In these cases, the "cysteine-rich domain" has been shown to be related to cell adhesion, such as in the cases of ADAM8, 12, 13, or to the proteolytic activity of TACE/ADAM17. For example, the recombinant disintegrin/cysteine-rich domain of ADAM8 mediates cell adhesion in cells expressing ADAM8 (17); the "cysteine-rich domain" of ADAM12 promotes the adhesion of fibroblasts and myoblasts (30); the disintegrin and cysteine-rich domains of ADAM13 bind to both fibronectin and to beta1-containing integrin receptors, and binding can be inhibited by antibodies against the cysteine-rich domain (23); the "cysteine-rich domain" of TACE/ADAM17 is required for shedding of IL-1R-II while affecting the inhibitor sensitivity of TNF-alpha shedding (31).

Despite the knowledge about the combined functions of both disintegrin and cysteine-rich domains, very little information is available about cysteine-rich-domain-specific functions. Iba *et al.* reported that it acts as a ligand for the cell-adhesion molecule syndecan as shown for the cysteine-rich domain of ADAM12 (32, 33). Dr. DeSimone's group recently showed that the cysteine-rich domain of ADAM13 cooperates intramolecularly with the metalloproteinase domain of ADAM13 to regulate its function, providing the first evidence that a downstream extracellular adhesive domain plays an active role in the regulation of ADAM protease function *in vivo* (26). In this report, we have demonstrated that disulfide bonds paired between cysteine residues of N-fragment and one or more cysteine residues at C^{605}, C^{633}, C^{639}, and C^{643} within the fraction of the cysteine-rich domain of the C-fragment processed at E^{586}-S^{587} of hADAM19 are necessary for the association of the processed N-fragment with its C-fragment (Fig. 2), and play a critical role in the regulation of hADAM19 activity by stabilizing the enzyme and preventing its autolysis (Figs. 4, 5, 6, 7). Therefore, we

may speculate that these disulfide bonds are very likely to be formed interfragmently between the N-fragment, conta ining the metalloproteinase, disintegrin, and part of the cysteine rich domain of hADAM19, and the C-fragment, containing the other part of the cysteine-rich domain after processed at E^{586}-S^{587} of hADAM19. Our results provided first pieces of evidence *in vitro* to support the results of the *in vivo* ADAM13 studies discussed above (26), and gave a very reasonable explanation for the fact that the processing or shedding of hADAM19 occurred autolytically and intramolecularly within its cysteine-rich domain (24; Figs. 1, 4B; and data not shown).

It is possible that the disulfide bonds are formed between the disintegrin domain of hADAM19 and this region of the cysteine -rich domain of the C-fragment because the disintegrin domain of hADAM19 also plays a key role in the proteolytic activity of hADAM19. We have previously shown that our specific antibody against the disintegrin domain inhibited substrate cleavage *in vitro* (27), and the deletion mutant containing only the metalloproteinase domain of hADAM19 lacked proteolytic activity using alpha 2-M and peptide substrate assays *in vitro* (data not shown). Any one of four cysteine residues at C^{605}, C^{633}, C^{639}, and C^{643} in the part of cysteine-rich domain is indispensable for the association between the N-fragment and C-fragment processed at E^{586}-S^{587}. We presume three disulfide bonds may have formed. One formed between two cysteine residues of C^{605}, C^{633}, C^{639}, and C^{643} and two formed by the remaining two cysteine residues paired with two other cysteine residues with at least one occurring prior to the position of E^{586} in the N-fragment. Alternatively, four disulfide bonds may exist, formed by C^{605}, C^{633}, C^{639}, and C^{643} with four other cysteine residues, with at least one being before the position of E^{586}. These bonds ha ve a strong coordination with each other, and when one of these disulfide bonds is disrupted, the others will be subsequently disturbed. Therefore, we propose that three or four disulfide bonds linked by the four cysteine residues at C^{605}, C^{633}, C^{639}, and C^{643} with other cysteine residues in the N-fragment are responsible for the association between the N-fragment and C-fragment

processed at E^{586}-S^{587}. Currently, we are unable to speculate the identities of these disulfide bonds as there are total 43 cysteine residues available in the metalloproteinase, disintegrin, cysteine-rich and EGF-like domains of hADAM19. In the near future, we would like to determine the identity of these disulfide bonds using multiple approaches including structural biology, analytical chemistry, and biochemical methods.

Acknowledgements

We thank Margaret Seavy at the Bioanalytical Facility of Florida State University for protein N-terminal sequencing. We are also grateful to the members of Professor Sang's laboratory, Yewseok Suh for his excellent technical assistance, Robert G. Newcomer for his editorial assistance, and Dr. Hyun I. Park, Dr. Yunge Zhao, and Douglas Hurst for providing valuable suggestions and discussions.

REFERENCES

1. Blobel, C. P. (2000) *Curr. Opin. Cell. Biol.* **12**, 606-612
2. Schlondorff, J. and Blobel, C. P. (1999) *J. Cell Science* **112**, 3603-3617
3. Kheradmand, F. and Werb, Z. (2002) *BioEssay* **24**, 8-12
4. Seals, D. F., and Courtneidge, S. A. (2003) *Gene & Development* **17**, 7-30
5. Thathiah, A., Blobel, C. P., and Carson, D. D. (2003) *J. Biol. Chem.* **278,** 3386-3394
6. Brew, K., Dinakarpandian, D., and Nagase, H. (2000) *Biochim. Biophys. Acta*. **1477**, 267-283
7. Cal, S., Arguees, J. M., Fernandez, P. L., and Lopez-Otin, C. (2001) *J. Biol. Chem.* **276**, 17932-17940
8. Kuno, K., Terashima, Y., and Matsushima, K. (1999) *J. Biol. Chem.* **274,** 18821-18826

9. Loechel, F., Gilpin, B. J., Engvall, E., Albrechtsen, R., and Wewer, U.M. (1998) *J. Biol. Chem.* **273**, 16993-16997

10. Lum, L., and Blobel, C. P. (1997) *Dev. Biol.* **191**, 131-145

11. Lum, L., Reid, M. S., and Blobel, C. P. (1998) *J. Biol. Chem.* **273**, 26236-26247

12. Roghani, M., Becherer, J. D., Moss, M. L., Atherton, R. E., Erdjument-Bromage, H., Arribas, J., Blackburn, R. K., Weskamp, G., Tempst, P., and Blobel, C. P.(1999) *J. Biol. Chem.* **274**, 3531-3540

13. Kang, T., Zhao, Y. G., Pei, D., Sucic, J. F., and Sang, Q. X. (2002) *J. Biol. Chem.* **277**, 25583-25591

14. Cao, Y., Kang, Q., Zolkiewska, A. (2001) *Biochem J.* **357**, 353-361

15. Schlondorff, J., Becherer, J. D., and Blobel, C.P. (2000). *Biochem. J.* **347**:131-138

16. Gao, G., Westling, J., Thompson, V. P., Howell, T. D., Gottschall, P. E., and Sandy, J. D. *J. Biol. Chem.* (2002), **277** , 11034-11043

17. Schlomann, U., Wildeboer, D., Webster, A., Antropova, O., Zeuschner, D., Knight, C. G., Docherty, A. J., Lambert, M.,Skelton, L., Jockusch, H., and Bartsch, J. W. (2002) *J. Biol. Chem.* **277,** 48210-48219

18. Howard, L., Maciewicz, R. A., and Blobel, C. P. (2000) *Biochem. J.* **348** , 21-27

19. Anders, A., Gilbert, S., Garten, W., Postina, R., and Fahrenholz, F.. (2001) *FASEB J*. **15**:1837-1839

20. Fahrenholz, F., Gilbert, S., Kojro, E., Lammich, S., and Postina, R.. (2000) *Ann. N. Y. Acad. Sci*. **920,** 215-222

21. Milla, M. E., Leesnitzer M. A., Moss. M. L., Clay, W. C. Carter, H. L., Miller, A. B., Su, J., Lambert, M. H., Willard, D.H.,Sheeley, D. M., Kost, T. A., Burkhart, W., Moyer, M., Blackburn, R. K., Pahel, G. L., Mitchell, J. L., Hoffman, C. R., and Becherer, J. D. (1999) *J. Biol. Chem.* **274,** 30563-30570

22. Shirakabe, K., Wakatsuki, S., Kurisaki, T., and Fujisawa-Sehara, A. (2001) *J. Biol. Chem.* **276**, 9352-9358

23. Gaultier, A., Cousin, H., Darribere, T., and Alfandari, D. (2002) *J. Biol. Chem.* **277**, 23336-23344

24. Kang, T., Park, H. I., Suh. Y., Zhao, Y.G., Tschesche, H., Sang, Q.X. (2002) *J. Biol. Chem.* **277**, 48514-48522

25. Westling, J., Fosang, A. J., Last, K., Thompson, V. P., Tomkinson, K. N., Hebert, T., McDonagh, T., Collins-Racie, L. A., LaVallie, E. R., Morris, E. A., and Sandy, J. D. (2002) *J. Biol. Chem.* **277**,16059-16066

26. Smith, K. M., Gaultier, A., Cousin, H., Alfandari, D., White, J. M., and DeSimone, D. W. (2002) *J. Cell Biol.* **159**, 893-902

27. Zhao, Y. G., Wei, P., and Sang, Q. X. (2001) *Biochem. Biophys. Res. Commun.* **289**, 288-294

28. Marchand, P., Volkmann, M., and Bond, J. (1996). *J. Biol. Chem.* **271**,24236-24241

29. Ilan, N., Mohsenin, A., Cheung, L., and Madri, J.A. (2001) *FASEB J.* **15**, 362-372

30. Zolkiewka, A. (1999) *Exp. Cell. Res*. 252：423-431

31. Reddy, P., Slack, J. L., Davis, R., Cerretti, D. P., Kozlosky, C. J., Blanton, R. A., Shows, D., Peschon, J. J., and Black, R. A. (2000) *J. Biol. Chem.* **275,** 14608-14614

32. Iba, K., Albrechtsen, R., Gilpin, B., Frohlich, C., Loechel, F., Zolkiewska, A., Ishiguro, K., Kojima, T., Liu, W., Langford, J. K., Sanderson, R. D., Brakebusch, C., Fassler, R., and Wewer, U. M.. (2000). *J. Cell Biol.* **149**, 1143-1156

33. Iba, K., Albrechtsen, R., Gilpin, B., Loechel, F., and Wewer, U. M. (1999) *Am. J. Pathol.* **154**, 1489-1501

FIGURE LEGENDS

Figure 1. Processing at E^{586}-S^{587} of hADAM19 occurs intramolecularly. The MDCK cells stably expressing soluble inactive hADAM19 (D-E346A) were mixed equally at 24-wells with MDCK cells transfected with the blank vector (lane 4), D586 (lane 5), or D-CR (lane 6) for 24 hours in serum free media, then the conditioned media were subjected to Western blotting with anti-FLAG-M2. The soluble stable lines, D52-5 (lanes 1), D586 (lane 2), or D-CR (lane 3) alone were as controls. The processed C-fragments of soluble hADAM19 are indicated.

Figure 2. The N-fragments associate with the C-fragments processed at E^{586}-S^{587} of soluble hADAM19 by disulfide bonds. A) No detection of the processed forms by anti-FLAG-M2 under non-reducing conditions. The MDCK cells stably expressing soluble hADAM19, D52-5 were incubated in serum-free media for 24 hours, then the conditioned media was subjected to Western blotting by anti-FLAG-M2 under reducing (lane 2) or non-reducing conditions (lane 3). The medium from MDCK cells transfected with the blank vector was utilized as a control (lane 1). The processed C-fragments of soluble hADAM19 are indicated. **B)** Detection of the processed forms by the specific antibody against the disintegrin domain of hADAM19 (Anti-Dis). The same process was performed as **A**), but using Anti-Dis as the probe to detect soluble hADAM19. The processed N-fragments of soluble hADAM19 are indicated. **C)** Any one of the cysteine residues at C^{605}, C^{633}, C^{639}, and C^{643} is necessary for the association of the processed N-fragment with its C-fragment of soluble hADAM19 in COS1 transfected cells. COS1 cells were transfected with blank vector (lanes 1, 7), D52 (lanes 2, 8), soluble mutants with C^{605} to S^{605} (D-C605S, lanes 3, 9), C^{633} to S^{633} (D-C633S, lanes 4, 10), C^{639} to S^{639} (D-C639S, lanes 5, 11), or C^{643} to S^{643} (D-C643S, lanes 6, 12), followed by incubation for 24 hours in serum-free media. The conditioned media were

analyzed by Western blotting with anti-FLAG-M2 under reducing (lanes 1-6) or non-reducing conditions (lanes 7-12). The pro- and mature forms, and the processed C-fragments of soluble hADAM19 are indicated. Notice: Different profiles are detected for the pro-, mature, and processed soluble hADAM19 among these transient transfections, and any one of these Cys to Ser mutants induces two processing sites.

Figure 3. A schematic illustration of the mutants of hADAM19 inserted in the expression vector pCR3.1. All of the constructs have a C-terminal FLAG tag. SP: Signal peptide; Pro-: Prodomain; Cat-: Catalytic domain; Dis-: Disintegrin domain; Cys-: Cysteine-rich domain; EGF-: EGF-like domain; TM: Transmembrane domain; CD: Cytoplasmic domain; F: FLAG tag.

Figure 4. Different stabilities of soluble of hADAM19 with C to S mutants in stable MDCK transfectants. A) Soluble C to S mutants of hADAM19 in stable MDCK transfectants have different stabilities. Representative MDCK cells stably expressing D52 (D52-5, lane 2, 12), D-C633S (D-C633S-4 and D-C633S-5, lanes 3, 4, 13, 14), D-C639S (D-C639S-8 and D-C639S-10, lanes 5, 6, 15, 16), D-C605S (D-C605S-7 and D-C605S-8, lanes 7, 8, 17, 18), and D-C643S (D-C643S-6 and D-C643S-9, lanes 9, 10, 19, 20) were seeded in equal amounts into different wells of 24-well plates. After reaching 80% confluence, the cells were incubated in serum-free media for 24 hours, then the conditioned media (lanes, 1-10) and cell lysates (lanes, 11-20) were analyzed by Western blotting using anti-FLAG-M2. The mature forms and the processed C-fragments of soluble hADAM19 are indicated. MDCK cells transfected with the blank vector were used as a control. Notice: Different levels of mature or processed soluble hADAM19 appear in the media, but not in the cell lysates among these transfects. **B**) The novel processing induced by the mutated cysteine residues is an autolysis. The representative MDCK cells stably expressing soluble inactive hADAM19 (D-

E346A, lane 2), C^{633} to S^{633} and E^{346} to A^{346} (D-C633S/E346A-7 and D-C633S/E346A-10, lanes 3, 4), and C^{643} to S^{643} and E^{346} to A^{346} (D-C643S/E346A-20 and D-C643S/E346A-22, lanes 5, 6) were initiated in equal amounts and changed to serum-free media when the cells reached 80% confluence. The conditioned media were analyzed by Western blotting using anti-FLAG-M2. MDCK cells transfected with the blank vector was used as a control (lane 1). Notice: There is no processing at all in the media from the MDCK stable lines of these double mutants because the mutants with E346A have no catalytic activity, demonstrating the new processing is also autocatalytic.

Figure 5. The proteins of D-C633S and D586 are more vulnerable to trypsin digestion. The conditioned media from MDCK cells stably expressing soluble hADAM19 (D52-5, lanes 3-7), C^{633} to S^{633} (D-C633S-4, lanes 8-12), and D586 (lanes 13-17) were subjected to trypsin digestion as described in "Materials and Methods", with trypsin concentrations at 0 (lanes 3, 8, 13), 5 (lanes 4, 9, 14), 10 (lanes 5, 10, 15), 20 (lanes 6, 11, 16), 40 (lanes 7, 12, 17) ng/ul, and followed by SDS-PAGE and Western blotting with anti-FLAG-M2. The conditioned media from MDCK cells transfected with the blank vector were treated without (lane 1) or with (lane 2) 40 ng/ul of trypsin and its inhibitors at 2-fold excess of trypsin as controls.

Figure 6. The new processing at K^{543}-V^{544} induced by mutating the cysteines is independent of the normal processing at E^{586}-S^{587}. A) The independence of the new processing in transfected COS1 cells. COS1 cells were transfected with the blank vector (lane 1), soluble hADAM19 (D52, lane 2), soluble mutants of hADAM19 with E^{586} to D^{586} (D-E586D, lane 3), C^{633} to S^{633} (D-C633S, lane 4), C^{633} to S^{633} and E^{586} to D^{586} (D-C633S/E586D, lane 5), C^{639} to S^{639} (D-C639S, lane 6), or C^{639} to S^{639} and E^{586} to D^{586} (D-C639S/E586D, lane 7). After incubation for 24 hours in serum-free media, the conditioned media were analyzed by Western blotting with anti-FLAG-M2. The pro- and mature forms, and the processed C-

fragments of soluble hADAM19, are indicated. Notice: D-E586D had no processed forms, but both D-C633S/E586D and D-C639S/E586D demonstrate the novel processing in the absence of normal processing. **B)** The novel processing induced by the mutated cysteine residues occurs independently at K^{543}-V^{544}. The representative MDCK cells stably expressing soluble double mutants, C^{633} to S^{633} and E^{586} to D^{586} (D-C633S/E586D-9 and D-C633S/E586D-13, lanes 3, 4), were seeded in equal amounts and changed to serum-free media when the cells reached 80% confluence. The conditioned media were analyzed by Western blotting using anti-FLAG-M2. MDCK cells transfected with the blank vector (lane 1) and D-C633S-4 (lane 2) were used as the controls. The sequences for the processed C-terminal proteins are shown at the right. Notice: The processing site of K^{543}-V^{544} is the major one in the media from the MDCK cells stably expressing the soluble double mutants of C633S/E586D, while the predominant one is E^{586}-S^{587} in D-C633S.

Figure 7. Shedding of full length hADAM19 with cysteine to serine mutations. A) The shedding status of MDCK cells stably expressing full length mutants of hADAM19. The representative MDCK cells stably expressing wild type hADAM19 (F46, lanes 1, 6), or mutants with C^{633} to S^{633} (F-C633S-3 and F-C633S-9, lanes 2, 7, 3, 8), or C^{643} to S^{643} (F-C643S-4 and F-C643S-7, lanes 4, 9, 5, 10) were seeded at equal amount into different wells of 24-well plates, then changed to serum-free media when the cells achieved 80% confluence. After 24 hours incubation, the conditioned media (lanes 1-5) and the cell lysates (lanes 6-10) were subjected to Western blotting using anti-Dis (lanes 1-5) or anti-FLAG-M2 (lanes 6-10). The pro-, mature, and shed forms of hADAM19 are indicated. Notice: F-C633S shed significantly, but not F-C643S or F46. **B**) The regulation of shedding in MDCK cells stably expressing F-C633S. MDCK cells stably expressing F-C633S (F-C633S-3) were chosen to seed into 24-well plates equally, and the cells were treated with serum-free media alone (lane 2), or containing GM6001 (2.5 uM, lane 3), PMA (50 ng/ml, lane 4), W7 (100 uM, lane 5) or

A23187 (500 nM, lane 6) for 24 hours. The conditioned media were analyzed by Western blotting using Anti-Dis. The shed fragments of hADAM19 are indicated. MDCK cells transfected with wild type (F46) were used as a control (lane 1). Notice: The shedding F-C633S was inhibited by A23187 and W7, was little inhibited by GM6001, but was enhanced by PMA.

Kang et al., Fig. 1

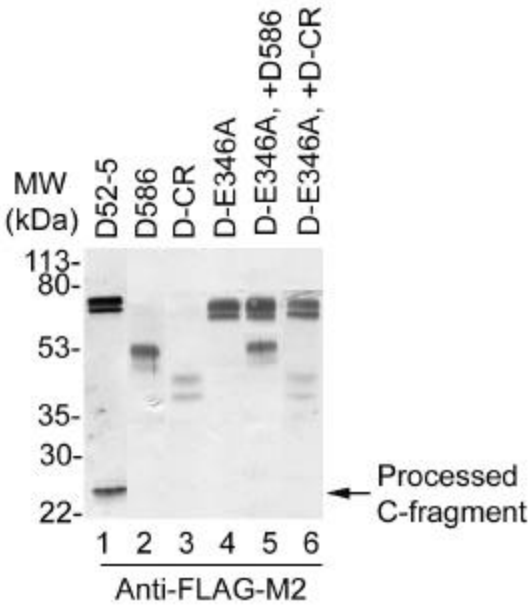

Kang et al., Fig. 2

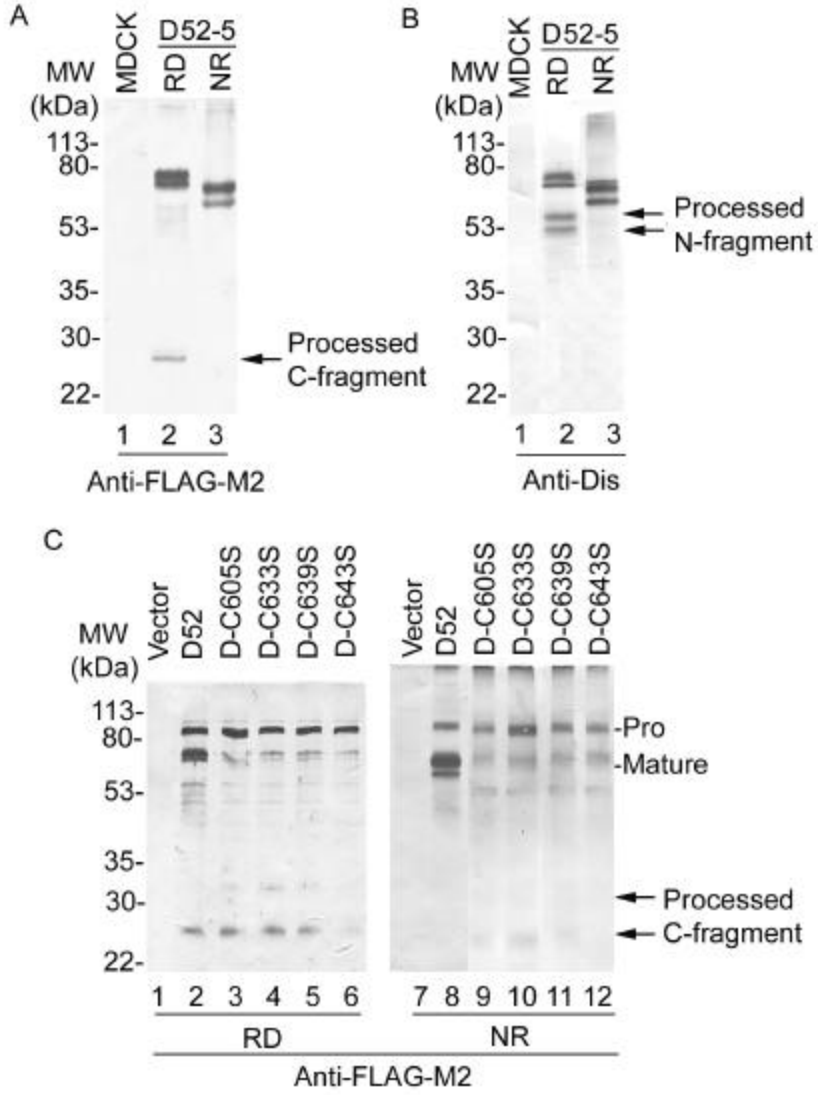

Kang et al. Fig. 3

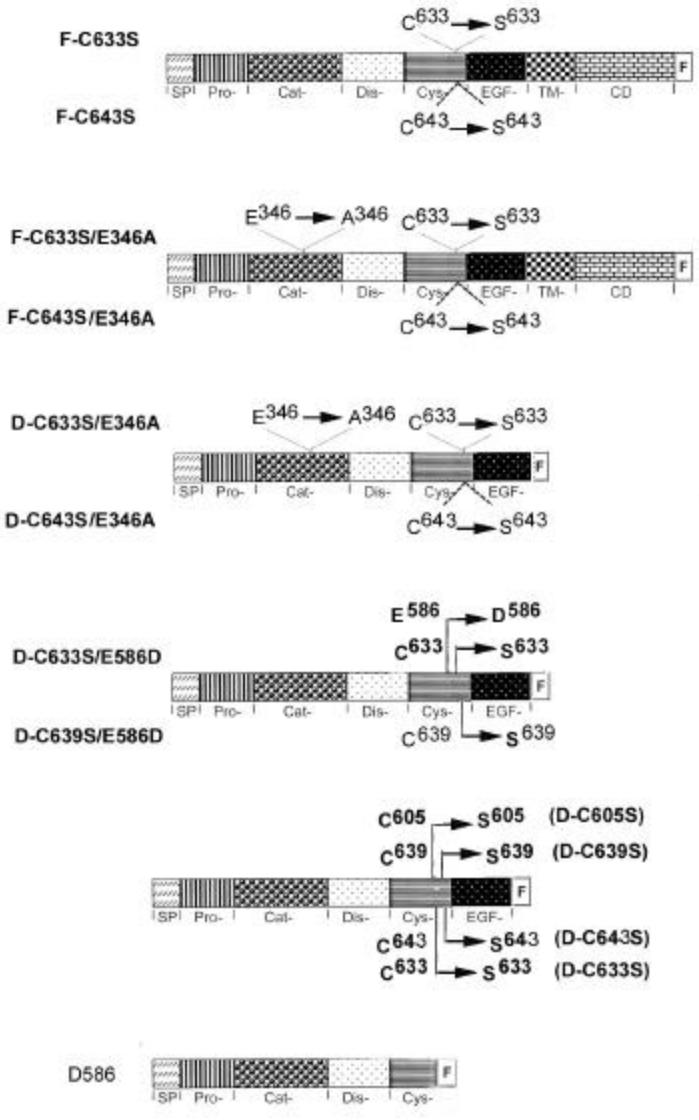

Kang et al. Fig. 4

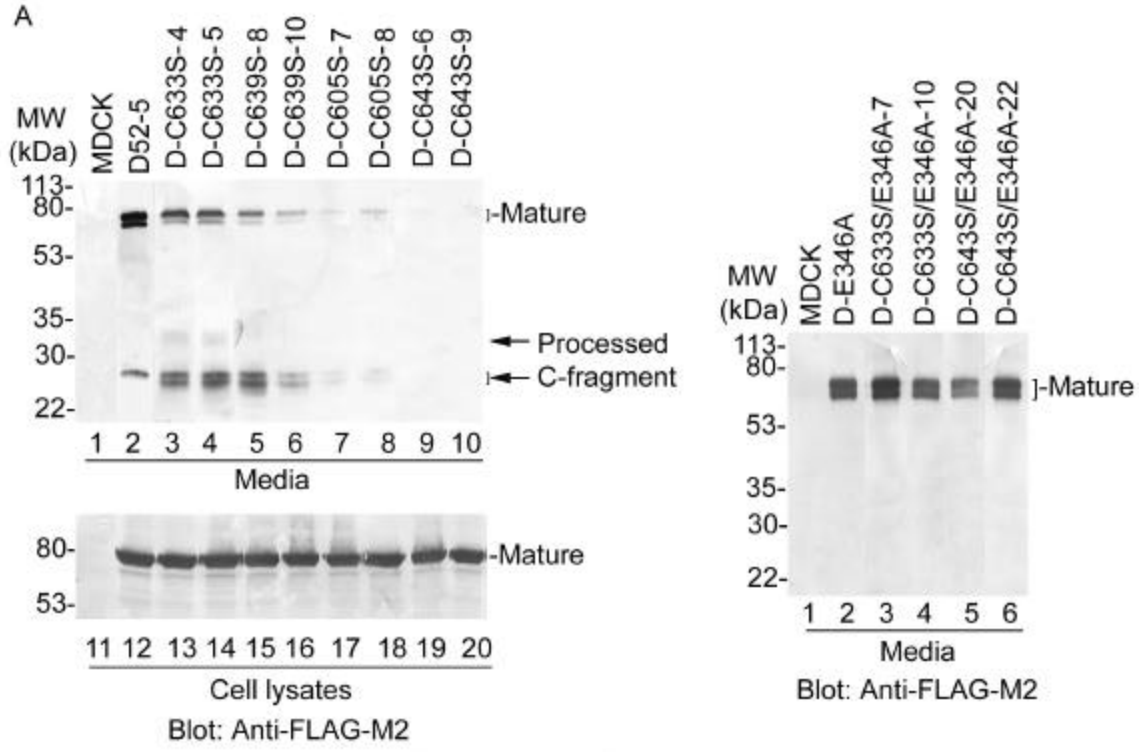

Kang et al., Fig. 5

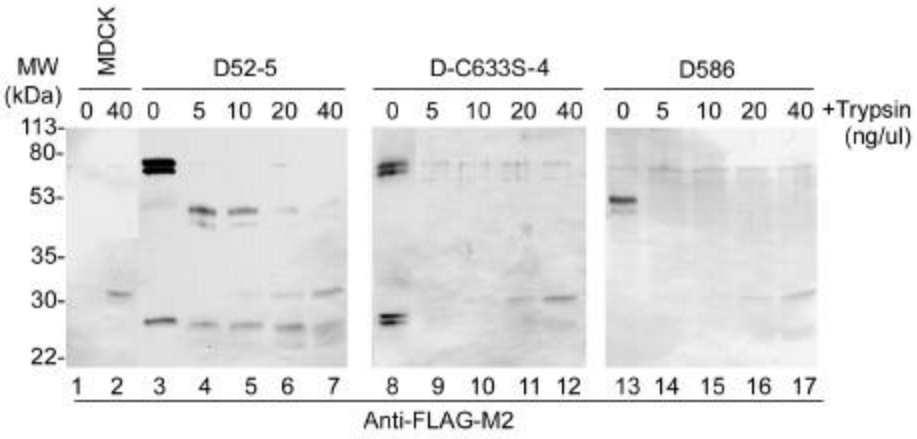

Kang et al., Fig. 6

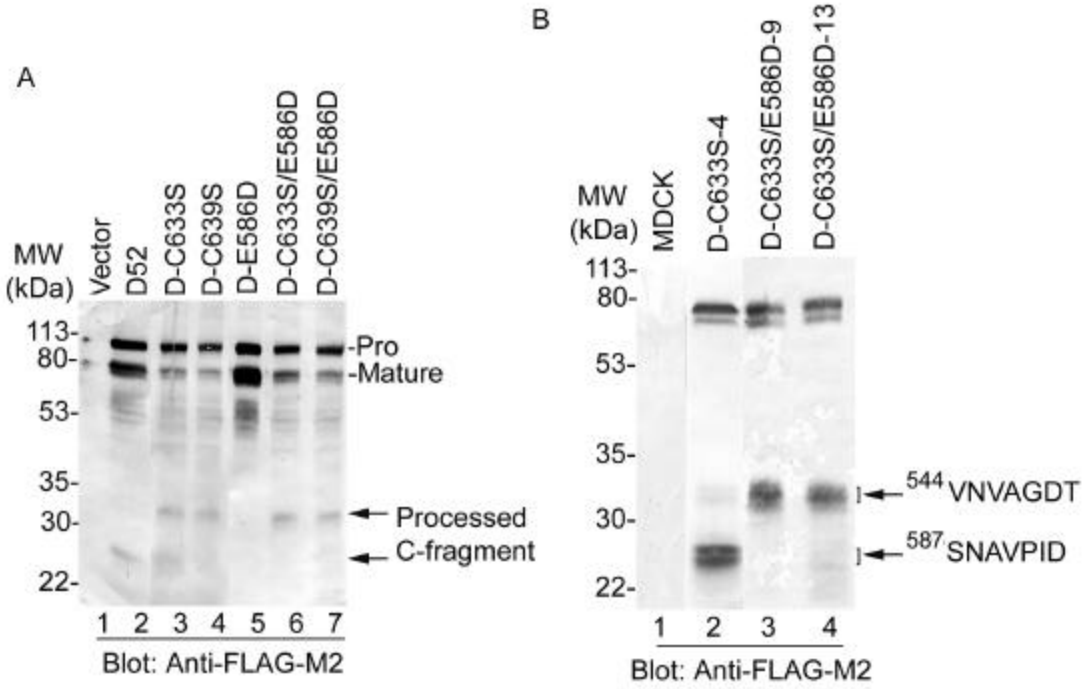

Kang et al., Fig. 7

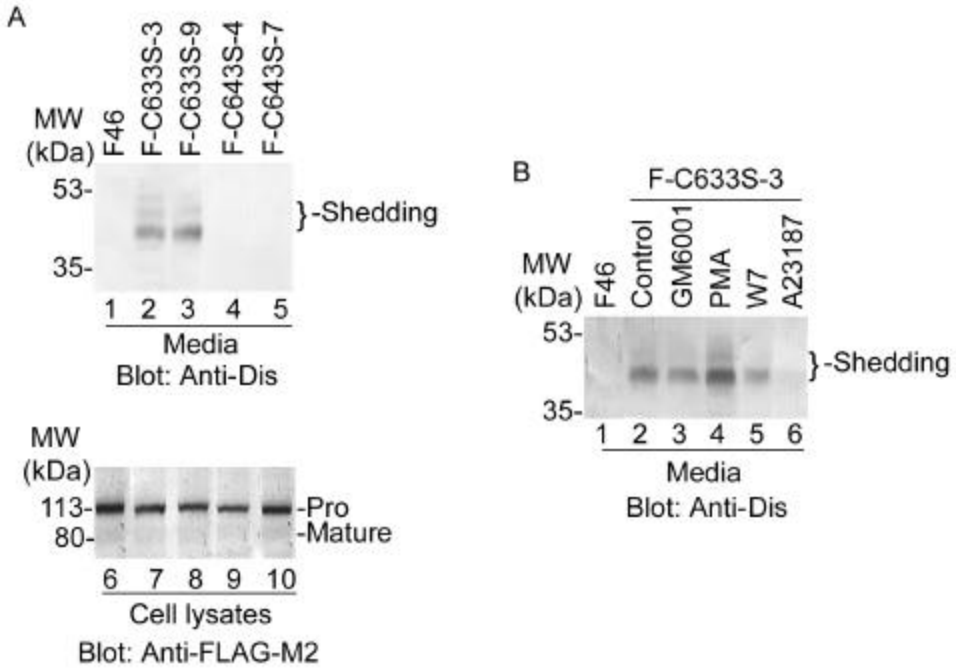

4. Discussion

4.1 *Furin and Metalloproteinases*

The PCs are a large family of serine proteinases, containing PACE(furin), PACE4, PC5/PC6, and PC7/PC8, that recognize dibasic motifs and cleave the peptide bond on the carboxyl side (Nakayama 1997, Steiner 1998, Molloy et al. 1999). As a major PC, furin is concentrated in the *trans*-Golgi network (TGN) and cycles between this compartment and the cell surface through the endocytic pathway. The autoactivation and intracellular trafficking of furin are well characterized. Numerous studies have shown that furin activates a large number of proproteins in multiple compartments (Nakayama 1997, Steiner 1998, Molloy et al. 1999). The minimal recognition sequence for furin requires basic residues at P_1 and P_4, but the efficient cleavage by furin is RXK/RR, and in some cases, at the P_1' position, an amino acid with a hydrophobic aliphatic side chain is not suitable (Nakayama 1997). The initial demonstration that furin is responsible for activation of metalloproteinases was shown in MMP11 (Pei and Weiss, 1995), and this mechanism was extended to some other MMPs, such as MMP14, 16, 24, and many ADAMs, including ADAM1, 9, 12, 15, 17 and 19 and ADAM-TS1, 4, 9, and 12 (Lum and Blobel 1997, Lum et al. 1998, Loechel et al. 1998, Kuno et al. 1999, Roghani et al. 1999, Schlondorff et al. 2000, Yana and Weiss 2000, Wang and Pei 2001, Cal et al. 2001, 2002, Guo et al. 2002, Cao et al. 2002, Kang et al. 2002a, 2002b, Somerville et al., 2003). Typically, there is only one furin recognition site between the pro- and catalytic- domain of metalloproteinases in most cases (Pei and Weiss 1995, Black et al. 1997, Moss et al. 1997, Nakayama 1997, Tortorella et al. 1999, Molloy et al. 1999, Stone et al, 1999, Primakoff and Myles 2000, Yana and Weiss 2000, Vu and Werb 2000, Yoshinaka et al. 2002, Kang et al. 2002a). I presented evidence for the first time that there are two consecutive functional furin recognition sites, $\underline{R}^{197}P\underline{RR}^{200}$ and $\underline{R}^{200}M\underline{KR}^{203}$, which adhere to the rules for efficient cleavage by furin (Nakayama 1997), between the pro- and catalytic-domain in hADAM19 (Kang et al. 2002b). However, N-terminal sequencing of wild type

mature forms confirmed that the primary intracellular cleavage site for hADAM19 activation is the one nearer to the catalytic domain, $\underline{R}^{200}M\underline{KR}^{203}$ as predicted before, and this motif is conserved in mice as $\underline{R}^{201}M\underline{KR}^{204}$ (Fritsche et al. 2000, Wei et al. 2001, Kang et al. 2002b). On the other hand, the farther one, $\underline{R}^{197}P\underline{RR}^{200}$ in humans, which was functional when the primary site was abolished (Kang et al. 2002b), is replaced with $Q^{198}PRR^{201}$ in mice (Inoue et al. 1998, Kurohara et al. 2000), which is not efficiently cleaved by furin. It is noticeable that there are also two potentially consecutive alternative furin recognition sites in other metalloproteinase zymogens, including ADAM11 (AB009675, $R^{292}LRRKR^{297}$), ADAM22 (AF 155382, $R^{219}PKRSKR^{205}$), ADAM-TS4 (AF148213, $R^{206}PRRAKR^{212}$), ADAM-TS9 (AA205581, $R^{280}TRRRTKR^{287}$), MT2-MMP (NM_002428, $R^{126}RRRKR^{131}$), and MT5-MMP (AJ010262, $R^{118}RRRNKR^{224}$). The ones nearer to the catalytic domains are conserved in different species, whereas the farther ones might be related to evolution. Although the significance of the two alternative recognition sites in these precursors remains poorly understood, I may speculate that the processing of these zymogens are crucial for some biological events; the zymogens will be activated by furin at a different site when the primary site is abrogated. Moreover, I provided evidence for the first time that furin was co-localized with both ADAM19 and MMP16 in the ER/Golgi complex and/or TGN, which were independent of their apparent enzyme-substrate relationship, demonstrating that some ADAMs and MMPs are physiologically relevent substrates activated by furin (Kang et al. 2002a, 2002b).

4.2 *Shedding of Metalloproteinases*.

Increasing evidence suggests that shedding is of vital importance for the regulation of metalloproteinase activity. For MT-MMPs, Dr. Pei´s group reported that MT5-MMP is shed by furin, down-regulating its activity, and that interleukin-8 triggers the signal for both release and activation of MT6-MMP by an unknown mechanism (Wang and Pei 2001, Kang et al.

2001). The activity of MT1-MMP can be autolytically terminated directly on the cell surface or via production of a soluble functional fragment, consequently down-regulating enzyme activity on the cell surface (Toth et al. 2002). Among ADAMs, ADAM13 and ADAM19 have been shown to shed or processed intracellularly by an autolytic mechanism, producing an active enzyme able to bind with alpha2-M and integrins (Gaultier et al. 2002), or cleave both alpha2-M and a peptide substrate *in vitro* (Kang et al 2002c, submitted), and ADAM8 was shown to be further autolytically processed to separate its metalloproteinase domain, which was active against MBP, from its disintegrin and cysteine-rich (DC) domains after the autolytic removal of its prodomain, subsquently, the DC domains mediate cell ahesion by dimerizing through the homophilic interaction (Schlomann et al. 2002). In addition, truncation of mature ADAM-TS4 at its C-terminus is required for its aggrecanase activity (Guo et al. 2002). It might, therefore, be a general regulatory mechanism that MT-MMPs, such as MT1-MMP and MT5-MMP, are down-regulated by shedding to release active forms from the cell surface, whereas ADAMs have to be shed, processed or truncated at the C-terminus to exert their functions, such as acting as a sheddase, binding with integrins, or forming homophilic dimer on the cell surface, or digesting components of the extracellular matrix. For the significance of autolytic processing or shedding in hADAM19, I have demonstrated that hADAM19 processing or shedding occurs at a different position removed from the normal processing site at E^{586}-S^{587} under certain conditions, as in the case of the disruption of disulfide bonds by mutation or reduction. This also produces an active enzyme, suggesting that there is an alternative site for the processing or shedding of hADAM19 within the cysteine-rich domain to achieve fully activated hADAM19, indicative of its very important roles in both physiological and pathological conditions (Kang et al. 2002b, 2002c, and submitted)

However, the signal pathways involved in shedding processes, especially of ADAMs, are poorly understood. In this dissertation (Kang et al., 2002c, submitted), I provided unique

characteristics of the regulation of hADAM19 processing or shedding within its cysteine-rich domain, which are distinguishable from those shown for other ADAMs, MT-MMPs, and other membrane-bound proteins. I found that PMA, a common inducer of shedding, also enhances the processing or shedding of hADAM19, and this probably involves the cytoplasmic domain, transmembrane domain, or both. This is consistent with the reports showing that the cytoplasmic domain of ADAM9 is required for PMA-induced shedding (Izumi et al. 1998), and that the membrane anchor of TACE is necessary for its processing of TNF-alpha (Reddy et al. 2000, Itai et al. 2001). However, in most cases, endogenous and/or inducer-mediated shedding is independent of the cytoplasmic domain (Crowe et al. 1995, Dethlefsen et al. 1998, Kahn et al. 1998, Vecchi et al. 1998, Diaz-Rodriguez et al. 2000). Calcium ionophore, A23187, and the inhibitors of Calmodulin (CaM) are also potent inducers of many protein shedding processes (Pandiella and Massague 1991, Yee et al. 1993, Vecchi et al. 1996, Dethlefsen et al. 1998, Kahn et al. 1998, Diaz-Rodriguez et al. 2000, Annabi et al. 2001, Fors et al. 2001). Nevertheless, I found that A23187 and inhibitors of CaM block or impair the processing or shedding of hADAM19. On the other hand, I revealed that neither tyrosine kinase, MAP kinase, phosphatase, nor PI-3K seemed to play roles in the processing of hADAM19, although they have been shown to participate in some shedding processes in the past (Desdouits-Magnen et al. 1998, Vecchi et al. 1998, Fan and Derynck 1999, Gechtman et al. 1999, Gutwein et al. 2000, Schlondorff et al. 2001, Nath et al. 2001).

In addition, the proteinases responsible for the shedding of many cell surface molecules seem to have broad sequence specificity as revealed by mutational analysis of residues around the cleavage site of pro-TGFalpha, APP, IL-6 receptor, L-selectin, and pro-TNFalpha (Wong et al. 1989, Sisodia 1992, Müllberg et al. 1994, Migaki et al. 1995, Tang et al. 1996). I used mutagenesis to show that the size of residues at both the E^{586} and S^{587} sites, especially the size of the side-chains, are extremely important for normal processing of hADAM19. Even delicate changes, such as E^{586} to D^{586} and S^{587} to T^{587}, caused dramatic decreases in the

processing (Kang et al. 2002c). Intriguingly, many studies have shown that some potent synthetic inhibitors of metalloproteinases, such as TAPI, BB94, and GM6001, can block most, if not all, shedding processes, and that many shedding processes are sensitive to TIMP3, a matrix-associated TIMP that preferably inhibits ADAMs (Crowe et al. 1995, Arribas et al. 1996, 1997, Hooper et al. 1997, Mullberg et al. 1997, Peschon et al. 1998, Hargreaves et al. 1998, Borland et al. 1999, Fitzgerald et al. 2000, Diaz-Rodriguez et al. 2000, Ilan et al. 2001, Nath et al. 2001, Bailly et al. 2002). However, neither GM6001 nor TIMP3 inhibits the processing or shedding of hADAM19, which is consistent with some reports showing that the shedding of MT5-MMP, MT6-MMP, and IL-6 receptor is not affected by metalloproteinase inhibitors (Müllberg et al. 1995, Wang and Pei 2001, Kang et al. 2001). Nevertheless, both GM6001 and TIMP3 are able to dramatically inhibit the activity of soluble hADAM19 against our peptide substrate *in vitro* (data not shown). One possibility, we speculate, is that shedding, in most cases, occurs at membrane-proximal regions on the cell surface, which are easily accessible to hydroxamate-based inhibitors and TIMP3 (Migaki et al. 1995, Arribas et al. 1997, Hooper et al. 1997, Alfalah et al. 2001). hADAM19 carries out the processing or shedding at a region distal from the transmembrane domain in the secretory pathway, which is less accessible to GM6001 and TIMP3 (Kang et al. 2002c, submitted).

4.3 *Regulations and Functions of ADAM19.*

Adamalysin 19/ADAM 19/ MDC19/ meltrin beta, cloned from mice and human, is a type I membrane-bound protein containing the fundamental domains of ADAMs, such as the prodomain, metalloprotease and disintegrin domains, cysteine-rich domain, EGF-like domain, transmembrane domain, and cytoplasmic domain (Inoue et al. 1998, Stone et al. 1999, Primakoff and Myles 2000, Kurohara et al. 2000, Fritsche et al. 2000, Wei et al. 2001). Synthesized as a zymogen in the ER, hADAM19 is cleaved by furin to remove its prodomain, and is then processed at E^{586}-S^{587} within the cysteine-rich domain by autolysis in the TGN

(Kang et al. 2002b, 2002c). This produces an active N-terminal fragment, which contains metalloproteinase and disintegrin domains and part of the cysteine-rich domain to exert its sheddase activity such as releasing beta type-NRG in the TGN (Shirakabe et al., 2001). Alternatively, the active N-terminal fragment is transported to cell surface, where it acts as a sheddase (Shirakabe et al., 2001) or binds with components in the ECM. Because proforms of hADAM19 exhibit no changes under reducing or non-reducing conditions (Kang et al. submitted), I may also propose that hADAM19 forms dimers, tetramers or higher multimers after prodomain cleavage and/or autolytic truncation at the cysteine-rich domain (Kang et al. submitted), probably through the metalloproteinase domain, in which there are 7 (an odd number) cysteine residues, as this domain is also able to form dimers, tetramers or higher multimers (data not shown), which then function in secretory pathways or on the cell surface. However, the pro- and mature- forms of hADAM19 without processing within its cysteine-rich domain might also be partially transported to cell surface as shown in other ADAMs, such as ADAM9, 12, 15, 17 (Loechel et al. 1998, Lum et al. 1998, Roghani et al. 1999, Schlondorff et al. 2000, Cao et al 2002).

Regarding the role of cysteine-rich domain in the activation and processing of hADAM19, the "cysteine-rich domain" is sometimes referred to the cysteine-rich domain together with the disintegrin domain. In these cases, the "cysteine-rich domain" has been shown to be related to cell adhesion, such as in the cases of ADAM8, 12, 13, or to the proteolytic activity of TACE/ADAM17. For example, the recombinant disintegrin/cysteine-rich domain of ADAM8 mediates cell adhesion in cells expressing ADAM8 (Schlomann et al. 2002). The "cysteine-rich domain" of ADAM12 promotes the adhesion of fibroblasts and myoblasts (Zolkiewka 1999). The disintegrin and cysteine-rich domains of ADAM13 bind to both fibronectin and beta1-containing integrin receptors, and binding can be inhibited by antibodies against the cysteine-rich domain (Gaultier et al. 2002). The "cysteine-rich domain" of TACE/ADAM17 is required for shedding of IL-1R-II while affecting the inhibitor

sensitivity of TNF shedding (Reddy et al. 2000). However, for cysteine-rich-domain-specific functions, there is little information available; Iba et al. reported that it acts as a ligand for the cell-adhesion molecule syndecan as shown for the cysteine-rich domain of ADAM12 (Iba et al. 1999, 2000, Thodeti et al., 2003). Dr. DeSimone's group recently showed that the cysteine-rich domain of ADAM13 cooperates intramolecularly with the metalloproteinase domain of ADAM13 to regulate its function, providing the first evidence that a downstream extracellular adhesive domain plays an active role in the regulation of ADAM protease function *in vivo* (Smith et al. 2002). In this dissertation, I have demonstrated that disulfide bonds paired with the cysteine residues at C^{605}, C^{633}, C^{639}, or C^{643} within the fraction of the cysteine-rich domain of the C-terminal fragment processed at E^{586}-S^{587} of hADAM19 are necessary for the association of the processed N-terminal with its C-terminal fragments, and play a critical role in the regulation of hADAM19 activity by stabilizing the enzyme and/or preventing its autolysis (Kang et al. submitted). Therefore, it is very likely that these disulfide bonds form intramolecularly between the metalloproteinase domain of hADAM19 and the part of the cysteine-rich domain of the C-terminal fragment processed at E^{586}-S^{587} of hADAM19. If this is the case, I provide the first evidence *in vitro* to support the results of the *in vivo* ADAM13 studies (Smith et al. 2002), and give a very reasonable explanation for the fact that the processing or shedding of hADAM19 occurs autolytically and intramolecularly within its cysteine-rich domain (Kang et al. 2002c, submitted). However, I am unable to rule out the possibility of the formation of disulfide bonds between the disintegrin domain of hADAM19 and this region of the cysteine-rich domain, because the disintegrin domain of hADAM19 also plays a key role in the proteolytic activity of hADAM19, as shown by specific antibody blocking assays *in vitro* (Zhao et al. 2001), and by the lack of proteolytic activity using alpha2-M and peptide substrate assays *in vitro* for the deletion mutant containing only the metalloproteinase domain of hADAM19 (data not shown). Any one of four cysteine residues at C^{605}, C^{633}, C^{639}, and C^{643} in the segment of cysteine-rich domain is indispensable for the

association between the N-terminal and C-terminal fragments processed at E^{586}-S^{587}. I presume three disulfide bonds, one formed between two cysteine residues of C^{605}, C^{633}, C^{639}, or C^{643} and two formed by the remaining cysteine residues paired with two other cysteine residues, with at least one occurring prior to the position of E^{586}. Alternatively, four disulfide bonds may exist, formed by C^{605}, C^{633}, C^{639}, and C^{643} with four other cysteine residues, with at least one being before the position of E^{586}. These bonds have a strong coordination with each other, and when one of these disulfide bonds is disrupted, the others will be subsequently disturbed. Therefore, I propose that three or four disulfide bonds linked by the four cysteine residues at C^{605}, C^{633}, C^{639}, and C^{643} are responsible for the association between the N-terminal and C-terminal fragments processed at E^{586}-S^{587}. However, I am currently limited to identify these four cysteine residue pairs, as there are total 43 cysteine residues available in the metalloproteinase, disintegrin, cysteine-rich and EGF-like domains of hADAM19.

With regard to the signal pathways related to the activation and the processing of hADAM19, I demonstrated in this dissertation that calcium signal is related to both the removal of the prodomain in ADAM19 by furin and the antolytic processing or shedding of hADAM19, and that both PKC and CaM signal pathways are involved in the processing or shedding of hADAM19 (Kang et al. 2002b, 2002c, submitted). However, for the processed C-terminal remnant, containing a fraction of the cysteine-rich domain, transmembrane domain and cytoplasmic domain, persumably localized on cell surface, its potential functions related to the signals remain to be uncovered, because two SH3 binding sites exist in its cytoplasmic domain. Interestingly, a meltrin beta mini, lacking the prodomain, metalloproteinase and disintegrin domains, was recently reported, in which showed that this novel meltrin beta isoform induced neurite outgrowth in neuronal cells (Kurisaki et al. 2002). Huang et al. showed that ADAM19 cytoplasmic tail specifically interacts with ArgBP1, beta-cop, ubiquitin and another unknown protein by a yeast two-hybrid screening (Huang et al. 2002). In addition, hADAM19 is an important marker for the differentiation and characterization of

dendritic cells and the distinction between macrophages and dendritic cells (Fritsche et al. 2000). But the mechanism for this function is unknown.

Regarding the proteolytic activity of ADAM19, soluble hADAM19 is able to form complex with alpha 2-M and generate two products *in vitro*, which can be blocked by the antibodies against its metalloproteinase domain and disintegrin domain, but not its prodomain, suggesting that the disintegrin of ADAM19 play a critical role in its proteolytic activity (Wei et al. 2001, Zhao et al. 2002, Kang et al. 2002b, 2002c). In this dissertation, I developed a peptide substrate, Ac-RPLESNAV, which can also be cleaved by soluble hADAM19 *in vitro* (Kang et al. 2002b, 2002c). My preliminary data show that TIMP3 can inhibit hADAM19 activity in this assay (data not shwon), which is similar to the results with ADAM10, 12, 17, and ADAM-TS4 and 5 *in vitro* (Amour et al. 1998, 2000, Loechel et al. 2000, Kashiwagi et al. 2001). Interestingly, ADAM-TS4 is truncated at E^{373}-A^{374}, the site for the cleavage of ADAM-TS4 and ADAM-TS5, but not MMPs. In contrast, the truncation site at N^{341}-F^{342} is mediated by MMPs, but not aggrecanases (Guo et al. 2002, Westling et al. 2002). Our mutational data showed that the E^{586}-A^{587} shedding site was also optimal for autolytic processing of hADAM19, indicating that our peptide substrates might be useful to determine the activity of other ADAMs, such as aggrecanases, ADAM-TS4 and 5. In this way, it is possible for us to establish unique inhibitor profiles for individual ADAMs. On the other hand, ADAM19 might be one of the aggrecanases to cleave aggrecan at at E^{373}-A^{374}, versican at E^{441}-A^{442}, and/or brevican at E^{395}-A^{396}, albeit the direct evidence remains to be provided. In an overall review, it is believable that ADAM19/meltrin beta/MDC19 may play a crucial role in osteoblast differentiation, early heart and central nervous system development, angiogenesis, rheumatoid arthritis and glioma.

5. References

1. Abbaszade, I., Liu, R. Q., Yang, F., Rosenfeld, S. A., Ross, O. H., Link, J. R., Ellis, D. M., Tortorella, M. D., Pratta, M. A., Hollis, J. M., Wynn, R., Duke, J. L., George, H. J., Hillman, M. C. Jr, Murphy, K., Wiswall, B. H., Copeland, R. A., Decicco, C. P., Bruckner, R., Nagase, H., Itoh, Y., Newton, R. C., Magolda, R. L., Trzaskos, J. M., Hollis, G. F., Arner, E. C., and Burn, T. C. (1999) Cloning and characterization of ADAMTS11, an aggrecanase from the ADAMTS family. *J. Biol. Chem.* **274**, 23443-23450
2. Alfalah, M., Parkin, E. T., Jacob, R., Sturrock, E. D., Mentele, R., Turner, A. J., Hooper, N. M., and Naim, H. Y. (2001) A point mutation in the juxtamembrane stalk of human angiotensin I-converting enzyme invokes the action of a distinct secretase. *J. Biol. Chem.* **276**, 21105-21109
3. Alfandri, D., Cousin, H., Gaultier, A., Smith, K., White, J. M. Darribere, T., and DeSimone, D. W. (2001) Xenopus ADAM13 is a metalloprotease required for cranial neural crest-cell migration. *Curr. Biol.* **11**: 918-930
4. Amour, A., Knight, C. G., Webster, A., Slocombe, P. M., Stephens, P. E., Knauper, V., Docherty, A. J., and Murphy, G. (2000) The in vitro activity of ADAM-10 is inhibited by TIMP-1 and TIMP-3. *FEBS Lett.* **473**, 275-279
5. Amour, A., Slocombe, P. M., Webster, A., Butler, M., Knight, C. G., Smith, B. J., Stephens, P. E., Shelley, C., Hutton, M., Knauper, V., Docherty, A. J., and Murphy, G. (1998) TNF-alpha converting enzyme (TACE) is inhibited by TIMP-3. *FEBS Lett.* **435**, 39-44
6. Anders, A., Gilbert, S., Garten, W., Postina, R., and Fahrenholz, F. (2001) Regulation of the alpha-secretase ADAM10 by its prodomain and proprotein convertases. *FASEB J.* **15**:1837-1839
7. Annabi, B., Pilorget, A., Bousquet-Gagnon, N., Gingras, D., and Beliveau, R. (2001) Calmodulin inhibitors trigger the proteolytic processing of membrane type-1 matrix metalloproteinase, but not its shedding in glioblastoma cells. *Biochem. J.* **359**, 325-333
8. Arribas, J., Coodly, L., Vollmer, P., Kishimoto, T. K., Rose-John, S., and Massague, J. (1996) Diverse cell surface protein ectodomains are shed by a system sensitive to metalloprotease inhibitors. *J. Biol. Chem.* **271**, 11376-11382
9. Arribas, J., Lopez-Casillas, F., and Massague, J. (1997) Role of the juxtamembrane domains of the transforming growth factor-alpha precursor and the beta-amyloid precursor protein in regulated ectodomain shedding. *J. Biol. Chem.* **272**, 17160-17165
10. Asai, M., Hattori, C., Szabo, B., Sasagawa, N., Maruyama, K., Tanuma, S. and Ishiura, S. (2003) Putative function of ADAM9, ADAM10, and ADAM17 as APP alpha-secretase. *Biochem. Biophys. Res. Commun.* **301**, 231-235
11. Asakura, M., Kitakaze, M., Takashima, S., Liao, Y., Ishikura, F., Yoshinaka, T., Ohmoto, H., Node, K., Yoshino, K., Ishiguro, H., Asanuma, H., Sanada, S., Matsumura, Y., Takeda, H., Beppu, S., Tada, M., Hori, M., and Higashiyama, S. (2002) Cardiac hypertrophy is inhibited by antagonism of ADAM12 processing of HB-EGF: metalloproteinase inhibitors as a new therapy. *Nat. Med.* **8**, 35-40
12. Bailly, V., Zhang, Z., Meier, W., Cate, R., Sanicola, M., and Bonventre, J. V. (2002) Shedding of kidney injury molecule-1, a putative adhesion protein involved in renal regeneration. . *J. Biol. Chem.* **277**, 39739-39748
13. Black, R. A., Rauch, C. T., Kozlosky, C. J., Peschon, J. J., Slack, J. L., Wolfson, M. F., Castner, B. J., Stocking, K. L., Reddy, P., Srinivasan, S., Nelson, N., Boiani, N., Schooley, K. A., Gerhart, M., Davis, R., Fitzner, J. N., Johnson, R. S., Paxton, R. J., March, C. J., and Cerretti, D. P. (1997) A metalloproteinase disintegrin that releases tumour-necrosis factor-alpha from cells. *Nature.* **385**, 729-733
14. Black, R. A. and White J. M. (1998) ADAMs: focus on the protease domain. *Curr. Opin. Cell Biol.* **10**, 654-659
15. Blobel, C. P. (1997) Metalloprotease-disintegrins: links to cell adhesion and cleavage of TNF alpha and Notch. *Cell.* **90**, 589-592
16. Blobel, C. P. (2000) Remarkable roles of proteolysis on and beyond the cell surface. *Curr. Opin. Cell Biol.* **12**, 606-612
17. Borland, G., Murphy, G., and Ager, A. (1999) Tissue inhibitor of metalloproteinases-3 inhibits shedding of L-selectin from leukocytes. *J. Biol. Chem.* **274**, 2810-2815
18. Brew, K., Dinakarpandian, D., and Nagase, H. (2000) Tissue inhibitors of metalloproteinases: evolution, structure and function. *Biochim. Biophys. Acta.* **1477**, 267-283
19. Bridges, L. C., Tani, P. H., Hanson, K. R. Roberts, C. M., Judkins, M. B. and, Bowditch, R. D. (2002) The lymphocyte metalloprotease MDC-L (ADAM 28) is a ligand for the integrin alpha4beta1. *J. Biol. Chem.*, **277,** 3784-3792
20. Brou, C., Logeat, F., Gupta, N., Bessia, C., LeBail, O., Doedens, J. R., Cumano, A., Roux, P., Black, R. A., and Israel, A. (2000) A novel proteolytic cleavage involved in Notch signaling: the role of the disintegrin-metalloprotease TACE. *Mol. Cell.* **5**, 207-216.

21. Buxbaum, J. D., Liu, K. N., Luo, Y., Slack, J. L., Stocking, K. L., Peschon, J. J., Johnson, R. S., Castner, B. J., Cerretti, D. P., and Black, R. A. (1998) Evidence that tumor necrosis factor alpha converting enzyme is involved in regulated alpha-secretase cleavage of the Alzheimer amyloid protein precursor. *J. Biol. Chem*. **273**, 27765-27767
22. Cal, S., Arguees, J. M., Fernandez, P. L., and Lopez-Otin, C. (2001) Identification, characterization, and intracellular processing of ADAM-TS12, a novel human disintegrin with a complex structural organization involving multiple thrombospondin-1 repeats. *J. Biol. Chem.* **276**, 17932-17940
23. Cal, S., Obaya, A. J., Llamazares, M., Garabaya, C., Quesada, V., and Lopez-Otin, C. (2002) Cloning, expression analysis, and structural characterization of seven novel human ADAMTSs, a family of metalloproteinases with disintegrin and thrombospondin-1 domains. *Gene* **283,** 49-62
24. Cao, Y., Kang, Q., Zhao, Z., and Zolkiewska, A. (2002) Intracellular processing of metalloprotease disintegrin ADAM12. *J. Biol. Chem*. **277**, 26403-26411
25. Cao, Y., Kang, Q., and Zolkiewska A. (2001) Metalloprotease-disintegrin ADAM 12 interacts with alpha-actinin-1. *Biochem. J.* **357**, 353-361
26. Chantry, A., Gregson, N. A., and Glynn, P. (1989) A novel metalloproteinase associated with brain myelin membranes. Isolation and characterization. *J. Biol. Chem,* **264**:21603-21617
27. Chen, L. C., Noelken, M. E., and Nagase, H. (1993) Disruption of the cysteine-75 and zinc ion coordination is not sufficient to activate the precursor of human matrix metalloproteinase 3 (stromelysin 1). *Biochemistry* **32**, 10289-10295
28. Colciaghi, F., Borroni, B., Pastorino, L., Marcello, E., Zimmermann, M., Cattabeni, F., Padovani, A., and Di Luca, M. (2002) [alpha]-Secretase ADAM10 as Well as [alpha]APPs Is Reduced in Platelets and CSF of Alzheimer Disease Patients. *Mol. Med.* **8**, 67-74
29. Crowe, P. D., Walter, B. N., Mohler, K. M., Otten-Evans, C., Black, R. A., and Ware, C. F. (1995) A metalloprotease inhibitor blocks shedding of the 80-kD TNF receptor and TNF processing in T lymphocytes. *J. Exp. Med.* **181**, 1205-1210
30. Desdouits-Magnen, J., Desdouits, F., Takeda, S., Syu, L. J., Saltiel, A. R., Buxbaum, J. D., Czernik, A. J., Nairn, A.C., and Greengard, P. (1998) Regulation of secretion of Alzheimer amyloid precursor protein by the mitogen-activated protein kinase cascade. *J. Neurochem.* **70**, 524-530
31. Dethlefsen, S. M., Raab, G., Moses, M. A., Adam, R. M., Klagsbrun M., and Freeman M. R. (1998) Extracellular calcium influx stimulates metalloproteinase cleavage and secretion of heparin-binding EGF-like growth factor independently of protein kinase C. *J. Cell. Biochem.* **69**, 143-153
32. Diaz-Rodriguez, E., Esparis-Ogando, A., Montero, J. C., Yuste, L., and Pandiella, A. (2000) Stimulation of cleavage of membrane proteins by calmodulin inhibitors. *Biochem. J.* **346**, 359-367
33. Eto, K., Huet, C., Tarui, T., Kupriyanov, S., Liu, H. Z., Puzon-McLaughlin, W., Zhang, X. P., Sheppard, D., Engvall, E., and Takada, Y. (2002) Functional classification of ADAMs based on a conserved motif for binding to integrin alpha 9beta 1: implications for sperm-egg binding and other cell interactions. *J. Biol. Chem*. **277**, 17804-17810
34. Eto, K., Puzon-McLaughlin, W., Sheppard, D., Sehara-Fujisawa, A., Zhang, X. P., and Takada, Y. (2000) RGD-independent binding of integrin alpha9beta1 to the ADAM-12 and -15 disintegrin domains mediates cell-cell interaction. *J. Biol. Chem*. **275,** 34922-34930
35. Evans, J. P. (2001) Fertilin beta and other ADAMs as integrin ligands: insights into cell adhesion and fertilization. *BioEssay* **23**, 628-639
36. Fahrenholz, F., Gilbert, S., Kojro, E., Lammich, S., and Postina, R. (2000) Alpha-secretase activity of the disintegrin metalloprotease ADAM 10. Influences of domain structure. *Ann. N. Y. Acad. Sci.* **920,** 215-222
37. Fan, H. and Derynck, R. (1999) Ectodomain shedding of TGF-alpha and other transmembrane proteins is induced by receptor tyrosine kinase activation and MAP kinase signaling cascades. *EMBO J.* **18**, 6962-6972
38. Franzke, C. W., Tasanen, K., Schacke, H., Zhou, Z., Tryggvason, K., Mauch, C., Zigrino, P., Sunnarborg, S., Lee, D. C., Fahrenholz, F., and Bruckner-Tuderman, L. (2002) Transmembrane collagen XVII, an epithelial adhesion protein, is shed from the cell surface by ADAMs. *EMBO J.* **21**:5026-5035
39. Fitzgerald, M. L., Wang, Z., Park, P. W., Murphy, G., and Bernfield, M. (2000) Shedding of syndecan-1 and -4 ectodomains is regulated by multiple signaling pathways and mediated by a TIMP-3-sensitive metalloproteinase. *J. Cell Biol.* **148**, 811-824
40. Fors, B. P., Goodarzi, K., von Andrian, U. H. (2001) L-selectin shedding is independent of its subsurface structures and topographic distribution. *J. Immunol.* **167**, 3642-3651
41. Fritsche, J., Moser, M., Faust, S., Peuker, A., Buttner, R., Andreesen, R., and Kreutz, M. (2000) Molecular cloning and characterization of a human metalloprotease disintegrin--a novel marker for dendritic cell differentiation. *Blood* **96**, 732-739

42. Galazka, G., Windsor, L. J., Birkedal-Hansen, H., and Engler, J. A. (1996) APMA (4-aminophenylmercuric acetate) activation of stromelysin-1 involves protein interactions in addition to those with cysteine-75 in the propeptide. *Biochemistry* **35**, 11221-11227
43. Gao, G., Westling, J., Thompson, V. P., How ell, T. D., Gottschall, P. E., and Sandy, J.D. (2002) Activation of the proteolytic activity of ADAMTS4 (aggrecanase-1) by C-terminal truncation. *J. Biol. Chem.* **277**, 11034-11041
44. Garton, K. J., Gough, P. J., Blobel, C. P., Murphy, G., Greaves, D. R., Dempsey, P. J., and Raines, E. W. (2001) Tumor necrosis factor-alpha-converting enzyme (ADAM17) mediates the cleavage and shedding of fractalkine (CX3CL1). *J. Biol. Chem.* **276**, 37993-38001
45. Gaultier, A., Cousin, H., Darribere, T., and Alfandari D. (2002) ADAM13 disintegrin and cysteine-rich domains bind to the second heparin-binding domain of fibronectin. *J. Biol. Chem.* **277**, 23336-23344
46. Gechtman, Z., Alonso, J. L., Raab, G., Ingber, D. E., and Klagsbrun, M. (1999) The shedding of membrane-anchored heparin-binding epidermal-like growth factor is regulated by the Raf/mitogen-activated protein kinase cascade and by cell adhesion and spreading. *J. Biol. Chem.* **274**, 28828-28835
47. Grams, F., Huber, R., Kress, L. F., Moroder, L., and Bode W. (1993) Activation of snake venom metalloproteinases by a cysteine switch-like mechanism. *FEBS Lett.* **335**, 76-80
48. Gutwein, P., Oleszewski, M., Mechtersheimer, S., Agmon-Levin, N., Krauss, K., and Altevogt, P. (2000) Role of Src kinases in the ADAM-mediated release of L1 adhesion molecule from human tumor cells. *J. Biol. Chem.* **275**, 15490-15497
49. Hargreaves, P. G., Wang, F., Antcliff, J., Murphy, G., Lawry, J., Russell, R. G., and Croucher, P. I. (1998) Human myeloma cells shed the interleukin-6 receptor: inhibition by tissue inhibitor of metalloproteinase-3 and a hydroxamate-based metalloproteinase inhibitor. *Br. J. Haematol.* **101**, 694-702
50. Hattori, M., Osterfied, M., and Flanagan, J. (2000) Regulated cleavage of a contact-mediated axon repellent. *Science* **289**, 1360-1365
51. Hooper, N. M., Karran, E. H., and Turner, A. J. (1997) Membrane protein secretases. *Biochem. J.* **321**, 265-279
52. Hooper, N. M. and Turner, A. J. The search"for alpha-secretase and its potential as a therapeutic approach to Alzheimer s disease. *Curr. Med. Chem.* **9**, 1107-1119
53. Howard, L., Maciewicz, R. A., and Blobel, C. P. (2000) Cloning and characterization of ADAM28: evidence for autocatalytic pro-domain removal and for cell surface localization of mature ADAM28. *Biochem. J.* **348**, 21-27
54. Howard, L., Nelson, K. K., Maciewicz, R. A., and Blobel, C. P. (1999) Interaction of the metalloprotease disintegrins MDC9 and MDC15 with two SH3 domain-containing proteins, endophilin I and SH3PX1. *J. Biol. Chem.* **274**, 31693-31699
55. Howard, L., Zhang, Y., Horrocks, M., Maciewicz, R. A., and Blobel, C. P. (2001) Catalytic activity of ADAM28. *FEBS Lett.* **498**, 82-86
56. Huang, L., Feng. L., Yang, L., Zhou, W., Zhao, S., and Li, C. (2002) Screen and identification of proteins interacting with ADAM19 cytoplasmic tail. *Mol. Biol. Rep.* **29**, 317-323
57. Iba, K., Albrechtsen, R., Gilpin, B., Frohlich, C., Loechel, F., Zolkiewska, A., Ishiguro, K., Kojima, T., Liu, W., Langford, J. K., Sanderson, R. D., Brakebusch, C., Fassler, R., and Wewer UM. (2000) The cysteine-rich domain of human ADAM 12 supports cell adhesion through syndecans and triggers signaling events that lead to beta1 integrin-dependent cell spreading. *J. Cell Biol.* **149**, 1143-56
58. Iba, K., Albrechtsen, R., Gilpin, B., Loechel, F., and Wewer, U. M. (1999) Cysteine-rich domain of human ADAM 12 (meltrin alpha) supports tumor cell adhesion. *Am. J. Pathol.* **154**, 1489-1501
59. Ilan, N., Mohsenin, A., Cheung, L., and Madri, J.A. (2001) PECAM-1 shedding during apoptosis generates a membrane-anchored truncated molecule with unique signaling characteristics. *FASEB J.* **15**, 362-372
60. Inoue, D., Reid, M., Lum, L., Kratzschmar, J., Weskamp, G., Myung, Y. M., Baron, R., and Blobel, C. P. (1998) Cloning and initial characterization of mouse meltrin beta and analysis of the expression of four metalloprotease-disintegrins in bone cells. *J. Biol. Chem.* **273**, 4180-4187
61. Itai, T., Tanaka, M., and Nagata, S. (2001) Processing of tumor necrosis factor by the membrane-bound TNF-alpha-converting enzyme, but not its truncated soluble form. *Eur. J. Biochem.* **268**, 2074-2082
62. Izumi, Y., Hirata, M., Hasuwa, H., Iwamoto, R., Umata, T., Miyado, K., Tamai, Y., Kurisaki, T., Sehara-Fujisawa, A., Ohno, S., and Mekada, E. (1998) A metalloprotease-disintegrin, MDC9/meltrin-gamma/ADAM9 and PKCdelta are involved in TPA-induced ectodomain shedding of membrane-anchored heparin-binding EGF-like growth factor. *EMBO J.* **17**, 7260-7272
63. Kahn, J., Walcheck, B., Migaki, G. I., Jutila, M. A., and Kishimoto, T. K. (1998) Calmodulin regulates L-selectin adhesion molecule expression and function through a protease-dependent mechanism. *Cell* **92**, 809-812
64. Kang, Q., Cao, Y., and Zolkiewska, A. (2000) Metalloprotease-disintegrin ADAM 12 binds to the SH3 domain of Src and activates Src tyrosine kinase in C2C12 cells. *Biochem. J.* 2000 **352,** 883-892

65. Kang, Q., Cao, Y., and Zolkiewska A. (2001) Direct interaction between the cytoplasmic tail of ADAM 12 and the Src homology 3 domain of p85alpha activates phosphatidylinositol 3-kinase in C2C12 cells. *J. Biol. Chem*. **276**, 24466-24472
66. Kang, T., Nagase, H., and Pei, D. (2002a) Activation of membrane-type matrix metalloproteinase 3 zymogen by the proprotein convertase furin in the trans-Golgi network. *Cancer Res.* **62**, 675-681
67. Kang, T., Park, H. I., Suh, Y., Zhao, YG., Tschesche, H., and Sang, Q. X. (2002c). Autolytic processing at Glu(586)-Ser(587) within the cysteine-rich domain of human adamalysin 19/disintegrin-metalloproteinase 19 is necessary for its proteolytic activity. *J. Biol. Chem.* **277,** 48514-48522
68. Kang, T., Tschesche, H., and Sang, Q. X. (2003) Regulation of enzyme stabiltiy by the cysteine residues of the residual cysteine-rich domain of C-terminal fragment retained by the autocatalytic processing at Glu(586)-Ser(587) of human adamalysin19/ADAM19. Submitted to *J. Biol. Chem*.
69. Kang, T., Yi, J., Guo, A., Wang, X., Overall, C. M., Jiang, W., Elde, R., Borregaard, N., and Pei, D. (2001) Subcellular distribution and cytokine- and chemokine-regulated secretion of leukolysin/MT6-MMP/MMP-25 in neutrophils. *J. Biol. Chem.* **276**, 21960-21968
70. Kang, T., Zhao, Y. G., Pei, D., Sucic, J. F., and Sang, Q. X. (2002b) Intracellular activation of human Adamalysin 19/disintegrin and metalloproteinase 19 by furin occurs via one of the two consecutive recognition sites. *J. Biol. Chem.* **277,** 25583-25591
71. Kashiwagi, M., Tortorella, M., Nagase, H., and Brew, K. (2001) TIMP-3 is a potent inhibitor of aggrecanase 1 (ADAM-TS4) and aggrecanase 2 (ADAM-TS5). *J. Biol. Chem.* **276**, 12501-12504
72. Kheradmand, F. and Werb, Z. (2002) Shedding light on sheddases: role in growth and development. *BioEssay* **24**, 8-12
73. Koike, H., Tomioka, S., Sorimachi, H., Saido, T. C., Maruyama, K., Okuyama, A., Fujisawa-Sehara, A., Ohno, S., Suzuki, K., and Ishiura, S. (1999) Membrane-anchored metalloprotease MDC9 has an alpha-secretase activity responsible for processing the amyloid precursor protein. *Biochem. J.* **343**, 371-375
74. Kuno, K., Kanada, N., Nakashima, E., Fujiki, F., Ichimura, F., and Matsushima, K. (1997) Molecular cloning of a gene encoding a new type of metalloproteinase-disintegrin family protein with thrombospondin motifs as an inflammation associated gene. *J. Biol. Chem*. **272**, 556-562
75. Kuno, K., Okada, Y., Kawashima, H., Nakamura, H., Miyasaka, M., Ohno, H., Matsushima, K. (2000) ADAMTS-1 cleaves a cartilage proteoglycan, aggrecan. *FEBS Lett.* **478**, 241-245
76. Kuno, K., Terashima, Y., and Matsushima, K. (1999) ADAMTS-1 is an active metalloproteinase associated with the extracellular matrix. *J. Biol. Chem.* **274,** 18821-18826
77. Kurisaki, T., Wakatsuki, S., and Sehara-Fujisawa, A. (2002) Meltrin beta mini, a new ADAM19 isoform lacking metalloprotease and disintegrin domains, induces morphological changes in neuronal cells. *FEBS Lett.* **532**, 419-422
78. Kurohara, K., Masuda, Y., Nagabukuro, N., Tsuji, A., Amagasa, T., and Fujisawa-Sehara, (2000) Meltrin beta (ADAM19) gene: cloning, mapping, and analysis of the regulatory region. *Biochem. Biophys. Res. Commun.* **270:** 522-527
79. Liao, J. K. (2002) Shedding growth factors in cardiac hypertrophy. *Nat Med*. **8**: 20-21
80. Loechel, F., Fox, J. W., Murphy, G., Albrechtsen, R., and Wewer, U. M. (2000) ADAM 12-S cleaves IGFBP-3 and IGFBP-5 and is inhibited by TIMP-3. *Biochem. Biophys. Res. Commun.* **278**, 511-515
81. Loechel, F., Gilpin, B. J., Engvall, E., Albrechtsen, R., and Wewer, U.M. (1998) Human ADAM 12 (meltrin alpha) is an active metalloprotease. *J. Biol. Chem.* **273**, 16993-16997.
82. Loechel, F., Overgaad, M. T., Oxvig, C., Albrechtsen, R., and Wewer, U. M. (1999) Regulation of human ADAM 12 protease by the prodomain. Evidence for a functional cysteine switch. *J. Biol. Chem.* **274**, 13427-13433
83. Lum, L., and Blobel, C. P. (1997) Evidence for distinct serine protease activities with a potential role in processing the sperm protein fertilin. *Dev. Biol.* **191**, 131-145
84. Lum, L., Reid, M. S., and Blobel, C. P. (1998) Intracellular maturation of the mouse metalloprotease disintegrin MDC15. *J. Biol. Chem.* **273**, 26236-26247
85. Lum, L., Wong, B. R., Josien, R., Becherer, J. D., Erdjument-Bromage. H., Schlondorff. J., Tempst, P., Choi, Y., and Blobel, C. P. (1999) Evidence for a role of a tumor necrosis factor-alpha (TNF-alpha)-converting enzyme-like protease in shedding of TRANCE, a TNF family member involved in osteoclastogenesis and dendritic cell survival. *J. Biol. Chem.* **274**, 13613-13618
86. Manna, S. K. and Aggarwal, B. B. (1998) Interleukin-4 down-regulates both forms of tumor necrosis factor receptor and receptor-mediated apoptosis, NF-kappaB, AP-1, and c-Jun N-terminal kinase. Comparison with interleukin-13. *J. Biol. Chem.* **273**, 33333-33341
87. Marchand, P., Volkmann, M., and Bond, J. (1996) Cysteine mutations in the MAM domain result in monomeric meprin and alter stability and activity of the proteinase. *J. Biol. Chem.* **271**,24236-24241
88. Marchenko, N. D., Marchenko, G. N., and Strongin, A. Y. (2002) Unconventional activation mechanisms of MMP-26, a human matrix metalloproteinase with a unique PHCGXXD cysteine-switch motif. *J. Biol. Chem*. **277**, 18967-18972

89. Martin, J., Eynstone, L. V., Davis, M., Williams, J. D., and Steadman, R. (2002) The tole of ADAM15 in glomercular mesangial cell migration. *J. Biol. Chem*. **277**, 33683-33689
90. Matthews, R. T., Gary, S. C., Zerillo, C., Pratta, M., Solomon, K., Arner, E. C., and Hockfield, S. (2000) Brain-enriched hyaluronan binding (BEHAB)/brevican cleavage in a glioma cell line is mediated by a disintegrin and metalloproteinase with thrombospondin motifs (ADAMTS) family member. *J. Biol. Chem*. **275**, 22695-22703.
91. Mechtersheimer, S., Gutwein, P., Agmon-Levin, N., Stoeck, A., Oleszewski, M., Riedle, S., Fogel, M., Lemmon, V., and Altevogt, P. (2001) Ectodomain shedding of L1 adhesion molecule promotes cell migration by autocrine binding to integrins. *J. Cell Biol.* **155**, 661-673
92. Migaki, G. I., Kahn, J., and Kishimoto, T. K. (1995) Mutational analysis of the membrane-proximal cleavage site of L-selectin: relaxed sequence specificity surrounding the cleavage site. *J. Exp. Med.* **182**, 549-557
93. Milla, M. E., Leesnitzer M. A., Moss. M. L., Clay, W. C. Carter, H. L., Miller, A. B., Su, J., Lambert, M. H., Willard, D.H.,Sheeley, D. M., Kost, T. A., Burkhart, W., Moyer, M., Blackburn, R. K., Pahel, G. L., Mitchell, J. L., Hoffman, C. R., and Becherer, J. D. (1999) Specific sequence elements are required for the expression of functional tumor necrosis factor-alpha-converting enzyme (TACE). *J. Biol. Chem.* **274,** 30563-30570
94. Millichip, M. I., Dallas, D. J., Wu, E., and McKie, N. (1998) The metallo-disintegrin ADAM10 (MADM) from bovine kidney has type IV collagenase activity in vitro. *Biochem. Biophys. Res. Commun*. **245**, 594-598
95. Molloy, S. S., Anderson, E. D., Jean, F., and Thomas, G. (1999) Bi-cycling the furin pathway: from TGN localization to pathogen activation and embryogenesis. *Trends Cell. Biol.* **9**, 28-35
96. Moss, M. L., Jin, S. L., Milla, M. E., Bickett, D. M., Burkhart, W., Carter, H. L., Chen, W. J., Clay, W. C., Didsbury, J. R., Hassler, D., Hoffman, C. R., Kost, T. A., Lambert, M. H., Leesnitzer, M. A., McCauley, P., McGeehan, G., Mitchell, J., Moyer, M., Pahel, G., Rocque, W., Overton, L. K., Schoenen, F., Seaton, T., Su, J. L., and Becherer, J.D. (1997) Cloning of a disintegrin metalloproteinase that processes precursor tumour-necrosis factor-alpha. *Nature.* **385**, 733-736
97. Müllberg, J., Durie, F. H., Otten-Evans, C., Alderson, M. R., Rose-John, S., Cosman, D., Black, R. A., and Mohler, K. M. (1995) A metalloprotease inhibitor blocks shedding of the IL-6 receptor and the p60 TNF receptor. *J. Immunol.* **155**, 5198-5205
98. Müllberg, J., Oberthür, W., Lottspeich, F., Mehl, E., Dittrich, E., Graeve, L., Heinrich, P. C., and Rose-John, S. (1994) The soluble human IL-6 receptor. Mutational characterization of the proteolytic cleavage site. *J. Immunol.* **152**, 4958-4968
99. Müllberg, J., Rauch, C. T., Wolfson, M. F., Castner, B., Fitzner, J. N., Otten-Evans, C., Mohler, K. M., Cosman, D., and Black, R. A. (1997) Further evidence for a common mechanism for shedding of cell surface proteins. *FEBS Lett.* **401**, 235-238
100. Nakayama, K. (1997) Furin: a mammalian subtilisin/Kex2p-like endoprotease involved in processing of a wide variety of precursor proteins. *Biochem. J.* **327**, 625-635
101. Nath, D., Slocombe, P. M., Stephens, P. E., Warn, A., Hutchinson, G. R., Yamada, K. M., Docherty, A. J., and Murphy G. (1999) Interaction of metargidin (ADAM-15) with alphavbeta3 and alpha5beta1 integrins on different haemopoietic cells. *J. Cell Sci.* **112**, 579-587
102. Nath, D., Slocombe, P. M., Webster, A., Stephens, P. E., Docherty, A. J., and Murphy G. (2000) Meltrin gamma(ADAM-9) mediates cellular adhesion through alpha(6)beta(1)integrin, leading to a marked induction of fibroblast cell motility. *J. Cell Sci.* **113**, 2319-2328
103. Nath, D., Williamson, N. J., Jarvis, R., and Murphy, G. (2001) Shedding of c-Met is regulated by crosstalk between a G-protein coupled receptor and the EGF receptor and is mediated by a TIMP-3 sensitive metalloproteinase. *J. Cell Sci.* **114**, 1213-1220
104. Nelson, K. K., Schlondorff, J., and Blobel, C. P. (1999) Evidence for an interaction of the metalloprotease-disintegrin tumour necrosis factor alpha convertase (TACE) with mitotic arrest deficient 2 (MAD2), and of the metalloprotease-disintegrin MDC9 with a novel MAD2-related protein, MAD2beta. *Biochem. J.* **343**, 673-680
105. Pan, D., and Rubin, G. M. (1997) Kuzbanian controls proteolytic processing of Notch and mediates lateral inhibition during Drosophila and vertebrate neurogenesis. *Cell*. **90**, 271-280
106. Pandiella, A. and Massague, J. (1991) Multiple signals activate cleavage of the membrane transforming growth factor-alpha precursor. *J. Biol. Chem.* **266**, 5769-5773
107. Park, H. I., Turk, B. E., Gerkema, F. E., Cantley, L. C., and Sang, Q. X. (2002) Peptide substrate specificities and protein cleavage sites of human endometase/matrilysin-2/matrix metalloproteinase-26 *J. Biol. Chem.* **277**, 35168-35175
108. Pei, D. (1999) CA-MMP: a matrix metalloproteinase with a novel cysteine array, but without the classic cysteine switch. *FEBS Lett.* **457**, 262-270

109. Pei, D., Kang, T., and Qi, H. (2000) Cysteine array matrix metalloproteinase (CA-MMP)/MMP-23 is a type II transmembrane matrix metalloproteinase regulated by a single cleavage for both secretion and activation. *J. Biol. Chem.* **275**, 33988-33997
110. Pei, D., and Weiss, S. J. (1995) Furin-dependent intracellular activation of the human stromelysin-3 zymogen. *Nature.* **375**, 244-247
111. Peschon, J. J., Slack, J. L., Reddy, P., Stocking, K. L., Sunnarborg, S. W., Lee, D. C., Russell, W. E., Castner, B. J., Johnson, R. S., Fitzner, J. N., Boyce, R. W., Nelson, N., Kozlosky, C. J., Wolfson, M. F., Rauch, C. T., Cerretti, D. P., Paxton, R. J., March, C. J., and Black, R. A. (1998) An essential role for ectodomain shedding in mammalian development. *Science* **282**, 1281-1284
112. Poghosyan, Z., Robbins, S. M., Houslay, M.D., Webster, A., Murphy, G., and Edwards, D. R. (2002) Phosphorylation-dependent interactions between ADAM15 cytoplasmic domain and Src family protein tyrosine kinase. *J. Biol. Chem.* **277**, 4999-5007
113. Prenzel, N., Zwick, E., Daub, H., Leserer, M., Abraham, R., Wallasch, C., and Ullrich A. (1999) EGF receptor transactivation by G-protein-coupled receptors requires metalloproteinase cleavage of proHB-EGF. *Nature* **402**, 884-888
114. Primakoff, P., and Myles, D. G. (2000) The ADAM gene family: surface proteins with adhesion and protease activity. *Trends. Genet.* **16**, 83-87
115. Qi, H., Rand, M. D., Wu, X., Sestan, N., Wang, W., Rakic, P., Xu, T., and Artavanis-Tsakonas S. (1999) Processing of the notch ligand delta by the metalloprotease Kuzbanian. *Science*. **283**, 91-94
116. Reddy, P., Slack, J. L., Davis, R., Cerretti, D. P., Kozlosky, C. J., Blanton, R. A., Shows, D., Peschon, J. J., and Black, R. A. (2000) Functional analysis of the domain structure of tumor necrosis factor-alpha converting enzyme. *J. Biol. Chem.* **275,** 14608-14614
117. Rio, C., Buxbaum JD, Peschon JJ, Corfas G. (2000) Tumor necrosis factor-alpha-converting enzyme is required for cleavage of erbB4/HER4. *J. Biol. Chem*. **275**, 10379-10387
118. Rodriguez-Manzaneque, J. C., Westling, J., Thai, S. N., Luque, A., Knauper, V., Murphy, G., Sandy, J. D., and Iruela-Arispe, M. L. (2002) ADAMTS1 cleaves aggrecan at multiple sites and is differentially inhibited by metalloproteinase inhibitors. *Biochem. Biophys. Res. Commun*. **293**, 501-508
119. Roghani, M., Becherer, J. D., Moss, M. L., Atherton, R. E., Erdjument-Bromage, H., Arribas, J., Blackburn, R. K., Weskamp, G., Tempst, P., and Blobel CP. (1999) Metalloprotease-disintegrin MDC9: intracellular maturation and catalytic activity. *J. Biol. Chem*. **274**, 3531-3540
120. Rooke, J., Pan, D., Xu, T., and Rubin, G. M. (1996) KUZ, a conserved metalloprotease-disintegrin protein with two roles in Drosophila neurogenesis. *Science*. **273**, 1227-1231
121. Sandy, J. D., Thompson, V., Doege, K., and Verscharen, C. (2000) The intermediates of aggrecanase-dependent cleavage of aggrecan in rat chondrosarcoma cells treated with interleukin-1. *Biochem. J.* **351**, 161-166
122. Sandy, J. D., and Verscharen, C. (2001) Analysis of aggrecan in human knee cartilage and synovial fluid indicates that aggrecanase (ADAMTS) activity is responsible for the catabolic turnover and loss of whole aggrecan whereas other protease activity is required for C-terminal processing in vivo. *Biochem. J.* **358**, 615-626
123. Sandy, J. D., Westling, J., Kenagy, R. D., Iruela-Arispe, M. L., Verscharen, C., Rodriguez-Mazaneque, J. C., Zimmermann, D. R., Lemire, J. M., Fischer, J. W., Wight, T. N., and Clowes, A.W. (2001) Versican V1 proteolysis in human aorta in vivo occurs at the Glu441-Ala442 bond, a site that is cleaved by recombinant ADAMTS-1 and ADAMTS-4. *J. Biol. Chem.* **276,** 13372-13378
124. Schlomann, U., Wildeboer, D., Webster, A., Antropova, O., Zeuschner, D., Knight, C. G., Docherty, A. J., Lambert, M., Skelton, L., Jockusch, H., and Bartsch, J. W. (2002) The metalloprotease disintegrin ADAM8. Processing by autocatalysis is required for proteolytic activity and cell adhesion. *J. Biol. Chem.* **277,** 48210-48219
125. Schlondorff, J. and Blobel, C. P. (1999) Metalloprotease-disintegrins: modular proteins capable of promoting cell-cell interactions and triggering signals by protein-ectodomain shedding. *J. Cel. Sci.* **112**, 3603-3617
126. Schlondorff, J., Becherer, J. D., and Blobel, C.P. (2000) Intracellular maturation and localization of the tumour necrosis factor alpha convertase (TACE). *Biochem. J.* **347**:131-138
127. Schlondorff, J., Lum, L., and Blobel, C. P. (2001) Biochemical and pharmacological criteria define two shedding activities for TRANCE/OPGL that are distinct from the tumor necrosis factor alpha convertase. *J. Biol. Chem.* **276**, 14655-14674
128. Seals, D. F., and Courtneidge, S. A. (2003) The ADAMs family of metalloproteinease: multidomain proteins with multiple functions. *Gene & Dev*. **17**, 7-30
129. Shi Z, Xu W, Loechel F, Wewer UM, Murphy LJ. (2000) ADAM 12, a disintegrin metalloprotease, interacts with insulin-like growth factor-binding protein-3. *J. Biol. Chem*. **275**, 18574-18580
130. Shirakabe, K., Wasuda, S., Kurisaki, T., and Fujisawa-Sehara, A. (2001) Roles of Meltrin beta /ADAM19 in the processing of neuregulin. *J. Biol. Chem.* **276**, 9352-9358

131. Sisodia, S. S. (1992) Beta-amyloid precursor protein cleavage by a membrane-bound protease. *Proc. Natl. Acad. Sci. U. S. A.* **89**, 6075-6079
132. Smith, K. M., Gaultier, A., Cousin, H., Alfandari, D., White, J. M., and DeSimone, D. W. (2002) The cysteine-rich domain regulates ADAM protease function in vivo. *J. Cell Biol.* **159**, 893-902
133. Somerville, R. P. T., Longpre, J.-M., Jungers, K. A., Engle, J. M., Ross, M., Evanko, S., Wight, T. N., Leduc, R., and Apte, S. S. (2003) Characterization of ADAMTS-9 and ADAMTS-20 as a Distinct ADAMTS Subfamily Related to *Caenorhabditis elegans* GON-1 *J. Biol. Chem.* **278**: 9503-9513
134. Steiner, D. F. (1998) The proprotein convertases. *Curr. Opin. Chem. Biol.* **848**, 45-62
135. Stone, A. L., Kroeger, M., and Sang, Q. X. (1999) Structure-function analysis of the ADAM family of disintegrin-like and metalloproteinase-containing proteins (review). *J. Protein Chem.* **18**, 447-465
136. Sunnarborg, S. W., Hinkle, C. L., Stevenson, M., Russell, W. E., Raska, C. S., Peschon, J. J., Castner, B. J., Gerhart, M. J., Paxton, R. J., Black, R. A., and Lee, D.C. (2002) Tumor Necrosis Factor-α Converting Enzyme (TACE) Regulates Epidermal Growth Factor Receptor Ligand Availability *J. Biol. Chem.* **277**: 12838-12845
137. Suzuki, A., Kadota, N., Hara, T., Nakagami, Y., Izumi, T., Takenawa, T., Sabe, H., and Endo T. (2000) Meltrin alpha cytoplasmic domain interacts with SH3 domains of Src and Grb2 and is phosphorylated by v-Src. *Oncogene*. **19**, 5842-5850
138. Tang, B. L. (2001) ADAMTS: a novel family of extracellular matrix proteases. *Int. J. Biochem. Cell. Biol.* **33**, 33-44
139. Tang, P., Hung, M. C., and Klostergaard, J. (1996) Length of the linking domain of human pro-tumor necrosis factor determines the cleavage processing. *Biochemistry* **35**, 8226-8233
140. Thathiah, A., Blobel, C. P., and Carson, D. D. (2003) Tumor Necrosis Factor-α Converting Enzyme/ADAM 17 Mediates MUC1 Shedding. *J. Biol. Chem.* **278**: 3386-3394
141. Thodeti, C. K., Albrechtsen, R., Grauslund, M., Asmar, M., Larsson, C., Takada, Y., Mercurio, A. M., Couchman, J. R., and Wewer, UM. (2003) ADAM12/Syndecan-4 Signaling Promotes β_1 Integrin-dependent Cell Spreading through Protein Kinase Cα and RhoA. *J. Biol. Chem.* **278**: 9576-9584
142. Tortorella, M. D., Burn, T. C., Pratta, M. A., Abbaszade, I., Hollis, J. M., Liu, R., Rosenfeld, S. A., Copeland, R. A., Decicco, C. P., Wynn, R., Rockwell, A., Yang, F., Duke, J. L., Solomon, K., George, H., Bruckner, R., Nagase, H., Itoh, Y., Ellis, D. M., Ross, H., Wiswall, B. H., Murphy, G., Hillman Jr, M. C., Hollis, G. F., Newton, R. C., Magolda, R. L., Trzaskos, J. M. and Arner, E. C. (1999) Purification and cloning of aggrecanase-1: a member of the ADAMTS family of proteins. *Science.* **284**, 1664-1666
143. Tortorella, M. D., Pratta, M., Liu, R. Q., Abbaszade, I., Ross, H., Burn, T., and Arner E. (2000a) The thrombospondin motif of aggrecanase-1 (ADAMTS-4) is critical for aggrecan substrate recognition and cleavage. *J. Biol. Chem.* **275**, 25791-25797
144. Tortorella, M. D., Pratta, M., Liu, R. Q., Austin, J., Ross, O. H., Abbaszade, I., Burn, T., and Arner E. (2000b) Sites of aggrecan cleavage by recombinant human aggrecanase-1 (ADAMTS-4). *J. Biol. Chem.* **275**, 18566-18573
145. Van, E. P., Little, R. D., Dupuis, J., Del Mastro, R. G., Falls, K., Simon, J., Torrey, D., Pandit, S., McKenny, J., Braunschweiger, K., Walsh, A., Liu, Z., Hayward, B., Folz, C., Manning, S. P., Bawa, A., Saracino, L., Thackston, M., Benchekroun, Y., Capparell, N., Wang, L., Eir, R., Feng, Y., Dubois, J., FitzGerald, M. G., Huang, H., Gibson, R., Allen, K. M., Pedan, A., Danzig, M. R., Umland, S. P., Egan, R. W., Cuss, F. M., Rorke, S., Clough, J. B., Holloway, J. W., Holgate, S. T., and Keith, T. P. (2002) Association of the ADAM33 gene with asthma and bronchial hyperresponsiveness. *Nature*
146. Van Wart, H. E., and Birkedal-Hansen, H. (1990) The cysteine switch: a principle of regulation of metalloproteinase activity with potential applicability to the entire matrix metalloproteinase gene family. *Proc. Natl. Acad. Sci. U. S. A.* **87**, 5578-5582
147. Vecchi, M., Baulida, J., and Carpenter, G. (1996) Selective cleavage of the heregulin receptor ErbB-4 by protein kinase C activation. *J. Biol. Chem.* **275**, 15490-15497
148. Vecchi, M., Rudolph-Owen, L. A., Brown, C. L., Dempsey P. J., and Carpenter, G. (1998) Tyrosine phosphorylation and proteolysis. Pervanadate-induced, metalloprotease-dependent cleavage of the ErbB-4 receptor and amphiregulin. *J. Biol. Chem.* **273**, 20589-20595
149. Vincent, B., Paitel, E., Saftig, P., Frobert, Y., Hartmann, D., De Strooper, B., Grassi, J., Lopez-Perez, E., and Checler, F. (2001) The disintegrins ADAM10 and TACE contribute to the constitutive and phorbol ester-regulated normal cleavage of the cellular prion protein. *J. Biol. Chem.* **276**, 37743-37746
150. Velasco, G., Pendas, A. M., Fueyo, A., Knauper, V., Murphy, G., and Lopez-Otin, C. (1999) Cloning and characterization of human MMP-23, a new matrix metalloproteinase predominantly expressed in reproductive tissues and lacking conserved domains in other family members. *J. Biol. Chem.* **274**, 4570-4576
151. Vu, T. H., and Werb, Z. (2000) Matrix metalloproteinases: effectors of development and normal physiology. *Gene Dev.* **14**, 2123-2133

152. Wei, P., Zhao, Y.-G., Zhuang, L., Ruben, S., and Sang, Q.-X. (2001) Expression and enzymatic activity of human disintegrin and metalloproteinase ADAM19/meltrin beta. *Biochem. Biophys. Res. Commun.* **280,** 744-755
153. Westling, J., Fosang, A. J., Last, K., Thompson, V. P., Tomkinson, K. N., Hebert, T., McDonagh, T., Collins-Racie, L. A., LaVallie, E. R., Morris, E. A., and Sandy, J. D. (2002) ADAMTS4 cleaves at the aggrecanase site (Glu373-Ala374) and secondarily at the matrix metalloproteinase site (Asn341-Phe342) in the aggrecan interglobular domain. *J. Biol. Chem.* **277**, 16059-16066
154. Wolfsberg T. G., and White, J. M. (1996). ADAMs in fertilization and development. *Dev. Biol.* **180**, 389-401
155. Wong, S. T., Winchell, L. F., McCune, B. K., Earp, H. S., Teixidó, J., Massagué, J., Herman, B., and Lee, D. C. (1989) The TGF-alpha precursor expressed on the cell surface binds to the EGF receptor on adjacent cells, leading to signal transduction. *Cell* **56**, 495-506
156. Yan Y, Shirakabe K, Werb Z (2002) The metalloprotease Kuzbanian (ADAM10) mediates the transactivation of EGF receptor by G protein-coupled receptors. *J. Cell Biol.* **158**, 221-226
157. Yana, I., and Weiss, S. J. (2000) Regulation of membrane type-1 matrix metalloproteinase activation by proprotein convertases. *Mol. Biol. Cell* **11**, 2387-2401
158. Yavari, R., Adida, C., Bray-Ward, P., Brines, M., and Xu T. (1998) Human metalloprotease-disintegrin Kuzbanian regulates sympathoadrenal cell fate in development and neoplasia. *Hum. Mol. Genet.* **7**, 1161-1167
159. Yee, N. S., Langen, H., and Besmer, P. (1993) Mechanism of kit ligand, phorbol ester, and calcium-induced down-regulation of c-kit receptors in mast cells. *J. Biol. Chem.* **268**, 14189-14201
160. Yoshida, S., Setoguchi, M., Higuchi, Y., Akizuki, S., and Yamamoto, S**.** (1990) Molecular cloning of cDNA encoding MS2 antigen, a novel cell surface antigen strongly expressed in murine monocytic lineage. *Int. Immunol.* **2**, 585-591
161. Yoshinaka, T., Nishii, K., Yamada, K., Sawada, H., Nishiwaki, E., Smith, K., Yoshino, k., Ishiguro, H., and Higashiyama, H.. (2002) Identification and characterization of novel mouse and human ADAM33s with potential metalloprotease activity. *Gene.* **282**, 227-236
162. Zhang, X. P., Kamata, T., Yokoyama, K., Puzon-McLaughlin, W., Takada, Y. (1998) Specific interaction of the recombinant disintegrin-like domain of MDC-15 (metargidin, ADAM-15) with integrin alphavbeta3. *J. Biol. Chem.* **273**, 7345-7350
163. Zhao, Y., Wei, P., and Sang, Q-X. (2001) Inhibitory antibodies against endopeptidase activity of human adamalysin 19. *Biochem. Biophys. Re.s Commun.* **289**, 288-294
164. Zhou, M., Graham, R., Russell, G., and Croucher, P. I. (2001) MDC-9 (ADAM-9/Meltrin gamma) functions as an adhesion molecule by binding the alpha(v)beta(5) integrin. *Biochem. Biophys. Res. Commun.* **280**, 574-580
165. Zolkiewska, A. (1999) Disintegrin-like/cysteine-rich region of ADAM 12 is an active cell adhesion domain. *Exp. Cell. Res.* 252: 423-431

6. Abbreviations

Ab, antibody; ADAM, a disintegrin and metalloproteinase; ADAMTS, a disintegrin and metalloproteinase with thrombospondin-like motifs; alpha2-M, alpha-2-macroglobulin; APP, amyloid precursor protein; ArgBP1, Arg binding protein 1; BACE, beta-amyloid converting enzyme; BCIP, 5-bromo-4-chloro-3-indoyl phosphate; beta-cop, beta-subunit of Coatomer protein; BFA, brefeldin A; CaM, calmodulin; CLM, calmidazolium; decRVKR-CMK, decanoyl-Arg-Val-Lys-Arg-chloromethylketone; DMEM, Dulbecco's modified Eagle´s medium; ECM, extracellular matrix; EDTA, ethylenediaminetetraacetic acid; EGF, epidermal growth factor; EGFR, epidermal growth factor receptor; ER, endoplasmic reticulum; FBS, fetal bovine serum; GPCRs, G-protein-coupled receptors; MAP kinase, mitogen-activated protein kinase; MBP, myelin basic protein, MDC, Metalloprotease/Disintegrin/Cysteine-rich; MDCK, Madin-Darby canine kidney; MMPs, matrix metalloproteinases; MT-MMPs, membrane-type matrix metalloproteinases; NBT, nitro blue tetrazolium; NRG, neuregulin; pAT, alpha1-antitrypsin or alpha1-proteinase inhibitor (alpha-PI); pATp, Pittsburgh mutant of alpha-1 antitrypsin/proteinase inhibitor (alpha1-Pipitt or alpha1-PIp); PACE4, paired basic amino acid converting enzyme 4; PBS, phosphate buffered saline; PC, proprotein convertase; 7.P15 cells, furin-deficient monkey kidney COS-7 strain cells; PI-3K, phosphatidylinositol-3 kinase; PKC, protein kinase C; PMA, phorbol-12 myristate 13-acetate; RPE.40 cells, furin-deficient Chinese hamster ovary (CHO)-K1 strain cells; SDS-PAGE, sodium dodecyl sulfate polyacrylamide gel electrophoresis; TACE, tumor necrosis factor a convertase; TAPI, tumor necrosis factor-? proteinase inhibitor; TFP, trifluoperazine; TIMPs, tissue inhibitors of metalloproteinases; TGF-alpha, transforming growth factor-alpha?TNF-alpha, tumor necrosis factor-alpha; TRANCE, TNF-related activation-induced cytokine; W7, N-(6-aminohexyl)-5-chloro-1-naphthalenesulfonamide.

7. ACKNOWLEDGMENTS

This dissertation was supported in part by grants from the National Institutes of Health, CA78646, the DOD U.S. Army Medical Research Acquisition Activity, DAMD17-02-1-0238, the American Cancer Society, Florida Division F01FSU-1, and the Florida State University Research Foundation (to **Prof. Dr. Qing-Xiang Amy Sang**), as well as the Deutsche Forschungsgemeinschaft, Bonn, by the SFB 549, project A05 and the DFG-grant, Ts 8-35/3 (to **Prof. Dr. Harald Tschesche**)

Above all, I would like to thank my dissertation advisors, **Prof. Dr. Harald Tschesche**, Department of Biochemistry, Faculty of Chemistry, University of Bielefeld, Germany, and **Prof. Dr. Qing-Xiang Amy Sang**, Department of Chemistry and Biochemistry, Florida State University, USA for their continuous support and guidance throughout my graduate work. Their remarkable patience and enlightening suggestions, along with their faith in my abilities, have been instrumental in shaping this work. I am grateful for the opportunity to learn form them, greatly fortifying my desire to remain in the academic world.

I must also thank **Dr. Duanqing Pei**, Department of Pharmacology, University of Minnesota, USA for his giving me an excellent training when I was working at his lab for two and half years. Our numerous discussions have extended significantly my knowledge on the MMP field. I really appreciate that he has always been encouraging me to be a good scientist.

I am thankful to **Dr. Jörg-Walter Bartsche**, Biology Department, University Bielefeld, Germany for his valuable comments during my manuscript preparations for publications, and for his great help on my final dissertation. I also thank **Dr. Joseph F. Sucic**, Biology Department, University of Michigan-Flint, USA, for his valuable comments during my manuscript preparations for publications.

I am grateful for the help and cooperation from the team working at Dr. Sang´s lab, such as **Drs. Yunge zhao, Hyun I. Park,** and **Aizheng Xiao,** Graduate students**: Douglous H.**

Hurst, Yewseok Suh, and **Seakwoo Lee.** Specially, I truly appreciate **Sara C. Monroe** and **Robert Newcomer** for their editorial assistance with the manuscript preparations.

I also grateful for their kindness and help during my staying at the Department of Biochemistry, Faculty of Chemistry, University Bielefeld, Germany, especially **Prof. Dr. Jürgen Wienands**, **Dr. Herbert Wenzel, Dr. Abulizi Abudula** and **Dr. Mohamed Ayoub, Rainer Beckmann, Martina Mahne, Oliver Hiller, Jörg Stute, Tim Fischer, Hongbin Li, Björn Stork, Astrid Holtmann, Kai Dittmann, Michael Engelke, Niklas Engels, Annika Grabbe, Mareke Oley**, i.e.

Finally, I am really appreciated that my family including my wife, **Qiong Chen**, and my son, **Jason S. Kang** fully supported me during the period of my graduate work, and that my relatives including my mother, the parents-in-law, my sisters and brother, and my sisters and brothers-in law, and my friends, such as **Yansong Li, Xiaodong Li, Fuxian Yi, Chaojun Duan, Feng Lin, Xiyun Deng, Jianbo Yang, Yonggang Zhou,** and **Qian Chen**, i.e. supported me with their encouragement.